M.5 Shielding Evaluation

The radiation shielding evaluation for the Standardized NUHOMS® System (during loading, transfer and storage) for the 24P and 52B canisters is discussed in Sections 3.3.5, 7.0 and 8.0. The following radiation shielding evaluation specifically addresses the dose rates due to design-basis PWR fuel and Burnable Poison Rod Assemblies (BPRAs) loaded in a NUHOMS®-32PT DSC. The shielding analysis is carried out for the four DSC configurations of the NUHOMS®-32PT system described in Section M.2.1. The basket layout for these configurations is identical except for the length of the DSC components. For shielding purposes, the only difference between the 100-ton and 125-ton versions is the thickness of the shield plug designs. The 100-ton versions have somewhat thinner shield plugs than the 125-ton versions. Each of the configurations is designed to store up to 32 intact standard PWR fuel assemblies. The 32PT-L100 and 32PT-L125 are also designed to store up to 32 intact standard PWR fuel assemblies with or without BPRAs. Therefore, for shielding purposes, the two long-cavity versions bound the short-cavity versions because of the additional gamma source due to the BPRAs. Therefore, the shielding evaluation presented herein is performed only for the 32PT-L100 and 32PT-L125 with fuel plus BPRAs. To assure that this evaluation is conservative, the fuel source terms are not adjusted to account for the additional decay required to accommodate the BPRAs.

The design-basis PWR fuel source terms are derived from the bounding fuel, B&W 15x15 Mark B assembly design as described in Section M.5.2

The NUHOMS®-32PT DSCs can store intact PWR fuel assemblies and BPRAs with the characteristics described in Table M.2-1. The NUHOMS®-32PT DSC may store PWR fuel assemblies arranged in any of three alternate heat zoning configurations with a maximum decay heat of 1.2kW per assembly and a maximum heat load of 24 kW per canister. The heat load configurations are shown in Figure M.2-1, Figure M.2-2 and Figure M.2-3. Note that while the B&W, CE, and Westinghouse fuel designs are specifically listed, storing reload fuel designed by other manufacturers is also allowed provided an analysis is performed to demonstrate that the limiting features listed in Table M.2-1 bound the specific manufacturers replacement fuel. The limiting features are burnup, initial enrichment, cooling time, fissile material type, number of fuel rods, number of guide tube/instrument tube holes, cobalt impurities in the hardware and initial heavy metal.

The design-basis fuel source terms for this evaluation are defined as the source terms from fuel with the burnup/initial enrichment/cooling time combination given in Table M.2-5 through Table M.2-9 (without BPRAs) and located in the basket as shown in Figure M.2-1, Figure M.2-2 or Figure M.2-3, that gives the maximum dose rate on the surface of the HSM and/or OS197/OS197H Transfer Cask (TC). This approach is consistent with the method used to generate the fuel qualification tables for the Standardized NUHOMS®-24P and -52B canister designs.

The Heat Load Zoning Configuration 2 (Figure M.2-2) is the configuration that produces the highest dose rates on the surfaces of the HSM and TCs. These bounding gamma and neutron source terms are then used in the radiation shielding models to conservatively calculate dose rates on and around the NUHOMS®-32PT system. In order to model Heat Load Zoning

Configuration 2, all sixteen assemblies in the outer ring of the DSC are modeled with source terms consistent with 1.2 kW. Therefore, the source terms result in fairly conservative dose rates because the shielding analysis is based on a 28.8 kW heat load compared to the 24 kW heat load limit.

The bounding burnup, minimum initial enrichment and cooling time combinations used in this analysis are as follows:

- 30 GWd/MTU, 2.5 wt. % U-235, 8-year cooled – Inner sixteen assemblies in the HSM models,
- 41 GWd/MTU, 3.1 wt. % U-235, 5-year cooled – Outer sixteen assemblies in the HSM and TC models, and
- 45 GWd/MTU, 3.3 wt. % U-235, 23-year cooled - Inner sixteen assemblies in the TC models.

The design-basis source terms for the authorized BPRAs are taken from Appendix J. The design-basis source terms cover three BPRA designs: (1) B&W 15x15 Burnable Absorber Assemblies with up to 2 cycles burnup and 5-year cooled, (2) WE 17x17 Pyrex Burnable Absorber, 2-24 Rodlets with up to 2 cycles burnup and 10-year cooled, and (3) WE 17x17 WABA Burnable Absorber, 3-24 Rodlets with up to 2 cycles burnup and 10-year cooled. The properties used to calculate the design-basis source terms for the authorized BPRAs are reproduced in Table M.5-2.

The methodology, assumptions, and criteria used in this evaluation are summarized in the following subsections.

M.5.1 Discussion and Results

The maximum dose rates due to 32 design-basis PWR fuel assemblies with BPRAs in the NUHOMS®-32PT DSC loaded into the Standardized NUHOMS®-HSM are summarized in Table M.5-3 for both the 100-ton and 125-ton design configurations. Table M.5-4 provides maximum and surface average dose rates on the HSM loaded with the NUHOMS®-32PT DSC for both the 100-ton and 125-ton design configurations. Table M.5-5 provides a summary of the dose rates on and around the TC for canister transfer for 100- and 125-ton configurations.

A discussion of the method used to determine the design-basis fuel and BPRA source terms is included in Section M.5.2. The model specification and shielding material densities are given in Section M.5.3. The method used to determine the dose rates due to 32 design-basis fuel assemblies with BPRAs in the NUHOMS®-32PT DSC design configurations is provided in Section M.5.4. Thermal and radiological source terms are calculated with the SAS2H/ORIGEN-S modules of SCALE 4.4 [5.1] for the fuel. The shielding evaluation is performed with the DORT [5.2] code with the CASK-81 cross section library [5.3]. Sample input files used for calculating neutron and gamma source terms and dose rates are included in Section M.5.5.1.

M.5.2 Source Specification

Thermal and radiological source terms are calculated with the SAS2H/ORIGEN-S modules of SCALE 4.4 [5.1] for the fuel. The SAS2H/ORIGEN-S results are used to develop the fuel qualification tables listed in Table M.2-5 through Table M.2-14 and the design-basis fuel source terms suitable for use in the shielding calculations. The thermal and radiological source terms for the BPRAs are taken from Appendix J.

The B&W 15x15 assembly is the bounding fuel assembly design for shielding purposes because it has the highest initial heavy metal loading as compared to the 14x14, other 15x15, and 17x17 fuel assemblies which are also authorized contents of the NUHOMS®-32PT DSC. In addition, the maximum Co59 content of the hardware regions for each assembly type is less than that of the B&W 15x15 Mark B fuel assembly. The neutron flux during reactor operation is peaked in the in-core region of the fuel assembly and drops off rapidly outside the in-core region. Much of the fuel assembly hardware is outside of the in-core region of the fuel assembly. To account for this reduction in neutron flux, the fuel assembly is divided into four exposure "regions." The four axial regions used in the source term calculation are: the bottom (nozzle) region, the in-core region, the (gas) plenum region, and the top (nozzle) region. The B&W 15x15 fuel assembly masses for each irradiation region are listed in Table M.5-6. The light elements that make up the various materials for the various fuel assembly materials are taken from reference [5.4] and are listed in Table M.5-7. The design-basis heavy metal weight is 0.475 MTU. These masses are irradiated in the appropriate fuel assembly region in the SAS2H/ORIGEN-S models. To account for the reduction in neutron flux outside the In-Core regions neutron flux (fluence) correction factors are applied to light element composition for each region. The neutron flux correction factors are given in Table M.5-8.

The fuel qualification tables are generated based on the decay heat limits for the various heat load zoning configurations shown in Figure M.2-1, Figure M.2-2 and Figure M.2-3. SAS2H is used to calculate the minimum required cooling time as a function of assembly initial enrichment and burnup for each decay heat limit. The total decay heat includes the contribution from the fuel as well as the hardware in the entire assembly. The fuel qualification table for fuel plus BPRAs also includes 8 watts per BPRA to account for the design-basis decay heat from the BPRAs. Because the decay heat generally increases slightly with decreasing enrichment for a given burnup, it is conservative to assume that the required cooling time for a higher enrichment assembly is the same as that for a lower enrichment assembly with the same burnup. The required cooling time for initial enrichments that fall between any two SAS2H runs are assumed to be that of the lower enrichment case results.

The design-basis source terms are defined as the burnup/initial enrichment/cooling time combination given in the fuel qualification tables that result in the maximum dose rate on the surface of the HSM and OS197/OS197H TC. The 1-D discrete ordinates code ANISN [5.5] is used to determine these design-basis source terms. Finding the burnup/initial enrichment/cooling time combinations from the fuel qualification tables and decay heat load zoning configurations that produce the maximum dose rate on the HSM roof determine the design-basis source term for the HSM shielding calculations. Similarly the design-basis source terms for the OS197/OS197H TC are determined by finding the maximum surface dose rates on the side of the cask. This

approach is consistent with the method used to determine the fuel qualification tables for the Standardized NUHOMS® canister designs described in the FSAR. The radiological source terms generated in the SAS2H/ORIGEN-2 runs are used in the ANISN evaluations to calculate the surface dose rates. Heat load configuration 2 (Figure M.2-2) produced the bounding total surface dose rate for both the HSM and TC. The HSM design-basis source terms for the outer ring of assemblies (modeled as sixteen assemblies) are from fuel with 41 GWd/MTU burnup, an initial enrichment of 3.1 wt. % U-235 and 5-years cooling. The HSM design-basis source terms for the inner sixteen assemblies are from fuel with 30 GWd/MTU burnup, and initial enrichment of 2.5 wt. % U-235 and 8-years cooling. Note that using this approach in modeling the outer ring of sixteen assemblies with the 1.2 kW source terms for all of the shielding analyses results in fairly conservative dose rates because the shielding analysis is in reality based on a 28.8 kW heat load. The TC design-basis source terms for the outer ring of assemblies (conservatively modeled as sixteen assemblies) are from fuel with 41 GWd/MTU burnup, an initial enrichment of 3.1 wt. % U-235 and 5-years cooling. The TC design-basis source terms for the inner sixteen assemblies are from fuel with 45 GWd/MTU burnup, and initial enrichment of 3.3 wt. % U-235 and 23-years cooling.

A sample SAS2H/ORIGEN-S input file for the In-Core Region for the 41 GWd/MTU, 3.1 wt. % U-235 and 5-years cooling case is listed and commented in Section M.5.5.1.

M.5.2.1 Gamma Source

Four SAS2H/ORIGEN-S runs are required for each burnup/initial enrichment/cooling time combination to determine gamma source terms for the four regions of interest for each fuel assembly; the bottom, in-core, plenum and top regions. The only difference between the runs is in Block #10 "Light Elements" of the SAS2H input and the 81$$ card in the ORIGEN-S input. Each run includes the appropriate Light Elements for the region being evaluated and the 81$$ card is adjusted to have ORIGEN-S output the total gamma source for the in-core region and only the light element source for the plenum and top nozzle regions.

The design-basis source terms for the authorized BPRA designs are taken from Appendix J of the FSAR. The design-basis source terms from Appendix J of the FSAR cover three BPRA designs 1) B&W 15x15 Burnable Absorber Assemblies with up to 2 cycles burnup and 5-year cooled, 2) WE 17x17 Pyrex Burnable Absorber, 2-24 Rodlets with up to 2 cycles burnup and 10-year cooled, and 3) WE 17x17 WABA Burnable Absorber, 3-24 Rodlets with up to 2 cycles burnup and 10-year cooled.

The SAS2H/ORIGEN-S gamma ray source is output in the CASK-81 energy group structure.

Gamma source terms for the in-core region include contributions from actinides, fission products, and activation product. The bottom, plenum and top nozzle regions include the contribution from the activation products in the specified region only. These results for the 41 GWd/MTU, 3.1 wt. % U-235 and 5-years cooling case are shown in Table M.5-9. The results for the 30 GWd/MTU, 2.5 wt. % U-235 and 8-years cooling case are shown in Table M.5-10. Finally, the results for the 45 GWd/MTU, 3.3 wt. % U-235 and 23-years cooling case are shown in Table M.5-11.

As stated above the design-basis BPRA source terms are taken from Appendix J of the FSAR and are listed in Table M.5-12.

Gamma source terms for use in the shielding models are calculated by multiplying the assembly sources by the number of assemblies in the region of interest (16) and dividing by the appropriate inner/outer heat load region volume. The appropriate assembly region volumes for both the inner and outer heat load zones are listed in Table M.5-13.

M.5.2.2 Neutron Source Term

One SAS2H/ORIGEN-S run is required for each burnup/initial enrichment/cooling time combination to determine the total neutron source terms for the in-core regions. The results for each burnup/initial enrichment/cooling time combination of interest are summarized in Table M.5-14.

Neutron source terms for use in the shielding models are calculated by multiplying the assembly sources by the number of assemblies in the in-core region of interest (16) and dividing by the appropriate in-core inner/outer heat load region volume. The appropriate assembly region volumes for both the inner and outer heat load regions are listed in Table M.5-13.

M.5.2.3 Axial Peaking

Axial peaking factors for both neutron and gamma sources in PWR fuel are taken from Reference [5.6]. These peaking factors were derived from work performed by the Department of Energy in support of its Topical Report for burnup credit [5.7]. The neutron and gamma peaking factors are shown as a function of the core height in Table M.5-15. These factors are directly applied to each DORT interval in the fuel region. Neutron peaking factors in each zone are equal to the gamma factor raised to the fourth power to correctly account for the variation of neutron source with burnup. The axial source distribution defined in Table M.5-15 introduces some level of conservatism into this calculation because the length average peaking factor of 1.06 is greater than 1.

M.5.3 Model Specification

M.5.3.1 Material Densities

With the exception of the DSC basket and fuel, all material densities are taken directly from the calculations used to support Section 7 of the FSAR.

The material weight given in Table M.5-6 for the fuel assembly and Table M.5-2 for the BPRAs are used to calculate material densities for in-core, plenum, top and bottom regions of the fuel assembly. The poison in the BPRAs is modeled as pure aluminum because it is a relatively light element with little shielding capability. In addition, while the source terms account for 32 BPRAs the material densities conservatively account for only 24 BPRAs. For the HSM axial dose rates and all of the TC calculations, only 20% of the steel plates used to form the fuel compartments is modeled in the shielding analysis. All other components of the basket such as the neutron poison material; aluminum plates, etc., have been conservatively neglected for all models. For the lateral HSM DORT shielding model only, the homogenized fuel regions also include all of the steel from the DSC basket inner fuel compartment. The zircaloy is modeled as Zr and the inconel, carbon steel and stainless steel are all modeled as Fe. This assumption has little effect on the dose rate results. The smeared active fuel region volume of the basket is the sum of the inner and outer heat load region volumes given in Table M.5-13.

In order to account for subcritical multiplication, an initial enrichment of ~4.9 wt. % U-235 is used to calculate the amount of U-235 in the shielding models. For an initial enrichment of ~4.9%, there are 23,044 grams of U-235 per assembly and 451,956 grams of U-238.

The material densities used in the various models are summarized in Table M.5-16.

M.5.4 Shielding Evaluation

Dose rate contributions from the bottom, in core, plenum and top regions, as appropriate, from 32 fuel assemblies with BPRAs are calculated with the DORT Code [5.2] at various location on and around the NUHOMS® -32PT DSCs, HSM, and OS197/OS197H TC.

The radiation shielding evaluation for the Standardized NUHOMS® System during loading, transfer and storage for the 24P and 52B canisters is discussed in Sections 3.3.5, 7.0 and 8.0 of the FSAR. The following shielding evaluation discussion specifically addresses the NUHOMS®-32PT 100-ton and 125-ton DSCs in an HSM and TC using the design-basis source terms determined in Section M.5.2.

M.5.4.1 Computer Programs

DORT [5.2] determines the fluence of particles throughout one-dimensional or two-dimensional geometric systems by solving the Boltzmann transport equation using either the method of discrete ordinates or a diffusion theory approximation. Particles can be generated by either particle interaction with the transport medium or extraneous sources incident upon the system. Anisotropic cross-sections can be expressed in a Legendre expansion of arbitrary order.

The DORT code implements the discrete ordinates method as its primary mode of operation. Balance equations are solved for the flow of particles moving in a set of discrete directions in each cell of a space mesh and in each group of a multigroup energy structure. Iterations are performed until all implicitness in the coupling of cells, directions, groups, and source regeneration is resolved.

DORT was chosen for this application because of its ability to solve two dimensional, cylindrical, deep penetration radiation transport problems similar to the NUHOMS® System.

M.5.4.2 Spatial Source Distribution

The source components are:

- The neutron sources due to the active fuel regions of the inner sixteen and outer sixteen fuel assemblies,
- The gamma source due to the active fuel regions of the inner sixteen and outer sixteen fuel assemblies,
- The gamma source due to the plenum regions of the inner sixteen and outer sixteen fuel assemblies,
- The gamma source due to the top regions of the inner sixteen and outer sixteen fuel assemblies,
- The gamma source due to the bottom region of the inner sixteen and outer sixteen fuel assemblies,

- The gamma source due to the 32 BPRAs in the active fuel region,
- The gamma source due to the 32 BPRAs in the plenum region, and
- The gamma source due to the 32 BPRAs in the top region.

The U-235 fission spectrum is input into the 1* array of the DORT input file to account for subcritical multiplication, increasing the neutron source in the active fuel region. Axial peaking is accounted for in the active fuel region by inputting a relative flux factor at each node in the 97* array. The flux factor data is discussed in Section M.5.2.3.

M.5.4.3 Cross Section Data

The cross-section data used in this analysis is taken from the CASK-81 22 neutron, 18 gamma-ray energy group, coupled cross-section library [5.3]. CASK-81 is an industry standard cross-section library compiled for performing calculations of spent fuel shipping casks and is distributed by ORNL/RSIC. The cross-section data allows coupled neutron/gamma-ray dose rate evaluation to be made that account for secondary gamma radiation (n,γ).

Microscopic P_3 cross-sections are taken from the CASK-81 library and mixed using the GIP-PC computer program distributed with DORT [5.2] to provide macroscopic cross-sections for the materials in the cask model.

An additional element and material, "fluxdosium," is included in the cross-section data and mixing table in the GIP input file. Fluxdosium is used to provide flux-to-dose rate conversion factors as described in Section M.5.4.4 for use in activity calculations. The presence of fluxdosium in the cross-section data does not affect the actual flux calculations.

M.5.4.4 Flux-to-Dose-Rate Conversion

The flux distribution calculated by the DORT code is converted to dose rates using the same flux-to-dose rate conversion factors as those used in the FSAR from ANSI/ANS-6.1.1-1977. The flux-to-dose rate conversion factors are entered into DORT through the cross section tables as material "fluxdosium".

The dose rate at each node in the DORT models is calculated using the activity calculation feature of DORT. The "cross-section" data for "fluxdosium" is specified for the activity calculations, which determine the gamma and neutron dose rate at each node.

M.5.4.5 Methodology

The methodologies used in this calculation are similar to those previously used to support NUHOMS® storage and transportation applications. The computer codes, basic modeling techniques, and analyses are based in large part on those used to support the Sacramento Municipal Utility Districts storage license at their Rancho Seco Nuclear Generating Station (TAC Number L10017, Materials License Number SNM-2510) and to support the certificate of

compliance application for the NUHOMS®-61BT storage system [5.8]. The methodology used herein is summarized below.

1. Volumetric sources in the CASK-81 format are developed for all fuel regions using the source term data developed in Section M.5.2. Source regions include the active fuel region, bottom end fitting (including all materials below the active fuel region), plenum, and top end fitting (including all materials above the active fuel region). Sources for control components are added group-by-group to the fuel sources.

2. Suitable shielding material densities are calculated for the fuel, DSC, HSM, and TC.

3. The 2-D discrete ordinates code DORT [5.2] is used to calculate dose rates on and around the DSC, HSM, and TC. The DORT code is selected because of its ability to readily handle thick, multi-layered shields and account for streaming through both the HSM air vents and cask/DSC annulus. The simple NUHOMS® geometry lends itself to 2-D models (RZ models are used for the cask and both RZ and XY models are used for the HSM).

   The discrete-ordinates code DORT is selected over monte-carlo methods for this calculation because it can quickly and reliably calculate dose rate distributions around the cask and HSM without the need to fine-tune biasing parameters for each case addressed. Additionally, the surface or volume crossing estimators typically used in monte-carlo calculations tend to average dose rates across an area or volume and may therefore underpredict the magnitude of radiation streaming. While DORT is subject to instabilities commonly referred to as "ray effects", these tend to result in conservative overpredictions of radiation streaming.

4. The DORT results are used to calculate offsite exposures.

5. DORT models are also generated to determine the effects of accident scenarios including HSM sliding and loss of cask neutron shield.

M.5.4.6 Assumptions

The following general assumptions are used in the analyses.

Source Terms

- The primary neutron source in LWR spent fuel is the spontaneous fission of ^{244}Cm. For the ranges of exposures, enrichments, and cooling times in the fuel qualification tables, ^{244}Cm represents more than 85% of the total neutron source. The neutron spectrum is, therefore, relatively constant for the fuel parameters addressed herein. Surface gamma dose rates are calculated for the HSM and cask surfaces using the actual photon spectrum applicable for each case.

- The PWR heavy metal weight is assumed to be 0.475 MTU per assembly to bound existing PWR fuel designs.

Shielding Materials

- Source regions are homogenized (smeared) to simplify the shielding calculations.
- The HSM reinforcing bars (rebars) have been included in smeared regions in the HSM walls and roof. The rebar steel is included in three inch thick regions for each face of each HSM surface. This layered method of including the rebar in the shielding model is consistent with ANSI/ANS 6.4 Guidelines.

HSM Dose Rates

- The HSM design evaluated in this calculation dose not include the thicker door and steel vent liners described in Section 8.1.1.6.
- The DSC and fuel assemblies are positioned as close to the front door as possible to maximize the front wall dose rates.
- Cylindrical (RZ) models are used to calculate dose rates on the front and back walls. Planes of reflection are used to simulate adjacent HSMs. Although the actual HSM geometry is rectangular, the cylindrical models conservatively calculate dose rates along the centerline of each HSM surface.
- Cartesian (XY) models are used to calculate the peak dose rates on the roof and side walls. Additional cylindrical results are used to estimate the dose rate distribution along the DSC axis.
- In the cartesian models, the DSC and fuel are modeled as a square source region. The size of this region was selected to maintain the total source volume.
- Fully symmetric S16 quadrature is used for all cylindrical models. An upward biased, 210-direction quadrature set [5.9] is used for the cartesian models.
- Embedments in the HSM concrete are neglected.
- For the accident case, an HSM is assumed to slide against its neighbor, opening a 12-inch gap between HSMs.

Cask Dose Rates

- The cask and DSC are modeled in cylindrical coordinates.
- Three inches of supplemental neutron shielding and one inch of steel are placed on top of the DSC cover plates during welding.
- During the accident case, the water in the cask neutron shield is lost.

M.5.4.7 HSM Dose Rates for the 125-Ton Configuration

Dose rates on and around an HSM containing a design-basis NUHOMS®-32PT 125-ton DSC are calculated using the DORT 2-D discrete-ordinates code. Five sets of HSM models are generated, four for normal conditions and one for accident conditions. These models are discussed and listed in the following sections.

M.5.4.7.1 HSM Roof Model

The HSM roof model is a cylindrical model representing a vertical plane through the DSC, HSM front and back walls, and HSM roof. This model is used to calculate dose rates on and around the upper half of the HSM. Note that a similar model (discussed in the next section as HSM floor model) is used to calculate dose rates around the lower half of the HSM.

The geometry of the roof model is shown in Figure M.5-1. Sources and materials are as defined above.

M.5.4.7.2 HSM Floor Model

The HSM floor model is similar to the roof model. It is used to calculate the dose rates on the front and back walls of the HSM below the centerline of the DSC. The geometry of the floor model is shown in Figure M.5-2. As with the roof model, two sets of six runs are made to represent the six source regions and to model an adjacent HSM.

M.5.4.7.3 HSM Side Model

The HSM side model is similar to the roof and floor models. It is used to calculate the dose rates near the front vent and on the end shield wall. The geometry of the side model is shown in Figure M.5-3. This model represents a horizontal plane that includes the DSC centerline. As such, the air vents through the side wall (located well above and below the DSC centerline) are not included in the model. This is not expected to significantly affect the accuracy of the calculation. Previous experience loading NUHOMS® HSMs indicates that the remaining conservatisms in the shielding models, including applying bounding 2-D dose rates on 3-D surfaces, more than outweigh this modeling choice. The impact of this choice is further reduced because the vents are well away from the DSC and particles would have to scatter several times before reaching the front screen. As with the roof model, two sets of six runs are made to represent the six source regions and to model an adjacent HSM.

M.5.4.7.4 HSM Top Model

The HSM Top models represent a vertical plane that is perpendicular to the longitudinal axis of the DSC. This model is used to calculate the dose rate distribution on the HSM roof and end shield wall. This XY cartesian model is shown in Figure M.5-4. The source region is modeled as a square 49.92 inches on a side in order to keep its volume (and hence the total source strength) the same as in the cylindrical models. The radial number densities are used in this model. Two sets of five runs are made to represent the five source regions (inner neutron, outer neutron in the $\pm$ Y directions, inner gamma, outer gamma in the + X direction, outer gamma in the $\pm$ Y directions) and to model an adjacent HSM. The presence of an adjacent HSM is

approximated using a plane of reflection in the center of the air vent. This model applies to both the 125- and 100-ton configurations.

M.5.4.7.5 HSM Accident

The postulated accident condition, consisting of an HSM sliding laterally 6-inches until it contacts its neighbor, results in increased dose rates on one of the affected HSM's air vents. Accordingly, the dose rates on the roof and front face of the HSM will increase because of this event.

The shielding models for the accident case are identical to the lateral and side models discussed above, except that the vent width is increased from 6 inches to 12 inches. Reflection in the air vent is assumed for both.

M.5.4.8 HSM Models for the 100-Ton Configuration

The 100-ton NUHOMS®-32PT DSC is the same length and carries the same payload as the 125-ton configuration. The main differences are the thicknesses of the top and bottom shield plugs. Accordingly, the DORT models described in Section M.5.4.7 are modified to create models applicable to the 100-ton configuration. All other dimensions and materials are the same. The 100-ton roof model geometry is shown in Figure M.5-5.

M.5.4.9 Data Reduction and HSM Dose Rate Results for the 125-Ton Configuration

The dose rate distribution for each case is calculated by summing the neutron and gamma DORT results. Surface average dose rates for each HSM surface are calculated as discussed below.

M.5.4.9.1 Front Surface for the 125-Ton Configuration

The dose rates on the HSM front are calculated using the floor (reflection at rear), roof (reflection at rear), and side (reflection in vent) models. The dose rates along the vertical centerline of the HSM front wall, from the floor and roof models, are shown in Figure M.5-6 for the 125-ton configuration. Also shown in Figure M.5-6 (for comparison) is the total dose rate from the side model.

Based on the information in Figure M.5-6, the average dose rate on the HSM front wall is conservatively estimated by using the surface average dose rate from the floor/top models in the center region of the HSM (18.4 mrem/hr gamma and 9.2 mrem/hr neutron) and the surface average dose rate from the side model in the areas adjacent to and including the vents (146.7 mrem/hr gamma and 2.3 mrem/hr neutron). This is shown in Figure M.5-7 and conservatively assumes that the peak front vent dose rate (at the same height as the DSC centerline) exists along the entire height of the front vent. The resulting maximum and average dose rates on the HSM front wall are shown in Table M.5-4.

M.5.4.9.2 Back Surface for the 125-Ton Configuration

The dose rates on the HSM rear shield wall are calculated using the floor and roof models (no reflection, rear shield wall included). Note that the side model results are bounded by the floor/roof models on the rear shield wall. The dose rates along the vertical centerline of the HSM front wall, from the floor and roof models, are shown in Figure M.5-8 for the 125-ton configuration. The surface average dose rate on the rear shield wall is conservatively estimated using the surface-average results from the floor and roof models (these results are taken on the DSC centerline). The rear shield wall maximum and average dose rates are shown in Table M.5-4.

M.5.4.9.3 Roof Surface for the 125-Ton Configuration

The HSM roof dose rates are calculated using the top and roof models. The top model provides the peak dose rates across the width of the HSM as shown in Figure M.5-9 (top model with adjacent HSM shown) for the 125-ton configuration. The roof model results, which are shown in Figure M.5-10 and are orthogonal to those in Figure M.5-9, are used to estimate an overall average on the HSM roof. The length-average dose rates from the top model (as shown in Figure M.5-9) are 73.7 mrem/hr and 1.36 mrem/hr for gammas and neutrons, respectively. Figure M.5-11 shows the geometry used in calculating surface area average dose rates. The resulting roof dose rates are listed in Table M.5-4.

M.5.4.9.4 End Shield Wall Surface for the 125-Ton Configuration

The HSM end shield wall dose rates are calculated using the top and side models. The top model provides the peak dose rates down the side of the end shield wall. The side model results, which are orthogonal to those in the top model, are used to estimate an overall average on the HSM end shield wall. The average dose calculation is performed in the same manner as was used on the HSM roof. The length-average dose rates from the lateral model are 2.5 mrem/hr and 0.088 mrem/hr for gammas and neutrons, respectively. Because the top model is a cross-section at the center of the DSC, these are the peak "average" dose rates along the DSC length. By multiplying these results by the ratio of average to centerline from the side model, an overall surface average dose rate can be estimated (refer to Figure M.5-11). The resulting end shield wall dose rates are listed in Table M.5-4.

M.5.4.9.5 HSM Accident Case for the 125-Ton Configuration

The accident dose rates are calculated using the models described in Section M.5.4.7.5. The resulting dose rates are tabulated in Table M.5-17.

M.5.4.10 HSM Dose Rates for the 100-Ton Configuration

The HSM dose rate results are summarized in Table M.5-4 for the 100-ton configuration.

M.5.4.10.1 Front Surface for the 100-Ton Configuration

The dose rate results are shown in Table M.5-4 and Figure M.5-12.

M.5.4.10.2 Back Surface for the 100-Ton Configuration

The dose rate results are shown in Table M.5-4 and Figure M.5-13.

M.5.4.10.3 Roof Surface for the 100-Ton Configuration

The dose rate results are shown in Table M.5-4 and Figure M.5-14 and Figure M.5-15.

M.5.4.10.4 End Shield Wall Surface for the 100-Ton Configuration

The dose rate results are shown in Table M.5-4.

M.5.4.10.5 HSM Accident Case for the 100-Ton Configuration

The dose rate results are shown in Table M.5-17.

M.5.4.11 TC Dose Rates for the 125-Ton Configuration

The NUHOMS® OS197/OS197H cask containing a NUHOMS®-32PT 125-ton DSC is modeled in cylindrical coordinates using 29 material zones as shown in Figure M.5-16. The materials used in zones 18-26 shown in Figure M.5-16 are varied to model the various welding and decontamination cases.

All cask cases use the same DORT model, with only the materials assigned to each zone being varied. The onsite transfer case, listed and commented below, includes all cask and DSC covers (zones 18, 19, 21-26), air in the DSC cavity (air versus helium has no effect on the results), air in the cask/DSC annulus (zones 7 and 16), and water in the neutron shield cavity (zone 9). The decontamination model includes water only in the cask/DSC annulus (all the way to the top of the DSC - zones 7 and 16), no water in the DSC cavity or neutron shield, and both the DSC and cask top covers removed. In the welding models, the DSC cavity is empty and the annulus is drained 12 inches below the top of the DSC. The inner cover welding case includes the DSC inner top cover (zone 18) and supplemental shielding consisting of three inches of NS-3 (zones 19 and 20, some NS-3 neglected for simplicity) and one inch of steel (zone 21). The outer cover welding case is identical except that the DSC outer cover (zone 19) is installed as well (supplemental NS-3 in zones 20-22, steel in zone 23).

M.5.4.11.1 Transfer Operations for 125-Ton Configuration

The cask normal operation (onsite transfer) dose rate results for 125-ton configuration are summarized in Table M.5-5 and Figure M.5-17. The results are applicable to most activities performed outside the plant reactor building. The relatively high dose rate on the cask bottom surface is due to the area with reduced shielding directly below the DSC grapple ring. The peak along the cask side near its top end is due to the presence of control components in the fuel assemblies.

M.5.4.11.2 Decontamination Operations for 125-Ton Configuration

The results from the cask decontamination models for 125-ton configuration are shown in Figure M.5-18.

M.5.4.11.3 Inner Cover Welding for 125-Ton Configuration

The dose rates during inner cover welding for 125-ton configuration are shown in Figure M.5-19.

M.5.4.11.4 Outer Cover Welding for 125-Ton Configuration

The dose rates during outer cover welding for 125-ton configuration are shown inFigure M.5-20.

M.5.4.12 Cask Dose Rates for 100-Ton Configuration

The dose rates around the NUHOMS® TC with the 100-ton configuration are calculated in the same manner as was used for the heavier 125-ton configuration. Data reduction for each case is summarized in the following sections. The 100-ton configuration geometry is shown in Figure M.5-21.

The shielding configurations are identical to those listed in Section M.5.4.11.1. However, some lifting operations of the 100-ton configuration are performed without water in the cavity and neutron shield. For these operations, the accident case results will be used to estimate dose rates and occupational exposures.

M.5.4.12.1 Transfer Operations for 100-Ton Configuration

The cask normal operation (onsite transfer) dose rate results are summarized in Table M.5-5 and Figure M.5-22. The results are applicable to most activities performed outside the plant reactor building. The relatively high dose rate on the cask bottom surface is due to the area with reduced shielding directly below the DSC grapple ring. The peak along the cask side near its top end is due to the presence of control components in the fuel assemblies.

M.5.4.12.2 Decontamination Operations for 100-Ton Configuration

The dose rates during the cask decontamination for 100-ton configuration are shown in Figure M.5-23.

M.5.4.12.3 Inner Cover Welding 100-Ton Configuration

The dose rates during inner cover welding for 100-ton configuration are shown in Figure M.5-24.

M.5.4.12.4 Outer Cover Welding 100-ton Configuration

The dose rates during outer cover welding for 100-ton configuration are shown in Figure M.5-25.

M.5.5 Appendix

Section M.5.5.1 includes a sample SAS2H/ORIGEN-S code input file used for the NUHOMS®-32PT system. The DORT code models are described in Section M.5.4. Section M.5.5.2 includes a sample DORT code input file used for the HSM analysis. Section M.5.5.3 includes a sample DORT code input file used for the TC analysis.

M.5.5.1 Sample SAS2H/ORIGEN-S Input File

M.5.6 References

5.1 Oak Ridge National Laboratory, RSIC Computer Code Collection, "SCALE: A Modular Code System for Performing Standardized Computer Analysis for Licensing Evaluations for Workstations and Personal Computers," NUREG/CR-0200, Revision 6, ORNL/NUREG/CSD-2/V2/R6.

5.2 "DORT-PC - Two-Dimensional Discrete Ordinates Transport Code System," CCC-532, Oak Ridge National Laboratory, RSIC Computer Code Collection, Version 2.10.1, October 1991.

5.3 CASK-81 - 22 Neutron, 18 Gamma-Ray Group, P3, Cross Sections for Shipping Cask Analysis," DLC-23, Oak Ridge National Laboratory, RSIC Data Library Collection, June 1987.

5.4 Ludwig, S.B., and J.P. Renier, "Standard- and Extended-Burnup PWR and BWR Reactor Models for the ORIGEN2 Computer Code," ORNL/TM-11018 Oak Ridge National Laboratory, December 1989.

5.5 "ANISN-ORNL - One-Dimensional Discrete Ordinates Transport Code System with Anisotropic Scattering", CCC-254, Oak Ridge National Laboratory, RSIC Computer Code Collection, April 1991.

5.6 NUHOMS® MP187 Multi-Purpose Cask Transportation Safety Analysis Report," Revision 10, NRC Docket Number 71-9255.

5.7 "Topical Report on Actinide-Only Burnup Credit for PWR Spent Nuclear Fuel Packages", Rev. 0, Office of Civilian Radioactive Waste Management, DOE/RW-0472 Rev. 0, May 1995.

5.8 "Addition of 61BT DSC to Standardized NUHOMS® System," Amendment No. 3, Revision 1 to NUHOMS® CoC 1004, January 2001, TAC No. L23137 (Amendment under review at NRC).

5.9 Jenal, J. P., P. J. Erickson, W. A. Rhoades, D. B. Simpson, and M. L. Williams, "The Generation of a Computer Library for Discrete Ordinates Quadrature Sets," ORNL/TM-6023, Oak Ridge National Laboratory, October 1977.

Table M.5-1
PWR Fuel Assembly Design Characteristics[3]

Assembly Class	B&W 15x15	WE 17x17	CE 15x15	WE 15x15	CE 14x14	WE 14x14
DSC Configuration	**Max Unirradiated Length (in)**					
32PT-S100	165.75	165.75	165.75	165.75	165.75	165.75
32PT-L100	171.71[1]	171.71[1]	171.71	171.71	171.71	171.71
32PT-S125	165.75	165.75	165.75	165.75	165.75	165.75
32PT-L125	171.71[1]	171.71[1]	171.71	171.71	171.71	171.71
Fissile Material	UO_2	UO_2	UO_2	UO_2	UO_2	UO_2
Maximum MTU/assembly[2]	0.475	0.475	0.475	0.475	0.475	0.475
Maximum Number of Fuel Rods	208	264	216	204	176	179
Maximum Number of Guide/ Instrument Tubes	17	25	9	21	5	17

(1) Maximum Assembly + BPRA Length (unirradiated)
(2) The maximum MTU/assembly is based on the shielding analysis. The listed value is higher than the actual.
(3) Maximum Co-59 content in the Top End Fitting Region is 15.6 grams per assembly.
Maximum Co-59 content in the Plenum Region is 5.0 grams per assembly.
Maximum Co-59 content in the In-Core Region is 24.7 grams per assembly.
Maximum Co-59 content in the Bottom Region is 12.8 grams per assembly.

Table M.5-2
Burnable Poison Rod Assembly Weight Data

Component Name: B&W 15 X 15 Burnable Absorber Assembly
Burnup: 2 cycle, 5-year cooled

Region	SS304 (Kgs)	Inconel-750 (Kgs)	Poison (Kgs)	Zr-4 (Kgs)
Top	3.602	0.058	0	0
Plenum	1.068	0	0.724	1.197
Core	2.468	0	9.146	11.98

Component Name: WE 17 X 17 Pyrex Burnable Absorber, 2 - 24 Rodlets (Worst Case)
Burnup: 2 cycle, 10-year cooled

Region	SS304 (Kgs)	Inconel-718 (Kgs)	Poison (Kgs)	Zr-4 (Kgs)
Top	2.62	0.42	0	0
Plenum	2.85	0	0	0
Core	11.9	0	5.08	0

Component Name: WE 17 X 17 WABA Burnable Absorber, 3 - 24 Rodlets (Worst Case)
Burnup: 2 cycle, 10-year cooled

Region	SS304 (Kgs)	Inconel-718 (Kgs)	Poison (Kgs)	Zr-4 (Kgs)
Top	2.95	0	0	0
Plenum	2.76	0	0	2.61
Core	0	0	2.5	14.8

Table M.5-3
Dose Rates Due to the 32 PWR Fuel Assemblies with BPRAs

Dose Rate Location	100-Ton Design Configuration			125-Ton Design Configurations		
	Gamma (mrem/hr)	Neutron (mrem/hr)	Total[1] (mrem/hr)	Gamma (mrem/hr)	Neutron (mrem/hr)	Total[1] (mrem/hr)
HSM Roof (centerline)	38.6	0.6	39.2	38.6	0.6	39.2
HSM Roof Birdscreen	1201	16.9	1218	1201	16.9	1218
HSM End Shield Wall Surface	5.4	0.2	5.6	5.4	0.2	5.6
HSM Door Exterior Surface (centerline)	158	36.3	185	77.5	28.1	99.3
HSM Front Birdscreen	780	7.3	788	745	6.8	752
HSM Back Shield Wall	1.45	0.05	1.50	1.37	0.05	1.41
Centerline Top DSC Cover Plate w/3"ns3+1" steel Dry Welding	123	18.7	142	36.7	15.0	51.7
Outer Edge Centerline Top DSC (Peak Annulus)	3834	132	3966	1458	111	1569
Cask Surface (Radial) Contact Normal Condition	784	261	950	784	259	947
3 ft from Cask Surface (Radial) Normal Condition	293	98.3	391	293	97.8	390
Cask Surface (Radial) Contact Accident Condition	1070	3780	4640	1070	3770	4630
Cask Top Axial Surface	94.8	32.6	107	37.7	27.5	48.7
Cask Bottom Axial Surface	758[2]	957[2]	1707[2]	193[3]	770[3]	960[3]

Notes:

(1) Gamma and Neutron peaks do not always occur at same location therefore the total is not always the sum of the gamma plus neutron.

(2) The peak bottom surface dose rate is directly below the grapple ring cut out in the bottom of the cask. The bottom average dose rates, including the grapple area, are 170 mrem/hr gamma, 115 mrem/hr neutron for a total average dose rate of 285 mrem/hr.

(3) The peak bottom surface dose rate is directly below the grapple ring cut out in the bottom of the cask. The bottom average dose rates, including the grapple area, are 48.7 mrem/hr gamma, 92.3 mrem/hr neutron for a total average dose rate of 141 mrem/hr.

Table M.5-4
Summary of HSM Dose Rates

Surface	Dose Rate Component	100-Ton Configuration		125-Ton Configurations	
		Maximum Dose Rate (mrem/hr)	Surface Average Dose Rate (mrem/hr)	Maximum Dose Rate (mrem/hr)	Surface Average Dose Rate (mrem/hr)
Rear[1]	Gamma	1.45	0.48	1.37	0.45
	Neutron	0.05	0.02	0.05	0.02
Front	Gamma	780	86.4	745	56.2
	Neutron	7.3	9.1	6.8	7.2
Roof	Gamma	1201	54.5	1201	54.2
	Neutron	16.9	0.75	16.9	0.75
Side[1]	Gamma	5.4	1.7	5.4	1.7
	Neutron	0.2	0.05	0.2	0.05

[1] Includes 24 inch shield wall.

Table M.5-5
Summary of Onsite TC Dose Rates (Maximum[1])

	100-Ton Configuration			125-Ton Configuration		
	Cask Surface			Cask Surface		
	Side (mrem/hr)	Top (mrem/hr)	Bottom[2] (mrem/hr)	Side (mrem/hr)	Top (mrem/hr)	Bottom[3] (mrem/hr)
Neutron	2.61E+02	3.26E+01	9.57E+02	2.59E+02	2.75E+01	7.70E+02
Gamma	7.84E+02	9.48E+01	7.58E+02	7.84E+02	3.77E+01	1.93E+02
Total	9.50E+02	1.07E+02	1.71E+03	9.47E+02	4.87E+01	9.60E+02
	1-Meter from Cask Surface			1-Meter from Cask Surface		
	Side (mrem/hr)	Top (mrem/hr)	Bottom[2] (mrem/hr)	Side (mrem/hr)	Top (mrem/hr)	Bottom[3] (mrem/hr)
Neutron	9.83E+01	1.13E+01	8.95E+01	9.78E+01	9.58E+00	7.14E+01
Gamma	2.93E+02	1.69E+01	1.85E+02	2.93E+02	6.63E+00	4.92E+01
Total	3.91E+02	2.52E+01	2.74E+02	3.90E+02	1.45E+01	1.21E+02
	2-Meters from Cask Surface			2-Meters from Cask Surface		
	Side (mrem/hr)	Top (mrem/hr)	Bottom[2] (mrem/hr)	Side (mrem/hr)	Top (mrem/hr)	Bottom[3] (mrem/hr)
Neutron	5.26E+01	4.47E+00	2.83E+01	5.24E+01	3.80E+00	2.25E+01
Gamma	1.73E+02	8.87E+00	8.07E+01	1.73E+02	3.28E+00	2.15E+01
Total	2.26E+02	1.31E+01	1.09E+02	2.25E+02	6.82E+00	4.40E+01

(1) Gamma and Neutron peaks do not always occur at same location therefore the total is not always the sum of the gamma plus neutron.

(2) This bottom surface dose rate is directly below the grapple ring cut out in the cask bottom. The bottom surface average dose rates are 115 neutron, 170 gamma or 285 total. These average dose rates include the area below grapple ring cutout in the cask.

(3) This bottom surface dose rate is directly below the grapple ring cut out in the cask bottom. The bottom surface average dose rates are 92.3 neutron, 48.7 gamma or 141 total. These average dose rates include the area below grapple ring cutout in the cask.

Table M.5-6
PWR Fuel Assembly Materials Weights

Item	Material	Average Weight (Kg/assembly)
In-Core Region		
Cladding	Zircaloy-4	108.16
Guide Tubes	Zircaloy-4	8.0
Instrument Tubes	Zircaloy-4	0.64
Spacers	Inconel-718	4.9
Grid Supports	Zircaloy-4	0.64
Plenum Region		
Cladding	Zircaloy	8.8
Springs	Stainless Steel	0.02
Spacer	Inconel-718	1.04
Top Region		
Top Nozzle	Stainless Steel	7.48
End Plugs & Nuts	Stainless Steel	0.57
Springs Retainer	Stainless Steel	0.91
Hold-Down Springs	Inconel-718	1.80
Bottom Region		
Bottom Spacer	Inconel-718	1.30
Lower Nuts	Stainless Steel	0.15
Bottom Nozzle	Stainless Steel	8.16

Table M.5-7
Elemental Composition of LWR Fuel-Assembly Structural Materials

Element	Atomic Number	Material Composition, grams per kg of material				
		Zircaloy-4	Inconel-718	Inconel X-750	Stainless Steel 304	UO_2 Fuel
H	1	1.30E-02	-	-	-	-
Li	3	-	-	-	-	1.00E-03
B	5	3.30E-04	-	-	-	1.00E-03
C	6	1.20E-01	4.00E-01	3.99E-01	8.00E-01	8.94E-02
N	7	8.00E-02	1.30E+00	1.30E+00	1.30E+00	2.50E-02
O	8	9.50E-01	-	-	-	1.34E+02
F	9	-	-	-	-	1.07E-02
Na	11	-	-	-	-	1.50E-02
Mg	12	-	-	-	-	2.00E-03
Al	13	2.40E-02	5.99E+00	7.98E+00	-	1.67E-02
Si	14	-	2.00E+00	2.99E+00	1.00E+01	1.21E-02
P	15	-	-	-	4.50E-01	3.50E-02
S	16	3.50E-02	7.00E-02	7.00E-02	3.00E-01	-
Cl	17	-	-	-	-	5.30E-03
Ca	20	-	-	-	-	2.00E-03
Ti	22	2.00E-02	7.99E+00	2.49E+01	-	1.00E-03
V	23	2.00E-02	-	-	-	3.00E-03
Cr	24	1.25E+00	1.90E+02	1.50E+02	1.90E+02	4.00E-03
Mn	25	2.00E-02	2.00E+00	6.98E+00	2.00E+01	1.70E-03
Fe	26	2.25E+00	1.80E+02	6.78E+01	6.88E+02	1.80E-02
Co	27	1.00E-02	4.69E+00	6.49E+00	8.00E-01	1.00E-03
Ni	28	2.00E-02	5.20E+02	7.22E+02	8.92E+01	2.40E-02
Cu	29	2.00E-02	9.99E-01	4.99E-01	-	1.00E-03
Zn	30	-	-	-	-	4.03E-02
Zr	40	9.79E+02	-	-	-	-
Nb	41	-	5.55E+01	8.98E+00	-	-
Mo	42	-	3.00E+01	-	-	1.00E-02
Ag	47	-	-	-	-	1.00E-04
Cd	48	2.50E-04	-	-	-	2.50E-02
In	49	-	-	-	-	2.00E-03
Sn	50	1.60E+01	-	-	-	4.00E-03
Gd	64	-	-	-	-	2.50E-03
Hf	72	7.80E-02	-	-	-	-
W	74	2.00E-02	-	-	-	2.00E-03
Pb	82	-	-	-	-	1.00E-03
U	92	2.00E-04	-	-	-	1.00E+03

Table M.5-8
Flux Correct Factors By Assembly Region

Assembly Region	Flux Factor
Bottom	0.20
In-Core	1.00
Plenum	0.20
Top	0.10

Table M.5-9
Gamma Source Term for 41 GWd/MTU, 3.1 wt. % U-235 and 5-Year Cooled Fuel

CASK-81 Energy Group	E_{upper} (MeV)	E_{mean} (MeV)	Top Region γ/s/assembly	Plenum Region γ/s/assembly	Fuel Region γ/s/assembly	Bottom Region γ/s/assembly
23	10	9	0.000E+00	0.000E+00	2.240E+05	0.000E+00
24	8	7.25	0.000E+00	0.000E+00	1.055E+06	0.000E+00
25	6.5	5.75	0.000E+00	0.000E+00	5.378E+06	0.000E+00
26	5	4.5	0.000E+00	0.000E+00	1.340E+07	0.000E+00
27	4	3.5	1.201E-09	1.380E-09	1.271E+10	1.735E-09
28	3	2.75	8.880E+04	5.535E+04	1.019E+11	1.444E+05
29	2.5	2.25	5.727E+07	3.570E+07	2.979E+12	9.311E+07
30	2	1.83	7.069E+02	4.866E+02	1.324E+12	1.155E+03
31	1.66	1.495	2.413E+12	1.504E+12	6.474E+13	3.923E+12
32	1.33	1.165	8.545E+12	5.326E+12	2.219E+14	1.389E+13
33	1	0.9	5.889E+10	5.157E+09	3.559E+14	1.076E+11
34	0.8	0.7	9.223E+08	2.682E+10	2.515E+15	1.330E+09
35	0.6	0.5	2.916E+07	4.978E+10	8.362E+14	4.741E+07
36	0.4	0.35	4.601E+08	2.522E+09	7.088E+13	7.480E+08
37	0.3	0.25	3.511E+08	7.843E+08	1.006E+14	5.707E+08
38	0.2	0.15	7.064E+09	1.386E+10	3.548E+14	1.149E+10
39	0.1	0.075	2.928E+10	1.888E+10	4.367E+14	4.760E+10
40	0.05	0.025	2.352E+11	2.778E+11	2.123E+15	3.826E+11

Table M.5-10
Gamma Source Term for 30 GWd/MTU, 2.5 wt. % U-235 and 8-Year Cooled Fuel

CASK-81 Energy Group	E_{upper} (MeV)	E_{mean} (MeV)	Top Region γ/s/assembly	Plenum Region γ/s/assembly	Fuel Region γ/s/assembly	Bottom Region γ/s/assembly
23	10	9	0.000E+00	0.000E+00	7.919E+04	0.000E+00
24	8	7.25	0.000E+00	0.000E+00	3.730E+05	0.000E+00
25	6.5	5.75	0.000E+00	0.000E+00	1.902E+06	0.000E+00
26	5	4.5	0.000E+00	0.000E+00	4.739E+06	0.000E+00
27	4	3.5	3.457E-11	4.016E-11	1.174E+09	5.032E-11
28	3	2.75	4.744E+04	2.959E+04	9.325E+09	7.711E+04
29	2.5	2.25	3.059E+07	1.908E+07	1.873E+11	4.973E+07
30	2	1.83	1.652E-02	2.174E+01	1.709E+11	2.643E-02
31	1.66	1.495	1.289E+12	8.040E+11	2.625E+13	2.096E+12
32	1.33	1.165	4.565E+12	2.847E+12	1.044E+14	7.421E+12
33	1	0.9	4.583E+09	1.161E+09	8.634E+13	8.097E+09
34	0.8	0.7	7.120E+08	9.788E+09	1.336E+15	1.026E+09
35	0.6	0.5	1.553E+07	1.734E+10	1.827E+14	2.525E+07
36	0.4	0.35	2.458E+08	9.316E+08	2.809E+13	3.995E+08
37	0.3	0.25	1.877E+08	3.140E+08	4.217E+13	3.050E+08
38	0.2	0.15	3.775E+09	5.647E+09	1.442E+14	6.136E+09
39	0.1	0.075	1.564E+10	9.968E+09	1.977E+14	2.543E+10
40	0.05	0.025	1.247E+11	1.167E+11	1.001E+15	2.025E+11

Table M.5-11
Gamma Source Term for 45 GWd/MTU, 3.3 wt. % U-235 and 23-Year Cooled Fuel

CASK-81 Energy Group	E_{upper} (MeV)	E_{mean} (MeV)	Top Region γ/s/assembly	Plenum Region γ/s/assembly	Fuel Region γ/s/assembly	Bottom Region γ/s/assembly
23	10	9	0.000E+00	0.000E+00	1.492E+05	0.000E+00
24	8	7.25	0.000E+00	0.000E+00	7.026E+05	0.000E+00
25	6.5	5.75	0.000E+00	0.000E+00	3.582E+06	0.000E+00
26	5	4.5	0.000E+00	0.000E+00	8.926E+06	0.000E+00
27	4	3.5	1.507E-11	1.829E-11	2.651E+07	2.259E-11
28	3	2.75	8.942E+03	5.575E+03	2.528E+08	1.454E+04
29	2.5	2.25	5.767E+06	3.595E+06	3.396E+09	9.375E+06
30	2	1.83	4.318E-03	3.072E+01	6.492E+10	6.219E-03
31	1.66	1.495	2.430E+11	1.515E+11	4.859E+12	3.951E+11
32	1.33	1.165	8.605E+11	5.365E+11	2.974E+13	1.399E+12
33	1	0.9	9.882E+08	1.116E+09	1.220E+13	1.430E+09
34	0.8	0.7	9.861E+08	1.425E+09	1.236E+15	1.420E+09
35	0.6	0.5	2.928E+06	5.651E+08	2.120E+13	4.760E+06
36	0.4	0.35	4.640E+07	5.428E+07	2.529E+13	7.542E+07
37	0.3	0.25	3.584E+07	2.904E+07	3.769E+13	5.817E+07
38	0.2	0.15	7.152E+08	5.551E+08	1.231E+14	1.162E+09
39	0.1	0.075	2.960E+09	1.858E+09	1.922E+14	4.810E+09
40	0.05	0.025	2.555E+10	1.779E+10	9.237E+14	4.131E+10

Table M.5-12
Design-Basis BPRA Source Terms

CASK-81 Energy Group	E_{upper} (MeV)	E_{mean} (MeV)	Top Region γ/s/BPRA	Plenum Region γ/s/BPRA	Fuel Region γ/s/BPRA
23	10	9	0.000E+00	0.000E+00	0.000E+00
24	8	7.25	0.000E+00	0.000E+00	0.000E+00
25	6.5	5.75	0.000E+00	0.000E+00	0.000E+00
26	5	4.5	0.000E+00	0.000E+00	0.000E+00
27	4	3.5	3.947E-15	6.520E-14	7.266E-18
28	3	2.75	3.942E+04	2.179E+04	5.495E+05
29	2.5	2.25	1.274E+07	7.040E+06	1.775E+08
30	2	1.83	9.577E+01	8.812E+01	9.153E-05
31	1.66	1.495	7.138E+11	3.946E+11	9.953E+12
32	1.33	1.165	1.690E+12	9.340E+11	2.356E+13
33	1	0.9	6.951E+09	4.180E+09	4.699E+09
34	0.8	0.7	4.155E+09	1.783E+10	2.835E+09
35	0.6	0.5	3.235E+07	3.854E+10	4.508E+08
36	0.4	0.35	7.014E+07	2.431E+10	9.776E+08
37	0.3	0.25	2.060E+08	3.482E+09	2.872E+09
38	0.2	0.15	1.217E+09	3.534E+09	1.697E+10
39	0.1	0.075	8.191E+09	5.176E+09	1.142E+11
40	0.05	0.025	8.484E+10	1.382E+11	1.170E+12

Table M.5-13
Inner/Outer Heat Load Zone Region Volumes

Assembly Region	Inner Heat Load Region (cm^3)	Outer Heat Load Region (cm^3)
Bottom	$1.710x10^5$	$1.710x10^5$
In-Core	$2.905x10^6$	$2.905x10^6$
Plenum	$1.783x10^5$	$1.783x10^5$
Top	$1.272x10^5$	$1.272x10^5$

Table M.5-14
Total Neutron Source Summary

CASK-81 Energy Group	E_{upper} (MeV)	E_{mean} (MeV)	Normalized Cm-244 Fission Source	Neutrons per second per assembly		
				41GWd/MTU 3.1 wt. % 5-year cooled	30 GWd/MTU 2.5 wt. % U-235 8-year cooled	45 GWd/MTU 3.3 wt. % U-235 23-year cooled
1	1.49E+01	1.36E+01	2.018E-04	7.848E+04	2.787E+04	5.263E+04
2	1.22E+01	1.11E+01	1.146E-03	4.457E+05	1.583E+05	2.989E+05
3	1.00E+01	9.09E+00	4.471E-03	1.739E+06	6.174E+05	1.166E+06
4	8.18E+00	7.27E+00	1.768E-02	6.876E+06	2.442E+06	4.611E+06
5	6.36E+00	5.66E+00	4.167E-02	1.621E+07	5.755E+06	1.087E+07
6	4.96E+00	4.51E+00	5.641E-02	2.194E+07	7.790E+06	1.471E+07
7	4.06E+00	3.54E+00	1.197E-01	4.655E+07	1.653E+07	3.122E+07
8	3.01E+00	2.74E+00	9.616E-02	3.740E+07	1.328E+07	2.508E+07
9	2.46E+00	2.41E+00	2.256E-02	8.774E+06	3.116E+06	5.884E+06
10	2.35E+00	2.09E+00	1.227E-01	4.772E+07	1.694E+07	3.200E+07
11	1.83E+00	1.47E+00	2.110E-01	8.206E+07	2.914E+07	5.503E+07
12	1.11E+00	8.30E-01	1.794E-01	6.977E+07	2.478E+07	4.679E+07
13	5.50E-01	3.31E-01	1.138E-01	4.426E+07	1.572E+07	2.968E+07
14	1.11E-01	5.72E-02	1.301E-02	5.060E+06	1.797E+06	3.393E+06
15	3.35E-03	1.97E-03	6.555E-05	2.549E+04	9.052E+03	1.710E+04
16	5.83E-04	3.42E-04	4.765E-06	1.853E+03	6.580E+02	1.243E+03
17	1.01E-04	6.50E-05	3.134E-07	1.219E+02	4.328E+01	8.173E+01
18	2.90E-05	1.96E-05	4.527E-08	1.761E+01	6.252E+00	1.181E+01
19	1.01E-05	6.58E-06	9.759E-09	3.795E+00	1.348E+00	2.545E+00
20	3.06E-06	2.09E-06	1.521E-09	5.915E-01	2.101E-01	3.967E-01
21	1.12E-06	7.67E-07	3.353E-10	1.304E-01	4.630E-02	8.745E-02
22	4.14E-07	2.12E-07	9.683E-11	3.766E-02	1.337E-02	2.525E-02
Total			**1.000E+00**	**3.889E+08**	**1.381E+08**	**2.608E+08**

Table M.5-15
Source Term Peaking Summary

Zone	Fraction of Core Height	Neutron Factor	Gamma Factor
1	0.00	0.33	0.76
2	0.05	0.78	0.94
3	0.10	1.57	1.12
4	0.20	1.57	1.12
5	0.30	1.57	1.12
6	0.40	1.57	1.12
7	0.50	1.57	1.12
8	0.60	1.57	1.12
9	0.70	1.57	1.12
10	0.80	1.46	1.10
11	0.90	0.72	0.92
12	0.95	0.24	0.70

Table M.5-16
Shielding Material Densities

Assembly Region Material Densities – Dry

Element	Atomic Number	Number Density (atoms/b-cm)				
		Fuel Radial	Fuel Axial	Top End Fitting	Plenum	Bottom End Fitting
H	1					
C	6					
N	7					
O	8	1.326E-02	1.326E-02		2.825E-05	
Na	11					
Mg	12					
Al	13	4.714E-04	4.714E-04	3.026E-05	1.101E-03	1.626E-05
Si	14					
K	19					
Ca	20					
Cr	24	1.142E-03	3.699E-04	3.928E-03	5.718E-04	2.171E-03
Fe	26	3.857E-03	1.131E-03	1.252E-02	1.452E-03	6.961E-03
Ni	28	6.197E-04	2.986E-04	2.908E-03	7.411E-04	1.561E-03
Zr	40	4.251E-03	4.251E-03		5.723E-03	
Pb	82					
U-235	92	3.251E-04	3.251E-04			
U-238	92	6.298E-03	6.298E-03			

Assembly Region Material Densities – Wet (atoms/bn-cm)

Element	Atomic Number	Number Density (atoms/b-cm)				
		Fuel Radial	Fuel Axial	Top End Fitting	Plenum	Bottom End Fitting
H	1	3.486E-02	3.486E-02	4.776E-02	3.430E-02	5.552E-02
C	6					
N	7					
O	8	3.069E-02	3.069E-02	2.388E-02	1.718E-02	2.775E-02
Na	11					
Mg	12					
Al	13	4.714E-04	4.714E-04	3.026E-05	1.101E-03	1.626E-05
Si	14					
K	19					
Ca	20					
Cr	24	1.142E-03	3.699E-04	3.928E-03	5.718E-04	2.171E-03
Fe	26	3.857E-03	1.131E-03	1.252E-02	1.452E-03	6.961E-03
Ni	28	6.197E-04	2.986E-04	2.908E-03	7.411E-04	1.561E-03
Zr	40	4.251E-03	4.251E-03		5.723E-03	
Pb	82					
U-235	92	3.251E-04	3.251E-04			
U-238	92	6.298E-03	6.298E-03			

Table M.5-16
Shielding Material Densities

(Continued)

Reinforced Concrete by HSM Region

Element	Atomic Number	Concrete Regions (atoms/bn-cm)					
		Roof Concrete	Front Concrete	Side Concrete	Rear Concrete	End Shield	Back Shield
H	1	7.261E-03	7.505E-03	7.389E-03	7.447E-03	7.277E-03	7.378E-03
C	6	0.000E+00	0.000E+00	0.000E+00	0.000E+00	0.000E+00	0.000E+00
N	7	0.000E+00	0.000E+00	0.000E+00	0.000E+00	0.000E+00	0.000E+00
O	8	4.099E-02	4.236E-02	4.171E-02	4.204E-02	4.108E-02	4.165E-02
Na	11	9.794E-04	1.012E-03	9.966E-04	1.004E-03	9.816E-04	9.951E-04
Mg	12	1.390E-04	1.436E-04	1.414E-04	1.425E-04	1.393E-04	1.412E-04
Al	13	2.233E-03	2.308E-03	2.272E-03	2.290E-03	2.238E-03	2.268E-03
Si	14	1.431E-02	1.479E-02	1.456E-02	1.467E-02	1.434E-02	1.454E-02
K	19	6.479E-04	6.697E-04	6.593E-04	6.645E-04	6.493E-04	6.583E-04
Ca	20	2.725E-03	2.817E-03	2.773E-03	2.795E-03	2.731E-03	2.769E-03
Fe	26	5.847E-03	3.195E-03	4.463E-03	3.829E-03	5.674E-03	4.579E-03

Other Shielding Materials

Element	Atomic Number	Number Density (atoms/b-cm)						
		NS-3	Concrete	Water	Air	Lead	Steel	Aluminum
H	1	4.591E-02	7.770E-03	6.687E-02				
C	6	8.252E-03						
N	7				1.980E-05			
O	8	3.780E-02	4.386E-02	3.343E-02	5.280E-06			
Na	11		1.048E-03					
Mg	12		1.487E-04					
Al	13	7.028E-03	2.389E-03					6.026E-02
Si	14	1.268E-03	1.531E-02					
K	19		6.933E-04					
Ca	20	1.484E-03	2.916E-03					
Cr	24							
Fe	26	1.063E-04	3.128E-04				8.487E-02	
Ni	28							
Zr	40							
Pb	82					3.296E-02		
U-235	92							
U-238	92							

Table M.5-17
HSM Accident Dose Rates

HSM Roof Accident Dose Rates (125-Ton Configuration)

	Neutron	Gamma	Total
Centerline	7.65E-01	4.23E+01	4.31E+01
Peak Vent	3.22E+01	2.43E+03	2.46E+03
Average	2.01E+00	1.81E+02	1.83E+02

HSM Front Accident Dose Rates (125-Ton Configuration)

	Neutron	Gamma	Total
Peak Door	2.81E+01	7.75E+01	9.93E+01
Peak Vent	1.74E+01	1.85E+03	1.87E+03
Average	7.91E+00	1.75E+02	1.83E+02

HSM Roof Accident Dose Rates (100-Ton Configuration)

	Neutron	Gamma	Total
Centerline	7.65E-01	4.23E+01	4.31E+01
Peak Vent	3.22E+01	2.43E+03	2.46E+03
Average	2.04E+00	1.82E+02	1.84E+02

HSM Front Accident Dose Rates (100-Ton Configuration)

	Neutron	Gamma	Total
Peak Door	3.63E+01	1.58E+02	1.85E+02
Peak Vent	1.79E+01	1.89E+03	1.91E+03
Average	9.74E+00	2.07E+02	2.16E+02

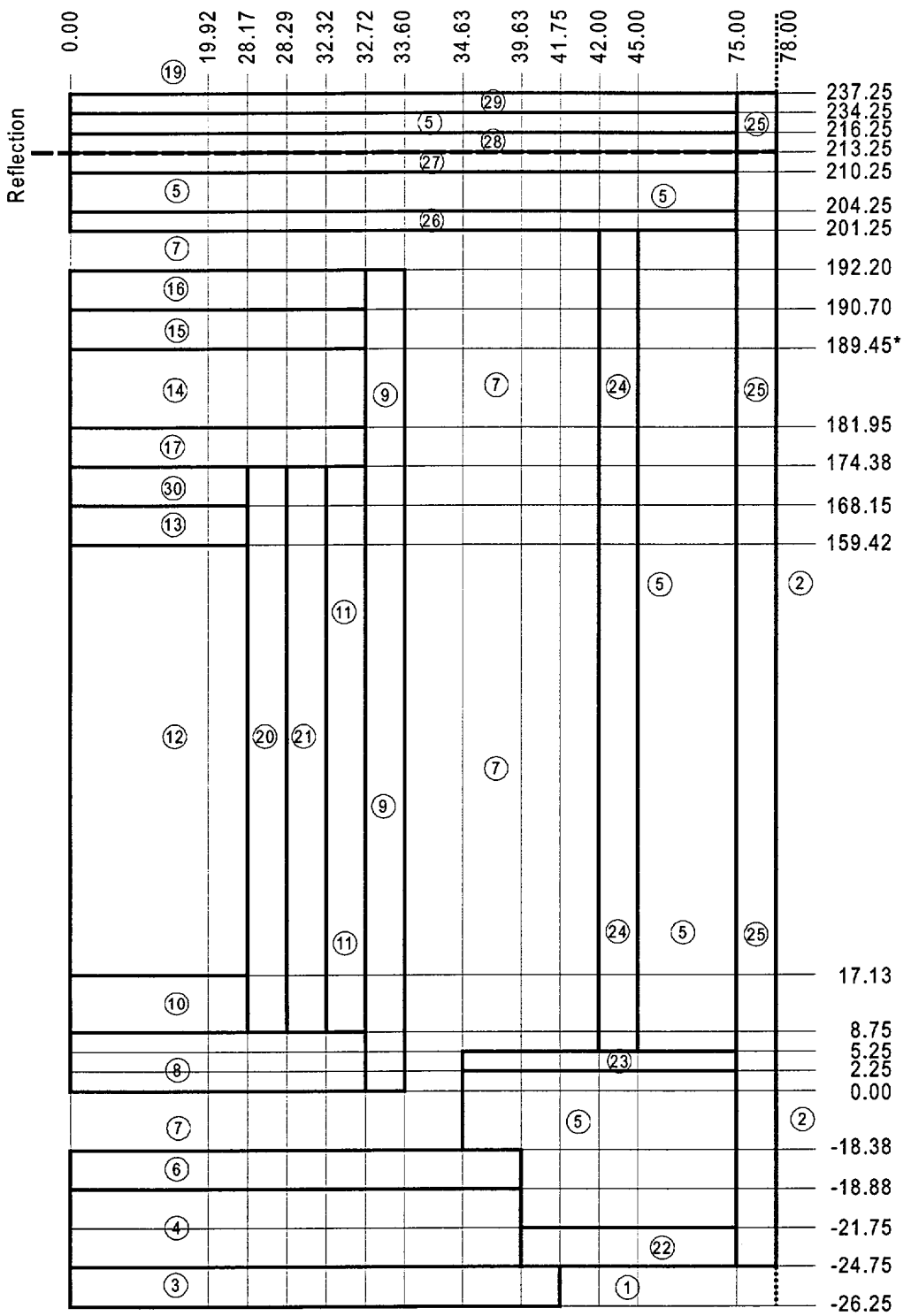

*** 189.70 used in models. This does not affect the results because regions 14 and 15 are both steel.**

Figure M.5-1
HSM Roof Model Geometry (125-Ton Configuration)

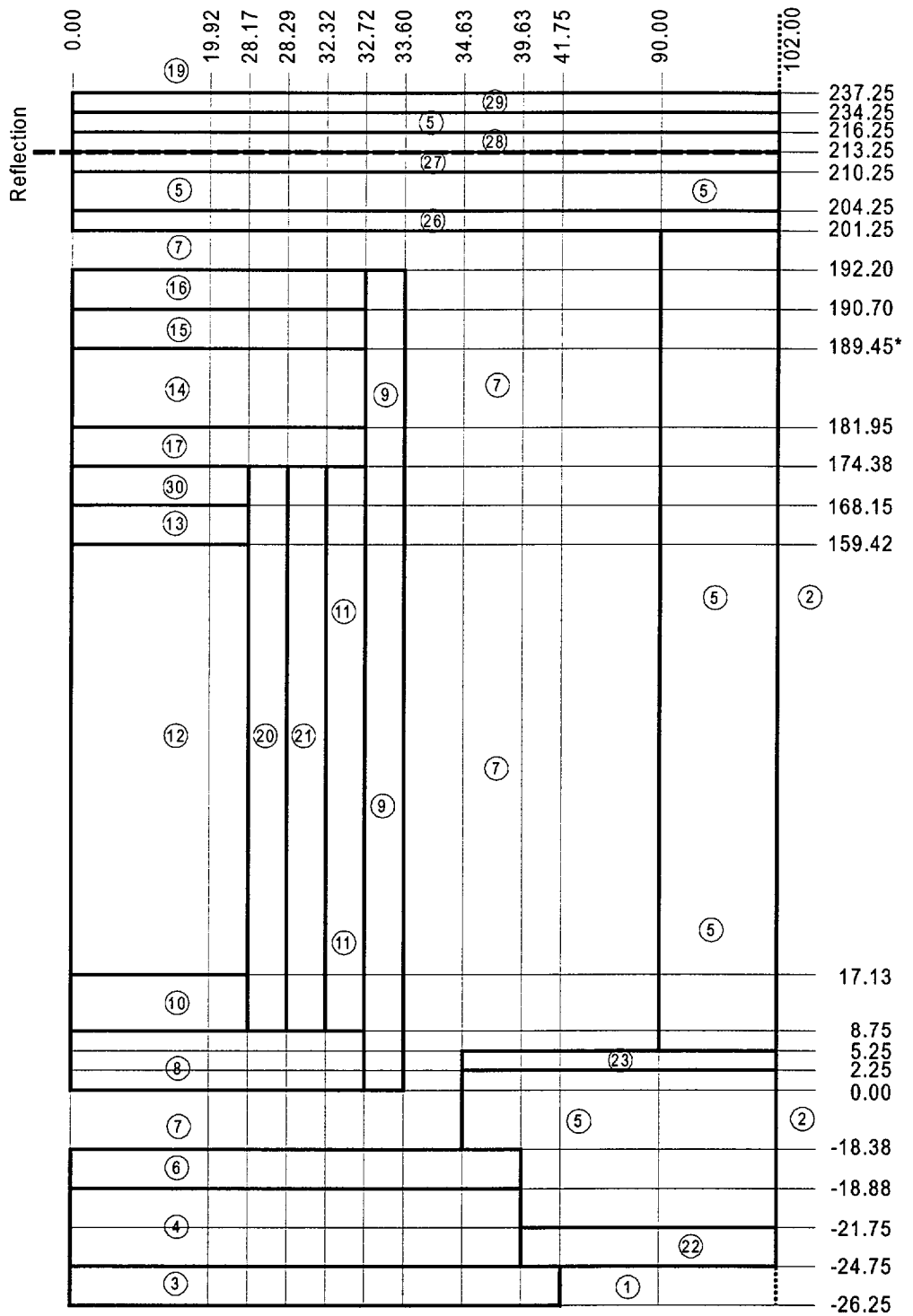

*** 189.70 used in models. This does not affect the results because regions 14 and 15 are both steel.**

Figure M.5-2
HSM Floor Model Geometry (125-Ton Configuration)

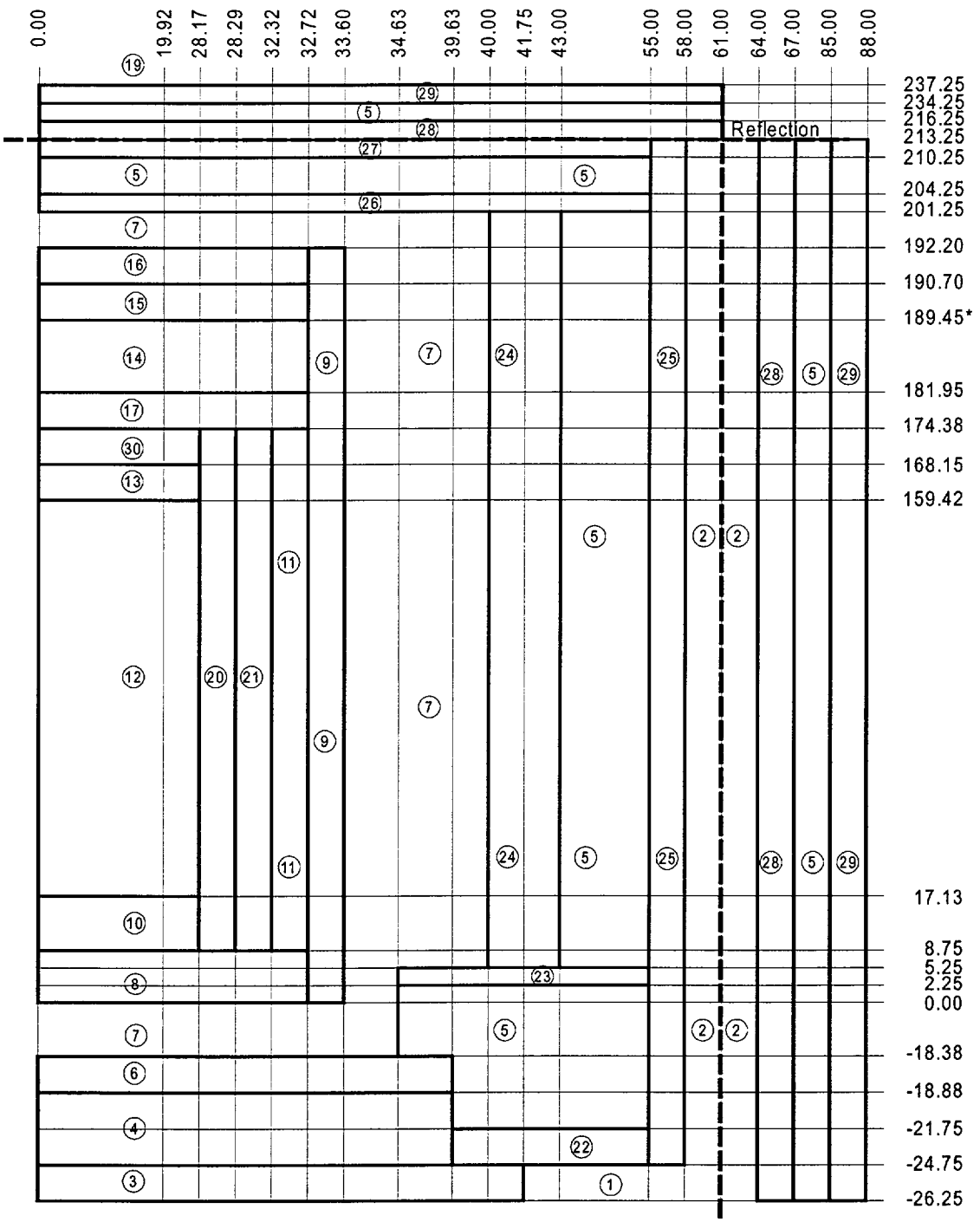

* 189.70 used in models. This does not affect the results because regions 14 and 15 are both steel.

Figure M.5-3
HSM Side Model Geometry (125-Ton Configuration)

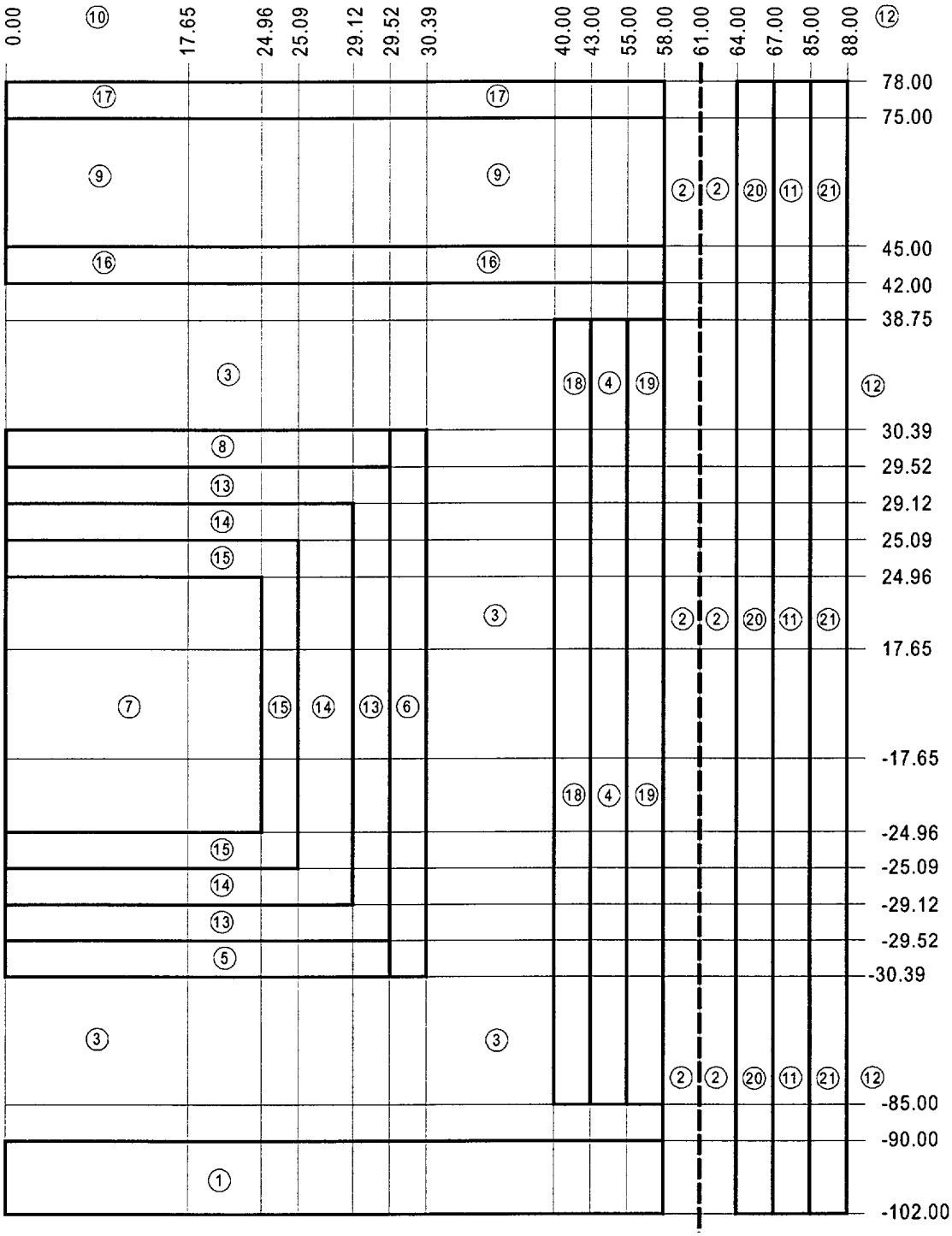

Figure M.5-4
HSM Top Model Geometry(125- and 100-Ton Configuration)

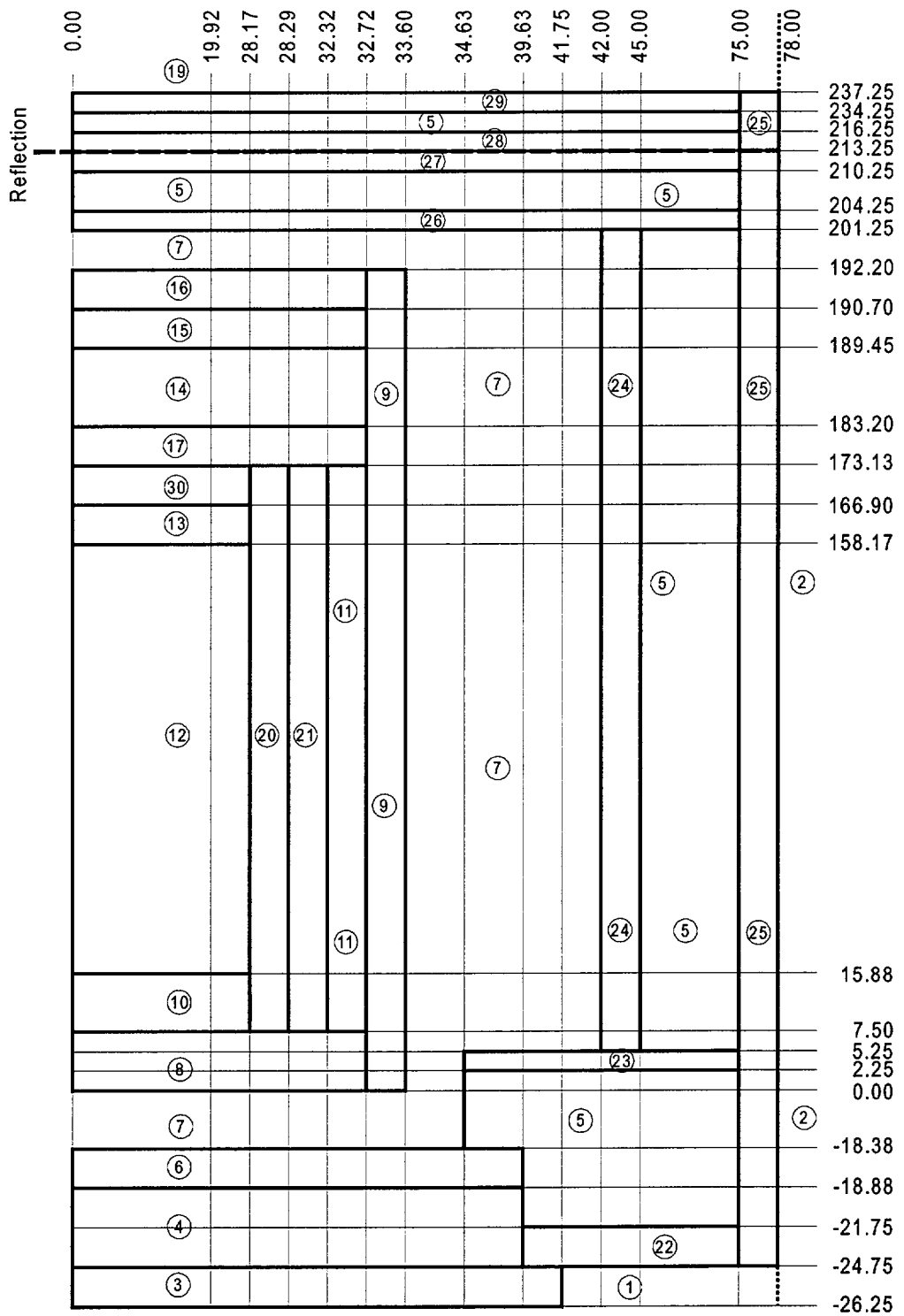

Figure M.5-5
HSM Roof Model Geometry (100-Ton Configuration)

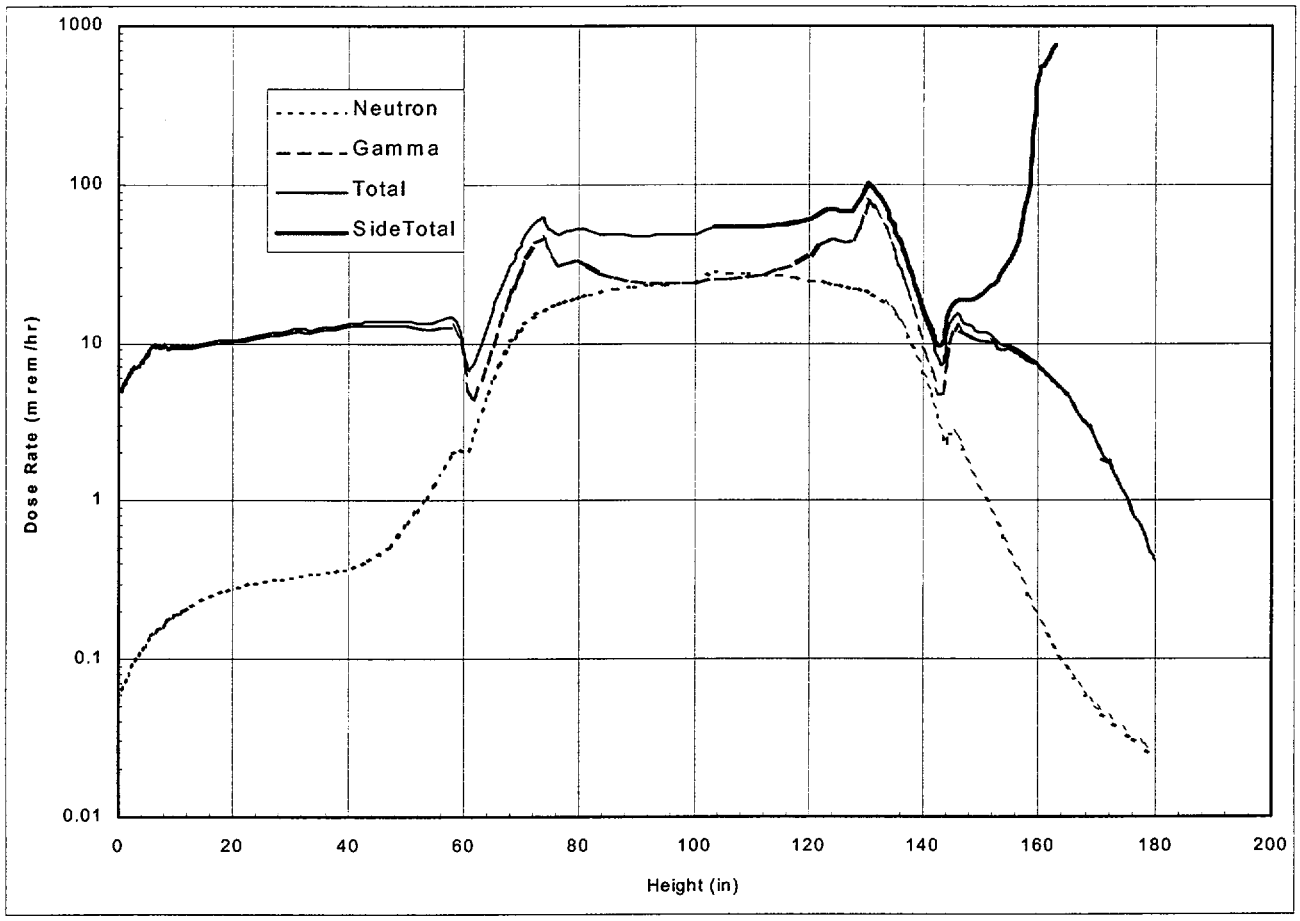

Figure M.5-6
HSM Front Wall Dose Rate Distribution (125-Ton Configuration)

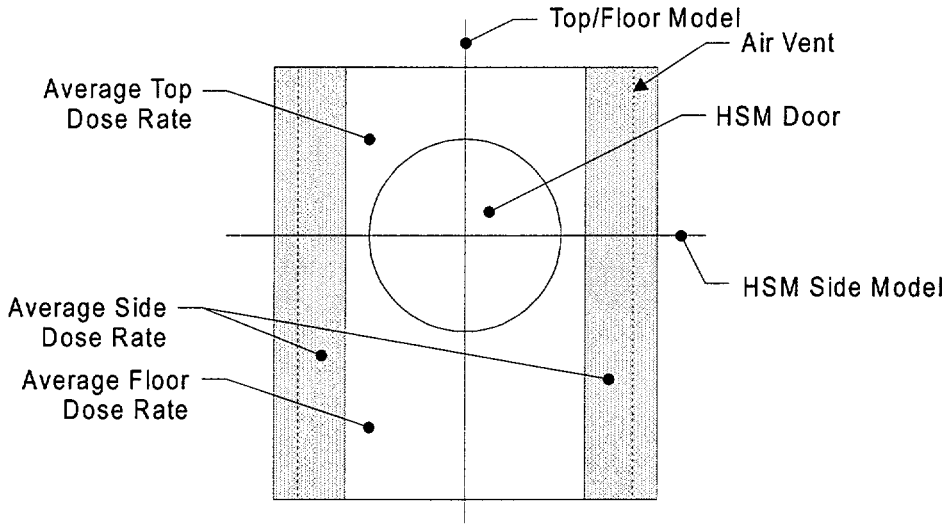

Figure M.5-7
Geometry for Front Wall Average Dose Rate Calculation

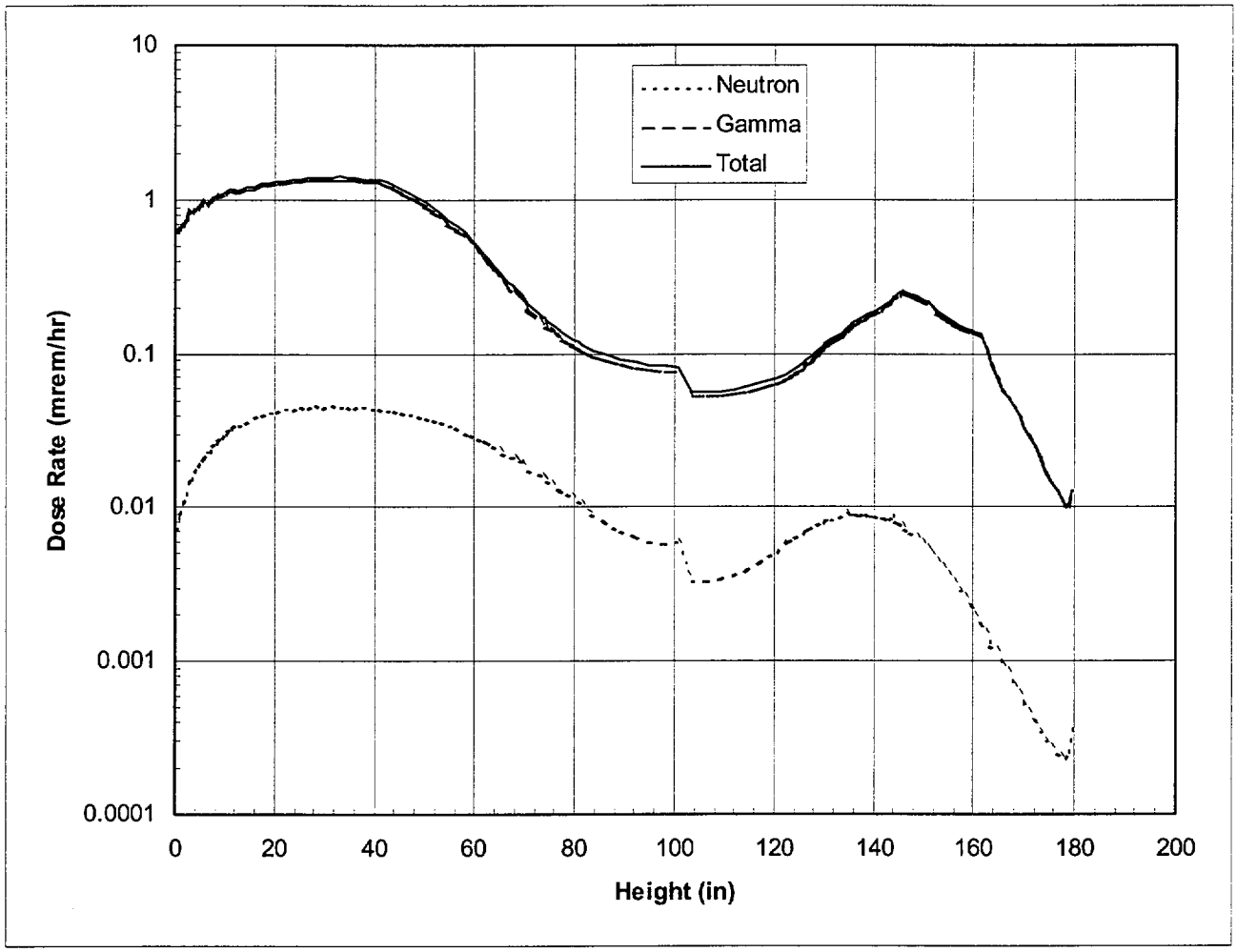

Figure M.5-8
HSM Back Wall Dose Rate Distribution (125-Ton Configuration)

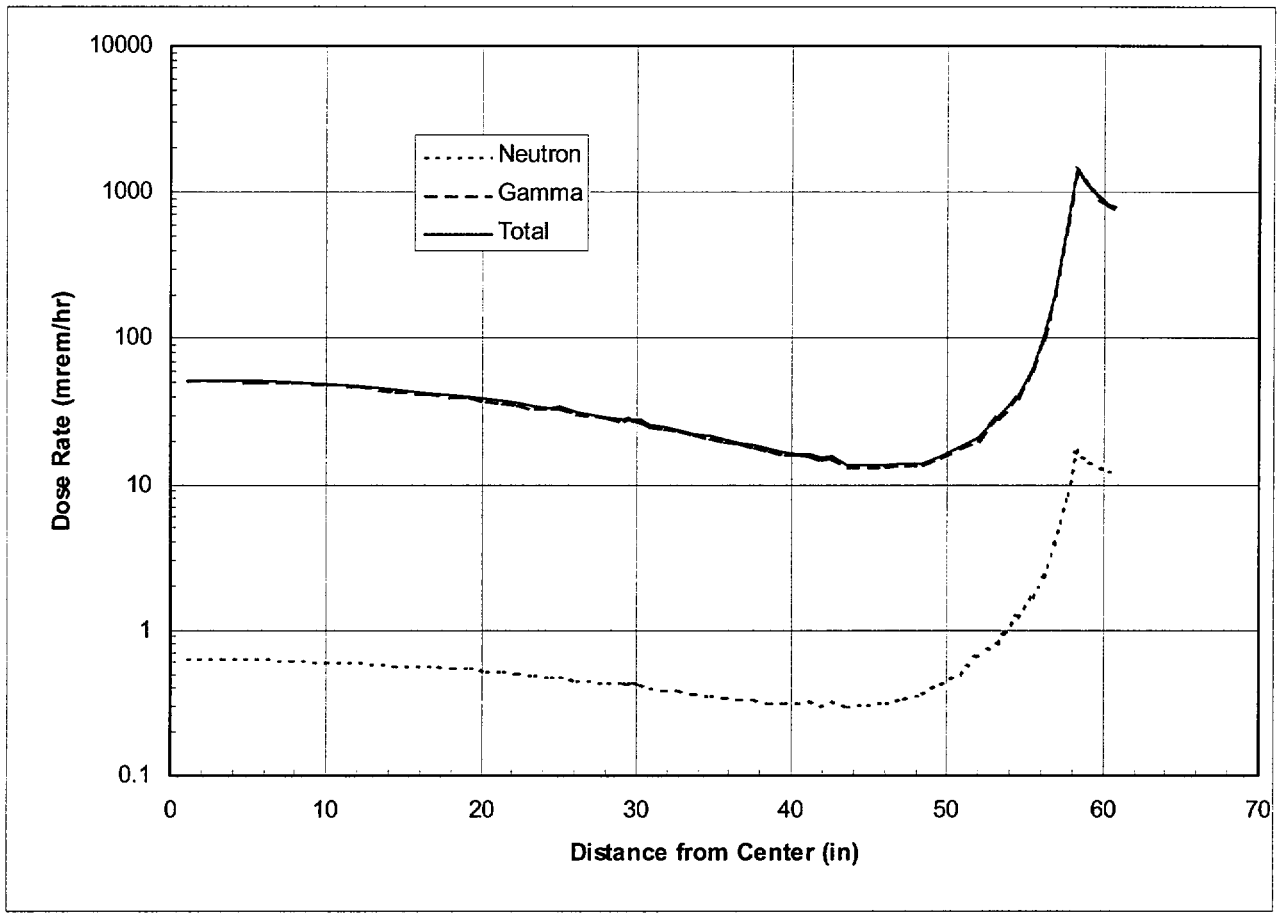

Figure M.5-9
HSM Roof Dose Rate Distribution Perpendicular to DSC Axis(125-Ton Configuration)

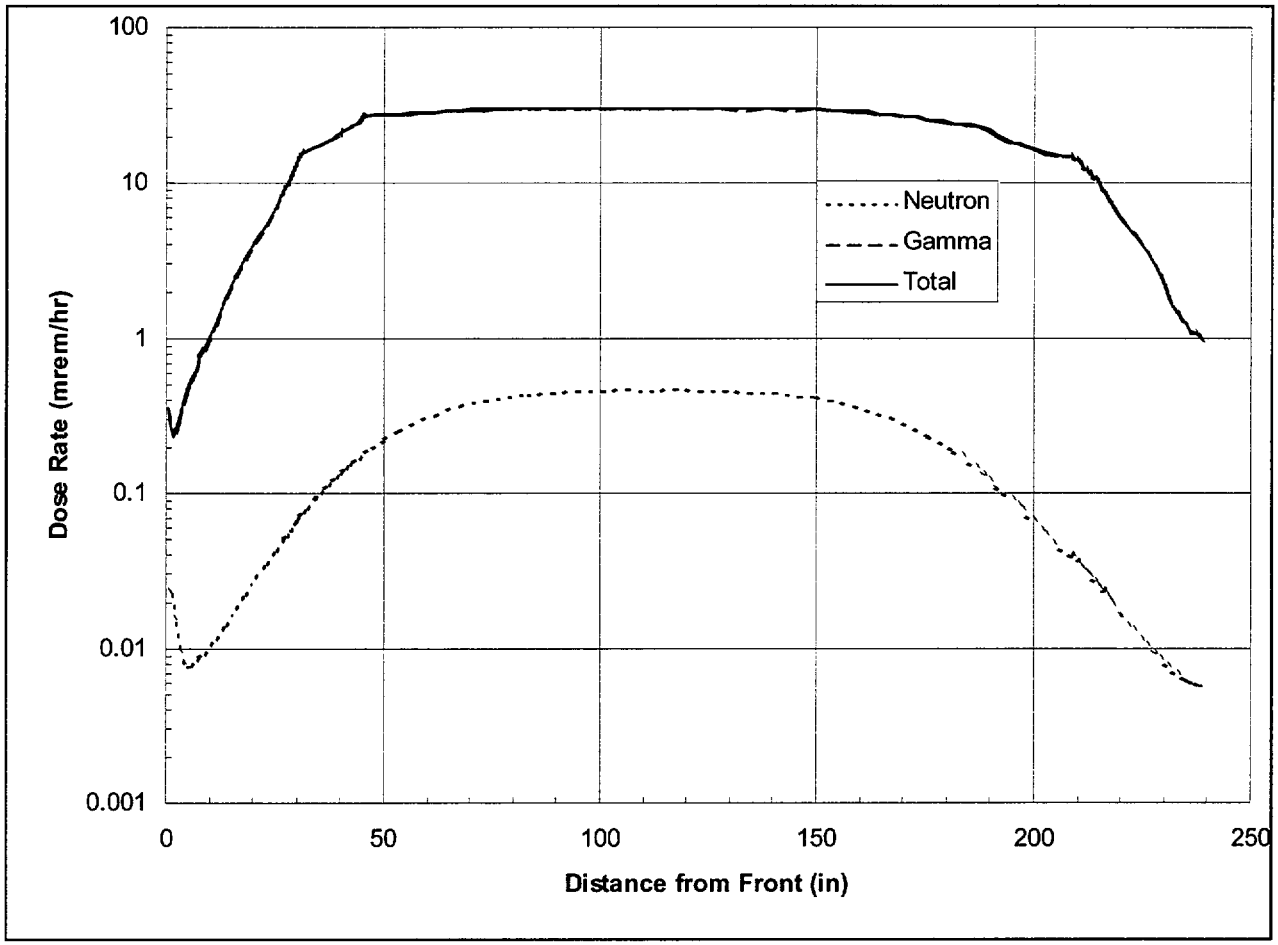

Figure M.5-10
HSM Roof Dose Rate Distribution Parallel to DSC Axis(125-Ton Configuration)

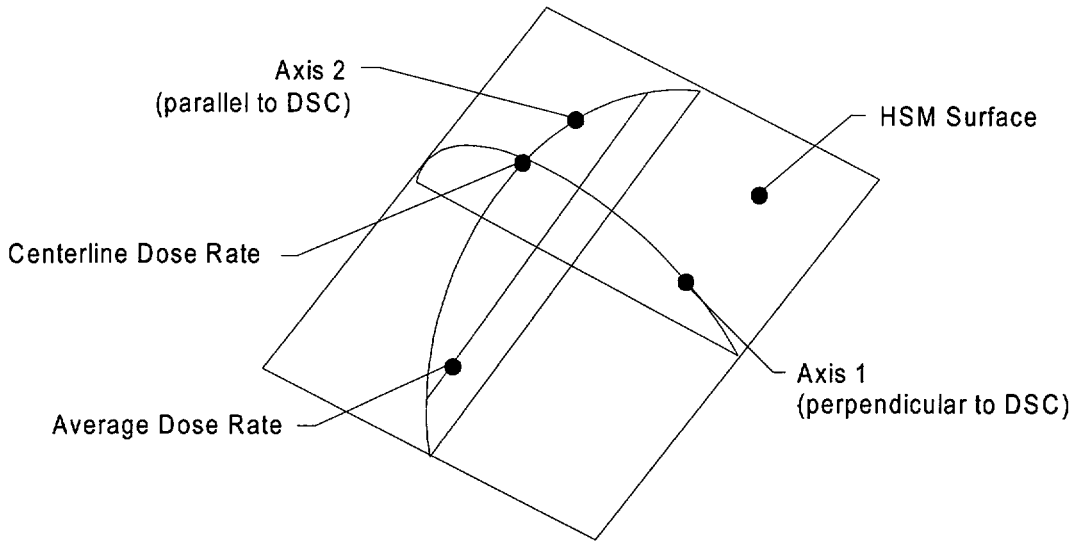

Figure M.5-11
Surface Average Calculation Geometry

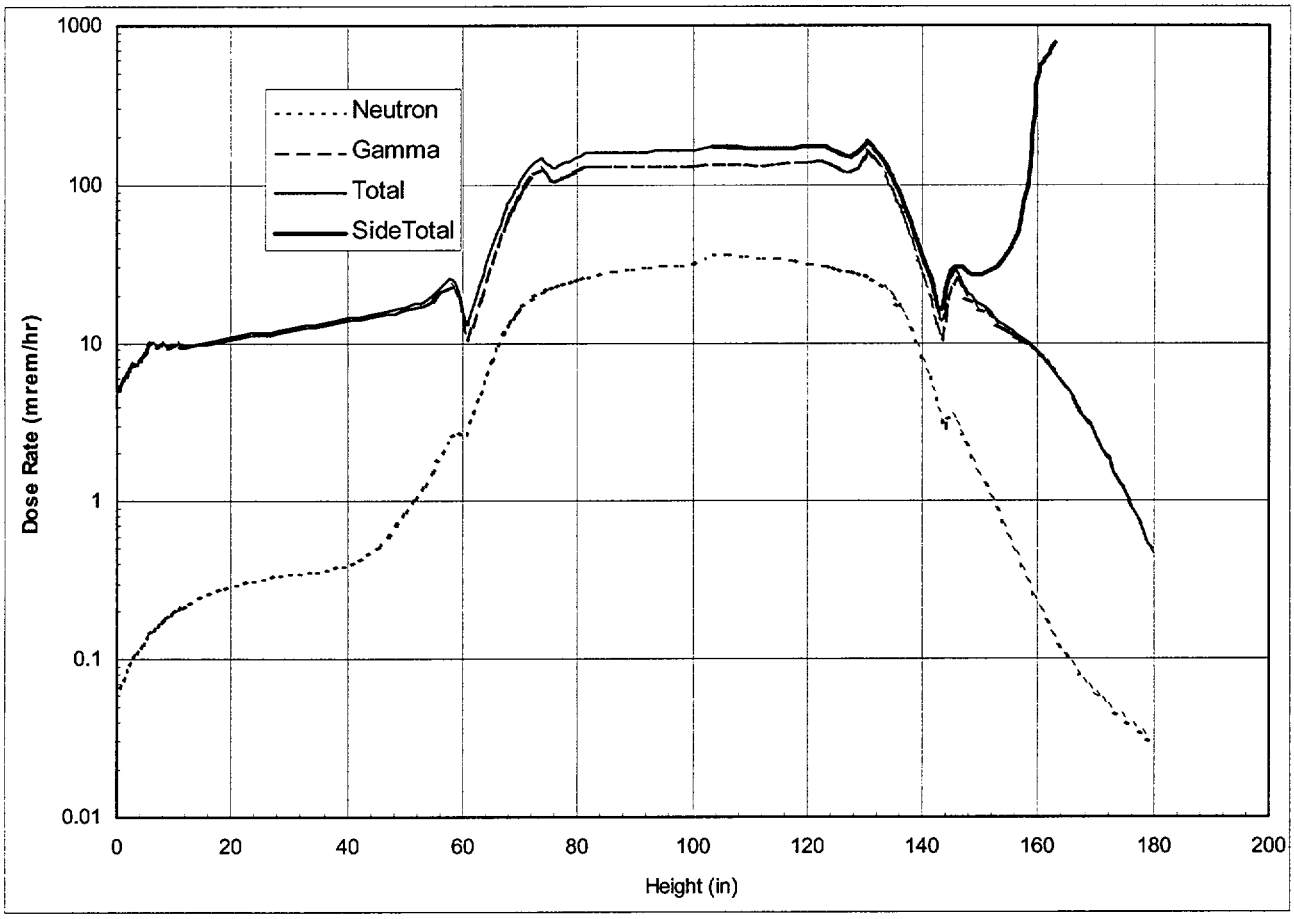

Figure M.5-12
HSM Front Wall Dose Rate Distribution (100-Ton Configuration)

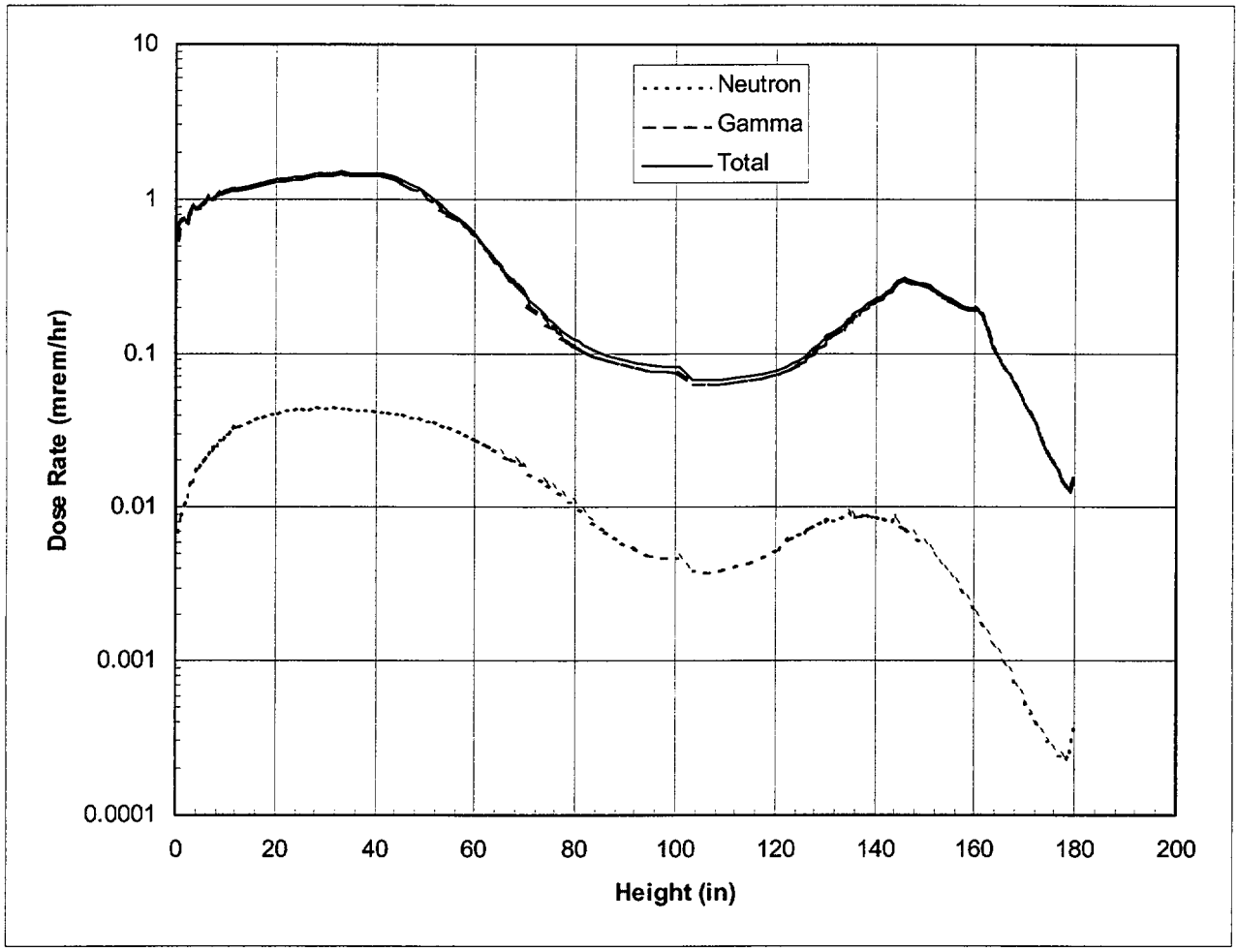

Figure M.5-13
HSM Back Wall Dose Rate Distribution (100-Ton Configuration)

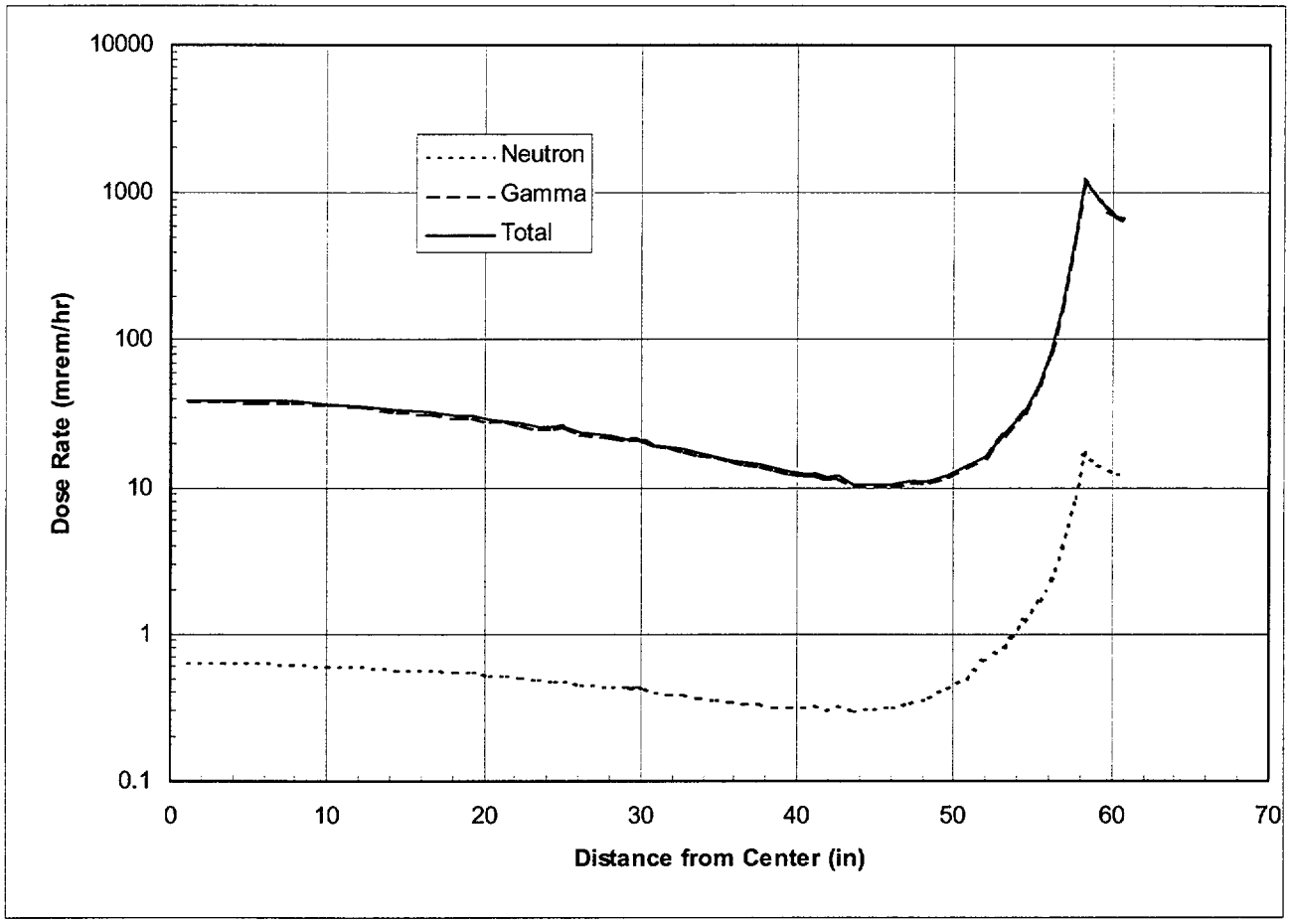

Figure M.5-14
HSM Roof Dose Rate Distribution Perpendicular to DSC Axis (100-Ton Configuration

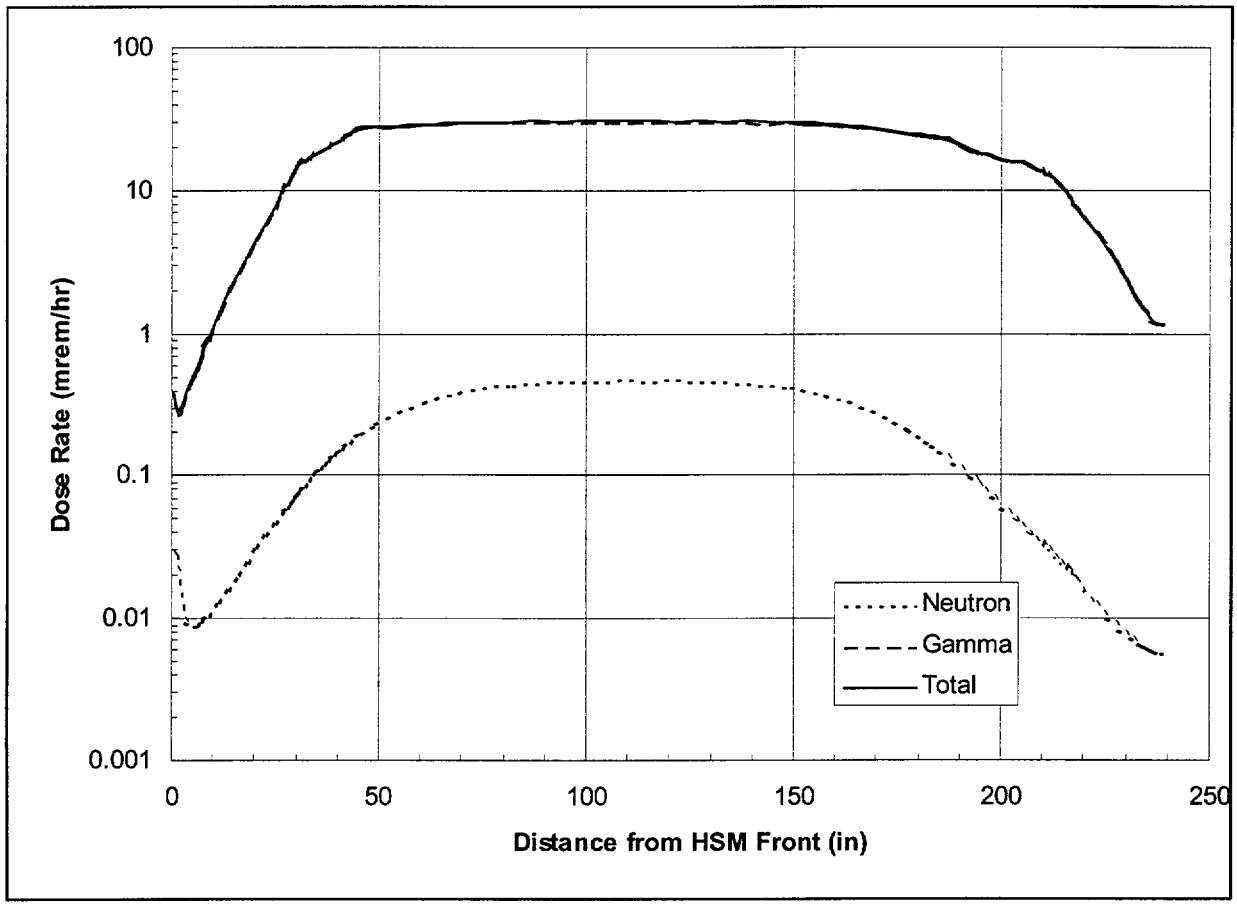

Figure M.5-15
HSM Roof Dose Rate Distribution Parallel to DSC Axis (100-Ton Configuration)

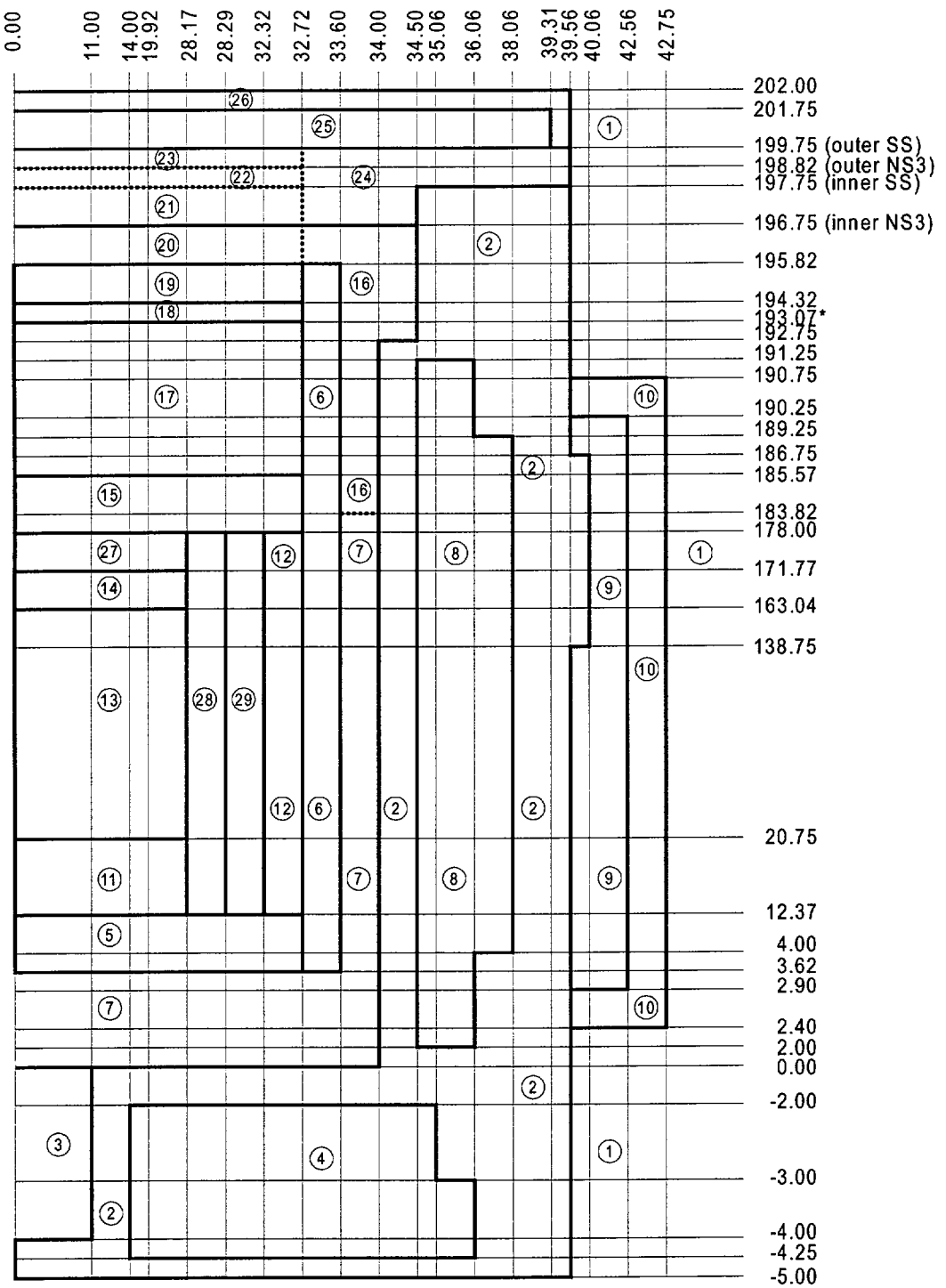

Figure M.5-16
Cask Model Geometry (125-Ton Configuration)

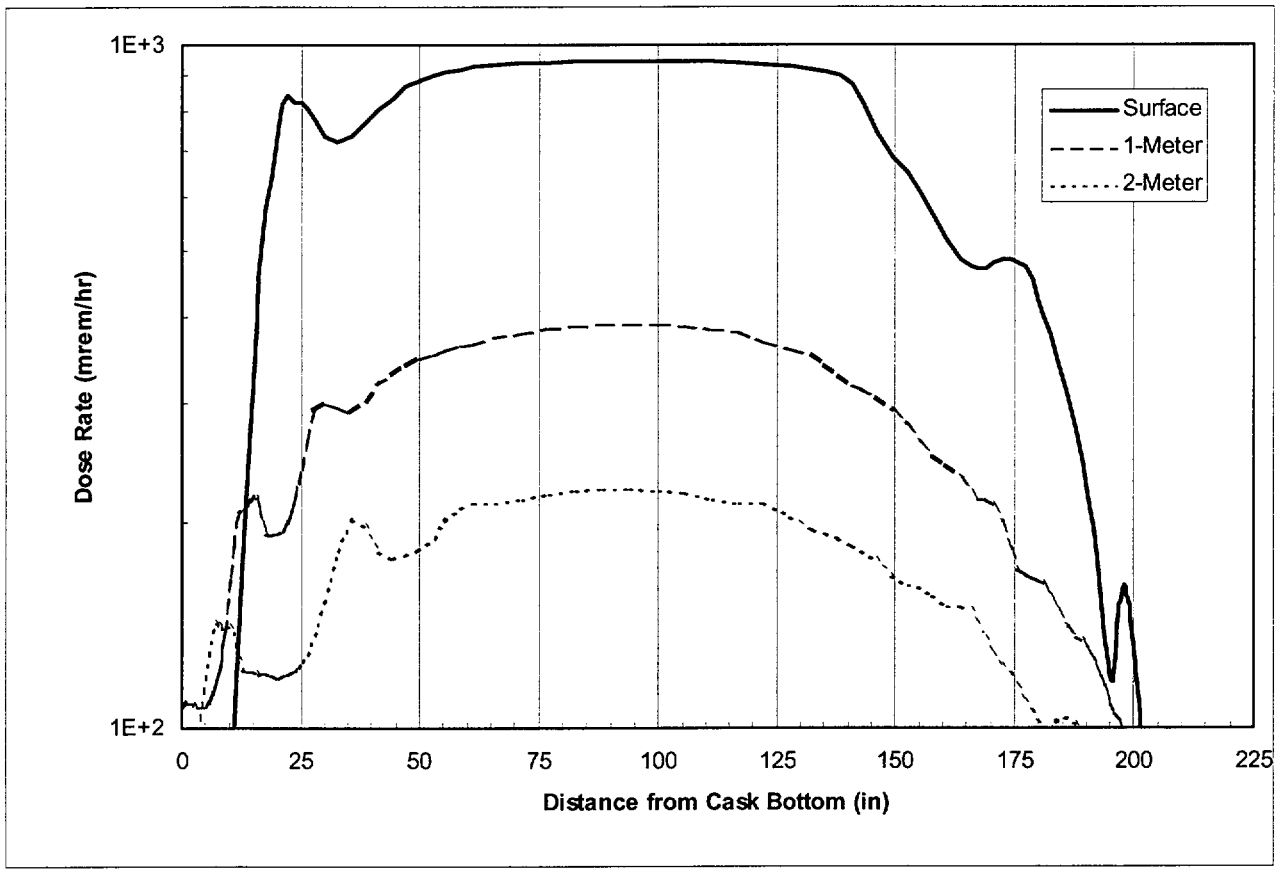

Figure M.5-17
Dose Rate Distribution Along Cask Side During Onsite Transfer (125-Ton Configuration)

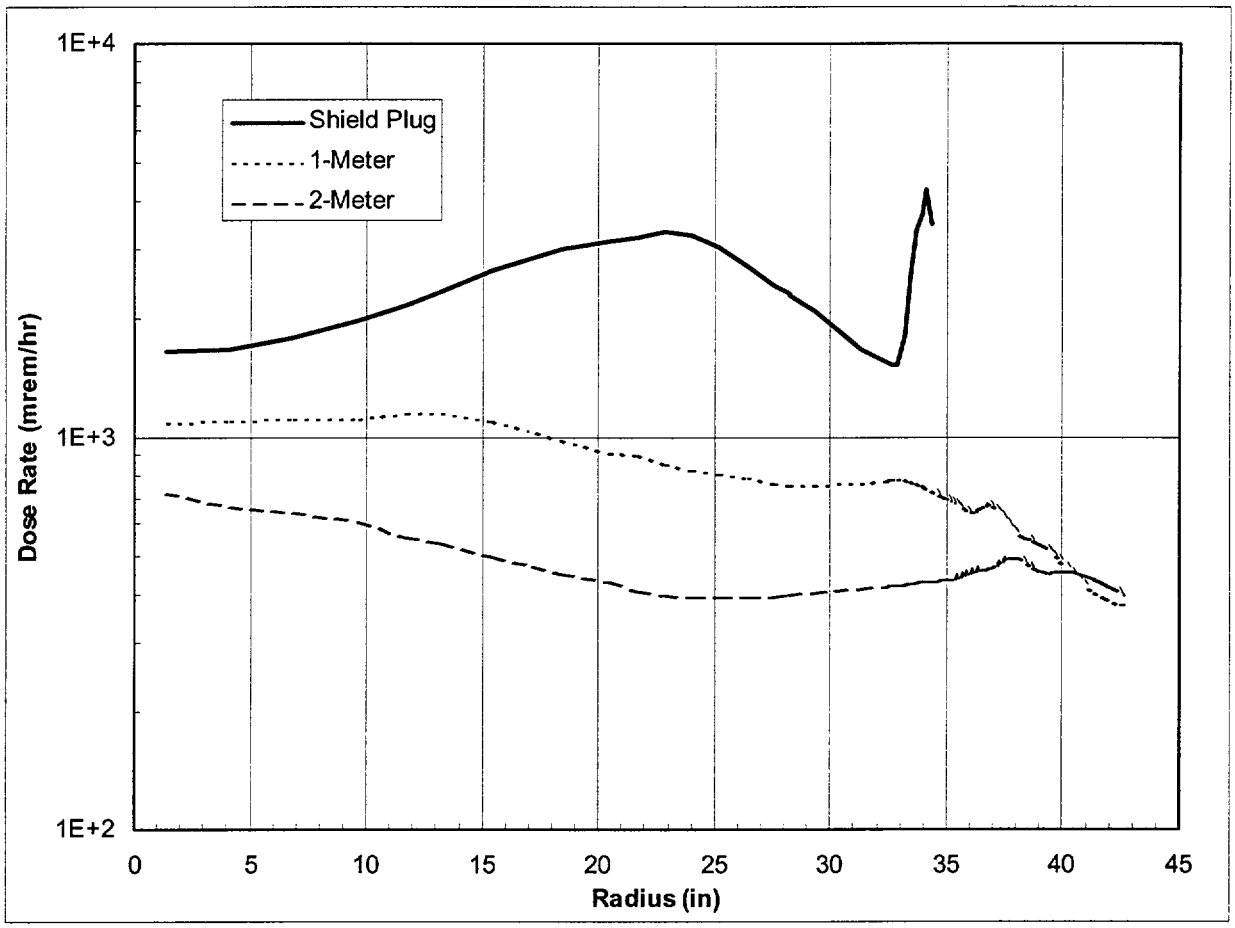

Figure M.5-18
Cask Top-End Dose Rates During Decontamination (125-Ton Configuration)

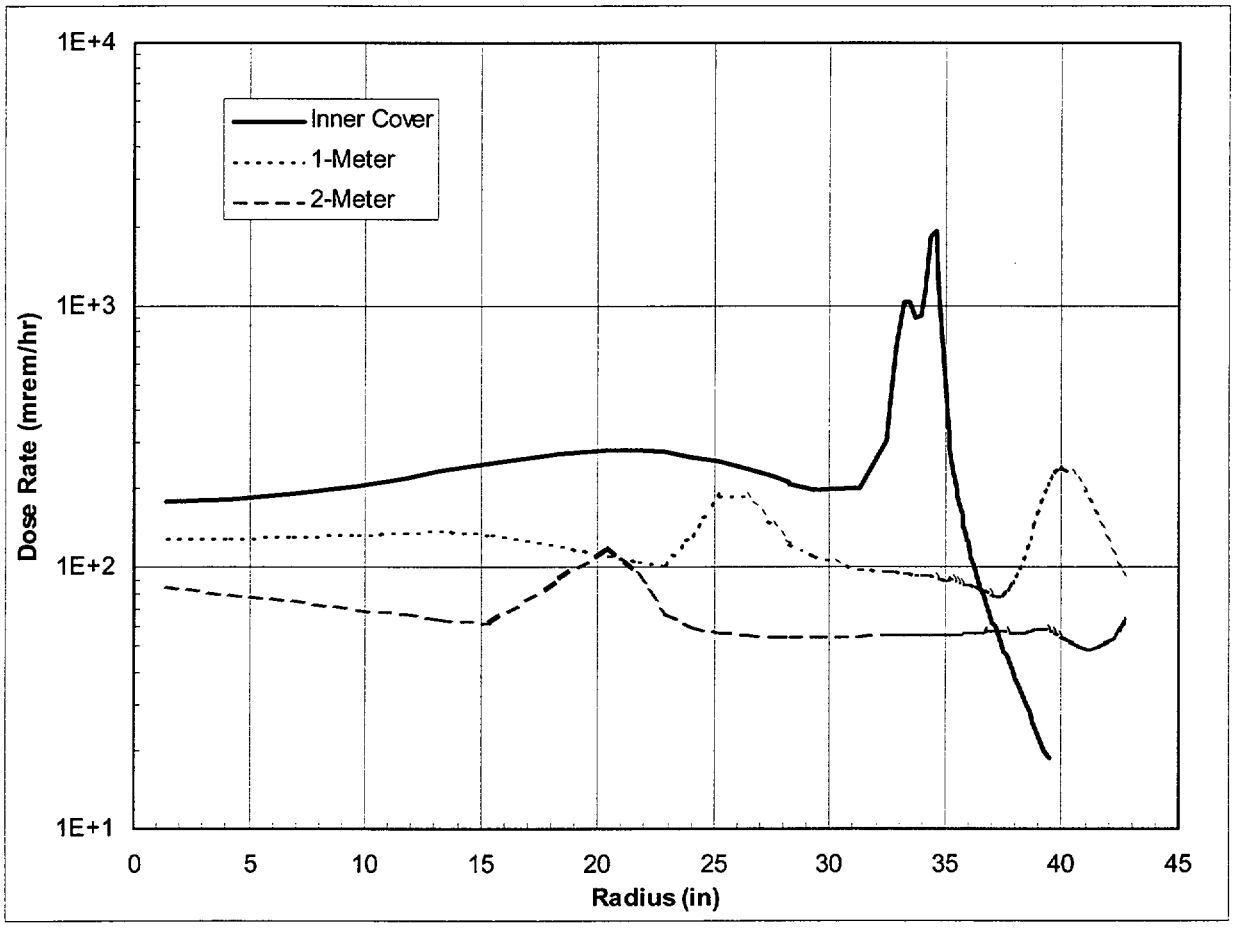

Figure M.5-19
Cask Top-End Dose Rates During Inner Cover Welding (125-Ton Configuration)

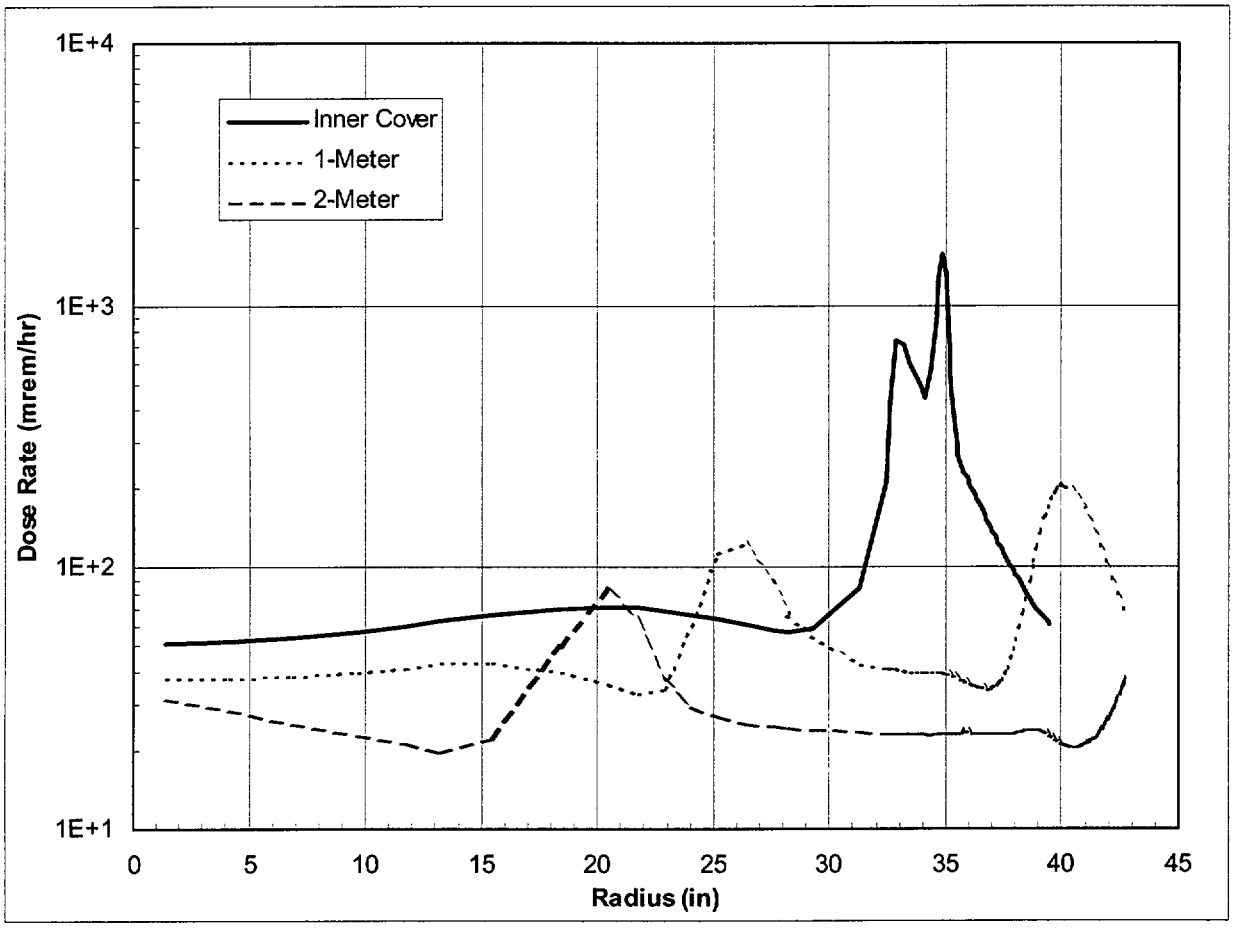

Figure M.5-20
Cask Top-End Dose Rates During Outer Cover Welding (125-Ton Configuratio

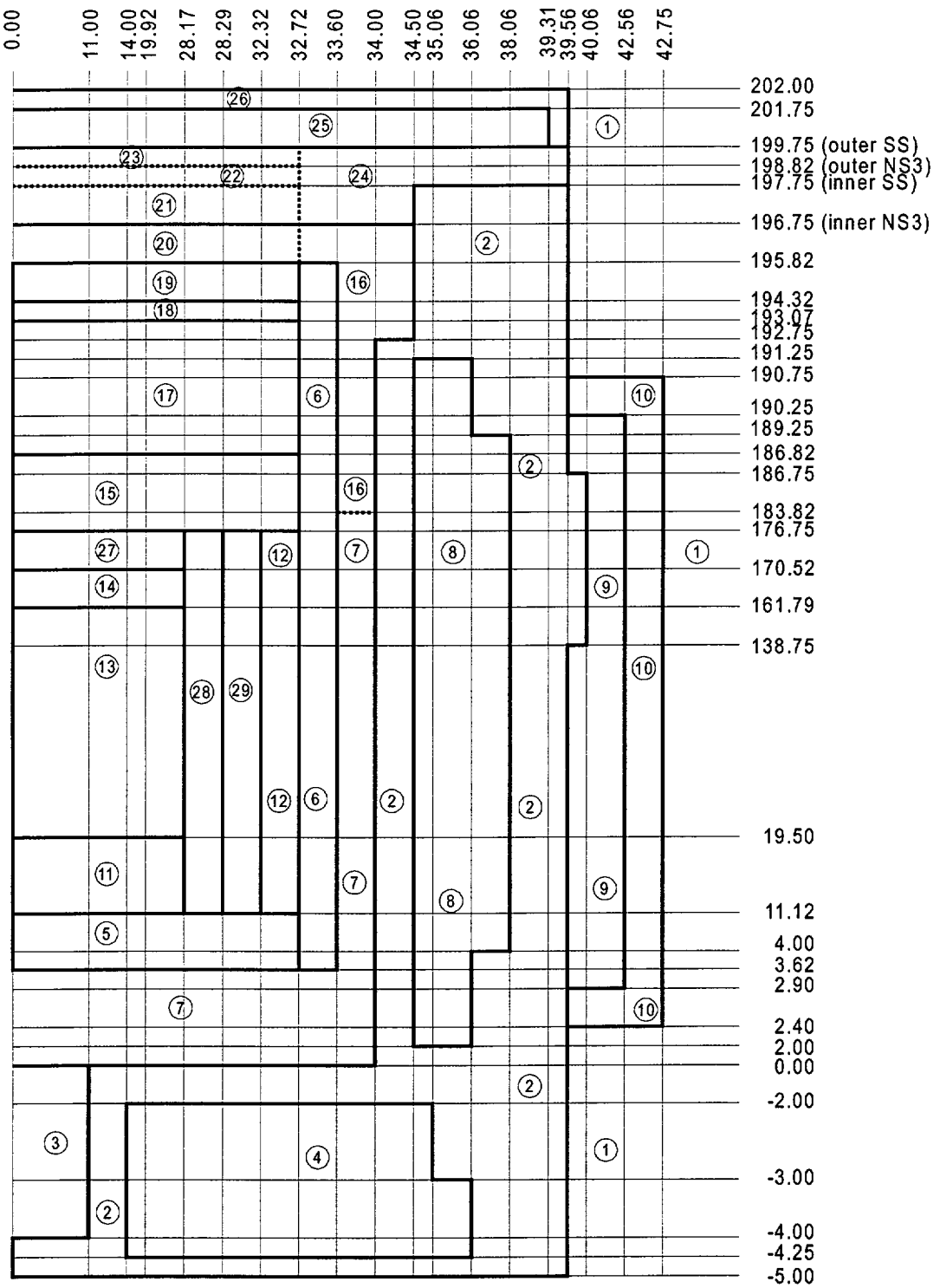

Figure M.5-21
Cask Model Geometry (100-Ton Configuration)

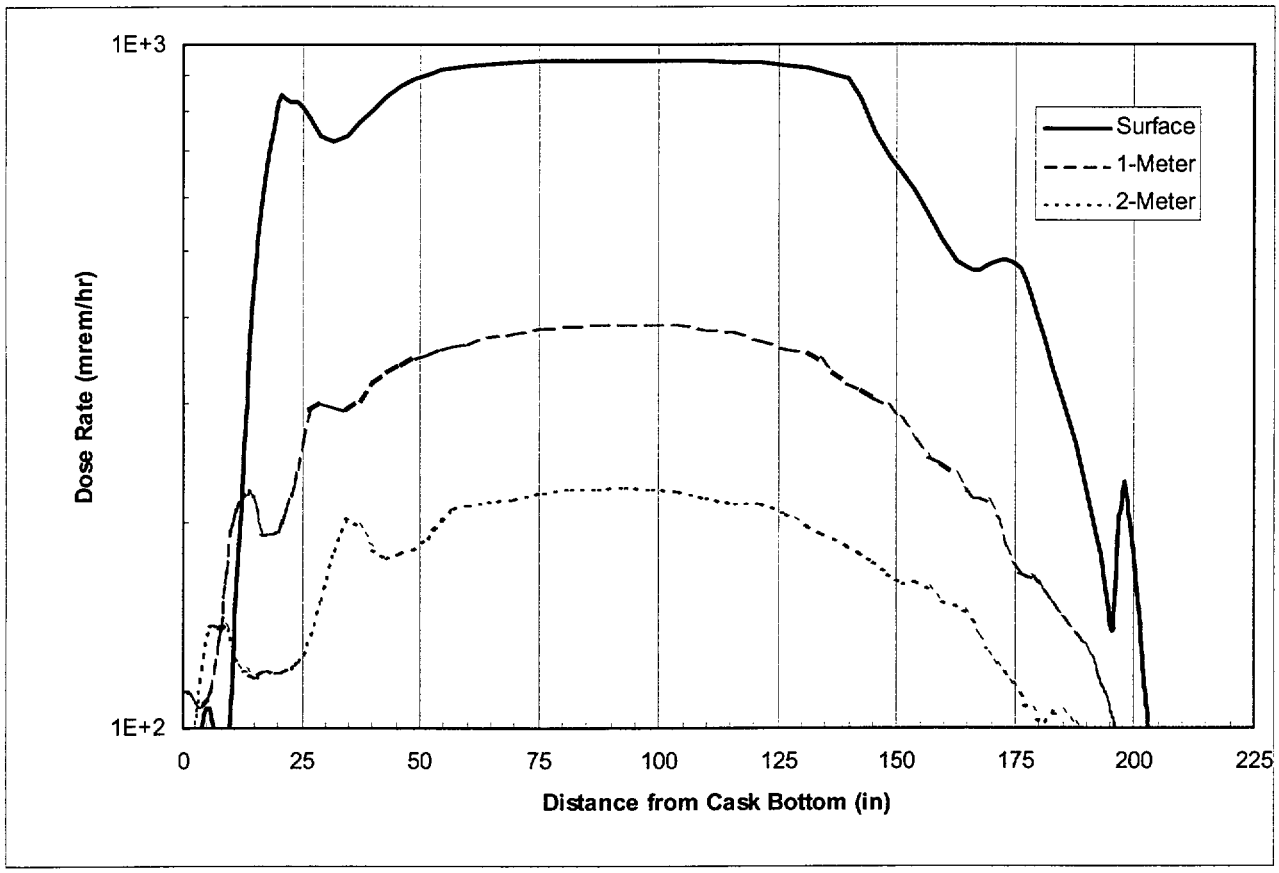

Figure M.5-22
Dose Rate Distribution Along Cask Side During Onsite Transfer (100-Ton Configuration)

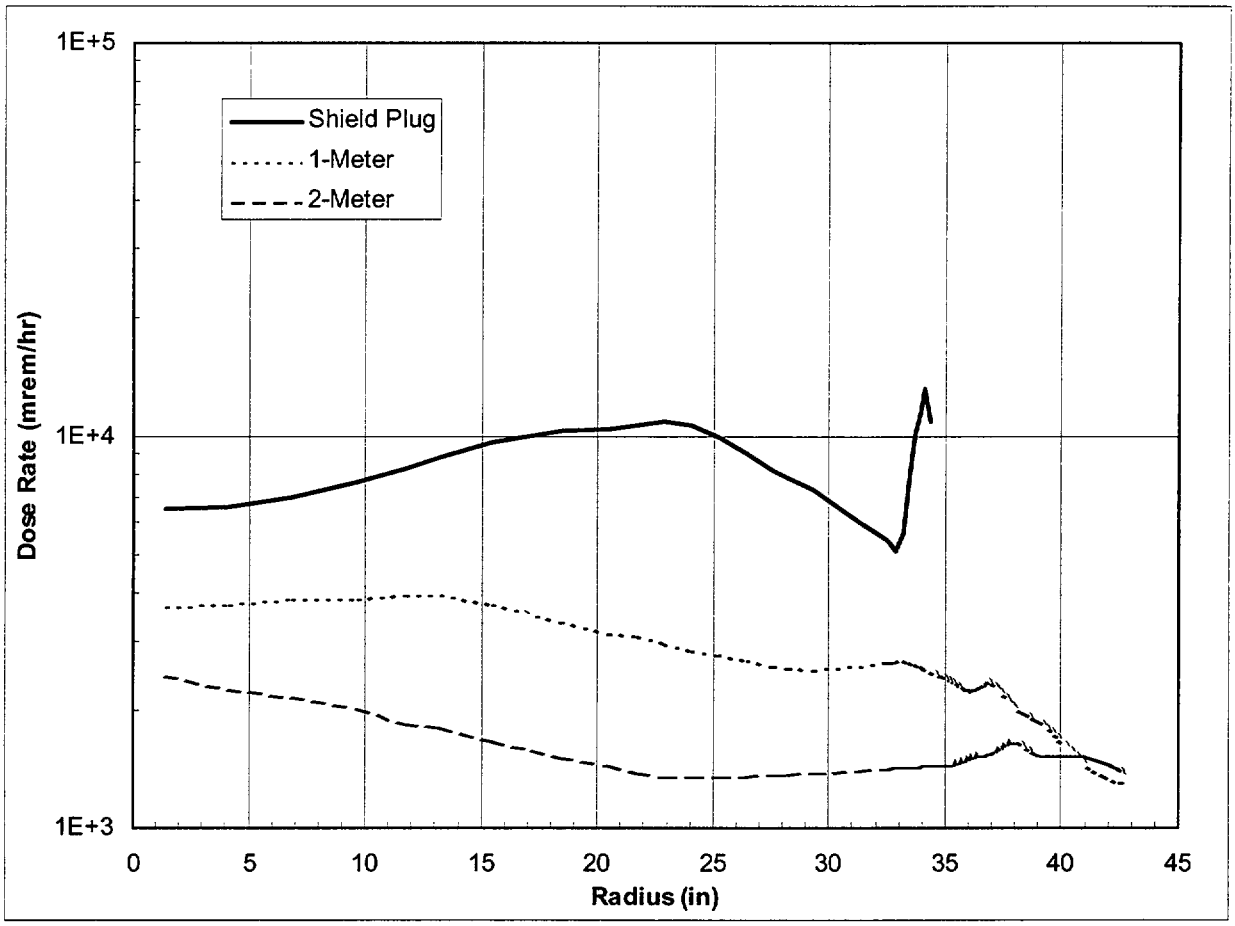

Figure M.5-23
Cask Top-End Dose Rates During Decontamination (100-Ton Configuration)

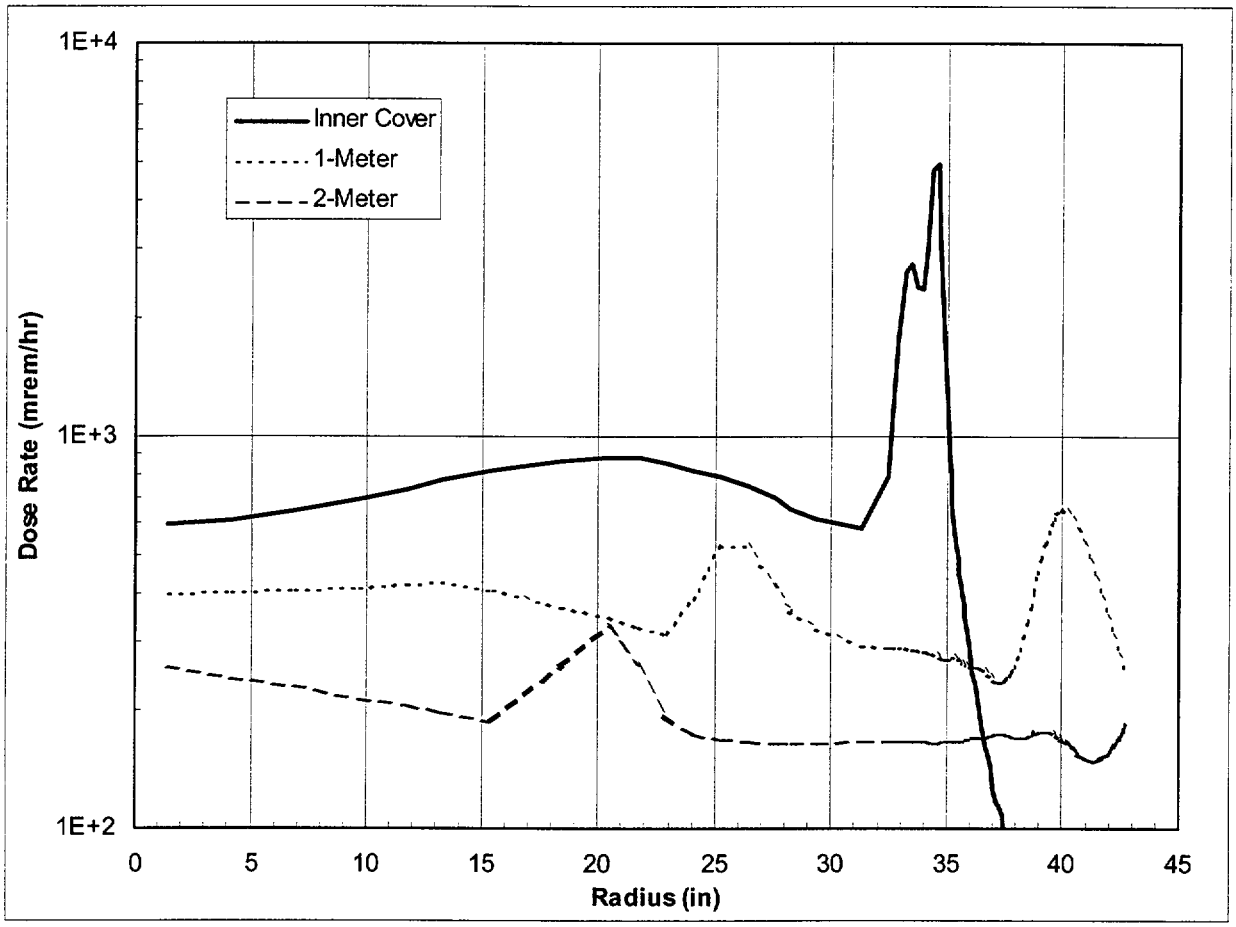

Figure M.5-24
Cask Top-End Dose Rates During Inner Cover Welding (100-Ton Configuration)

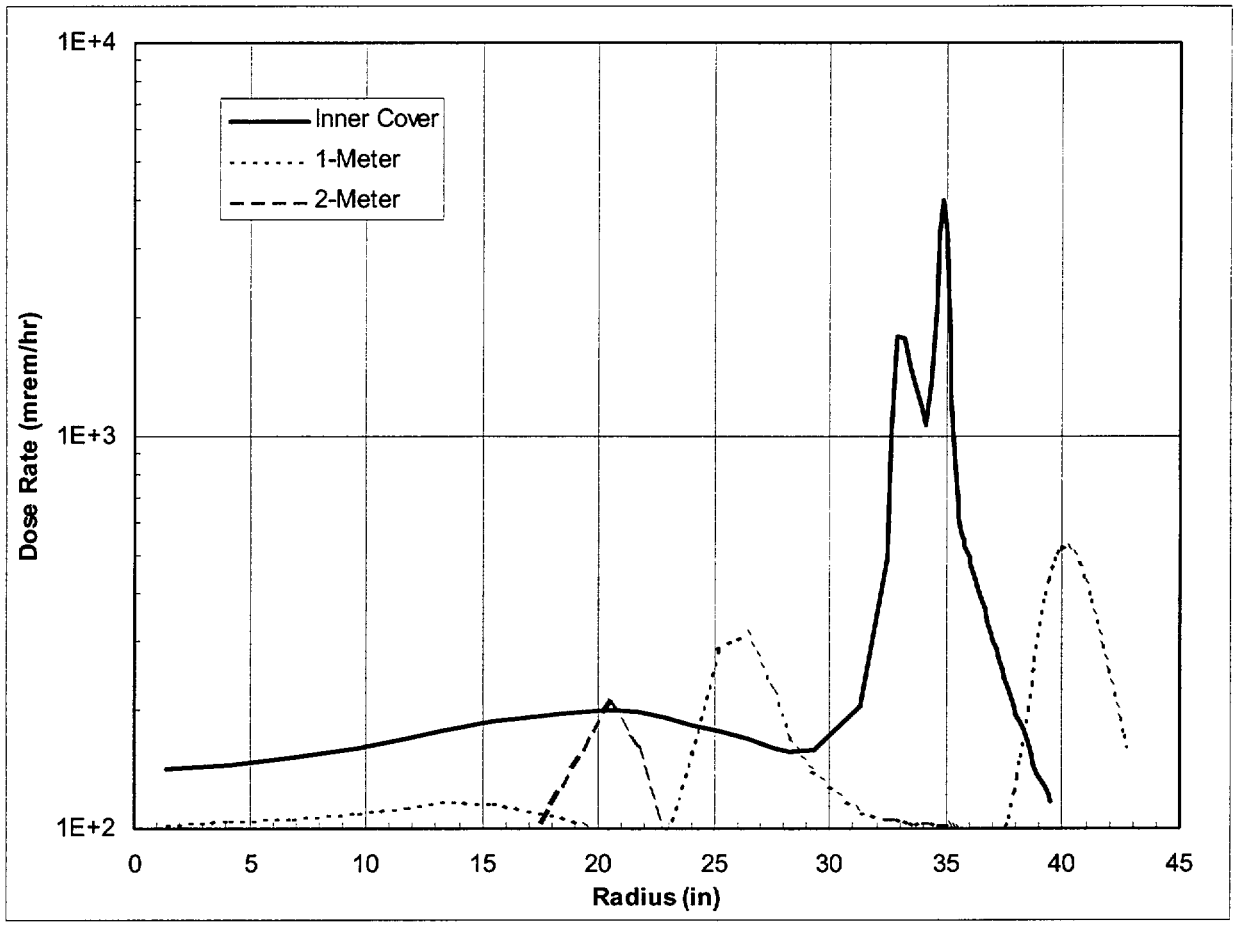

Figure M.5-25
Cask Top-End Dose Rates During Outer Cover Welding (100-Ton Configuration

M.6 Criticality Evaluation

The design criteria for the NUHOMS®-32PT DSC requires that the fuel loaded in the DSC remain subcritical under normal, and accident conditions as defined in 10CFR Part 72.

The NUHOMS®-32PT DSC system's criticality safety is ensured by fixed neutron absorbers, soluble boron in the pool and favorable geometry. Burnup credit is not taken in this criticality evaluation. The fixed neutron absorbers are present in the form of borated metallic plates and Poison Rod Assemblies (PRAs) which are inserted in the guide tubes of certain assemblies in the basket. These materials are ideal for long-term use in the radiation and thermal environments of a DSC. The minimum required boron-10 loading for the metallic plates is 0.0070 g/cm^2 (90% credit taken in the criticality analysis or 0.0063 g/cm^2). In addition to the fixed neutron poison in the basket, PRAs may be required for the center four, eight or sixteen assemblies depending on fuel assembly design and initial enrichment. The minimum required B_4C content of the PRAs is 40% Theoretical Density (TD) with 75% credit taken in the criticality analysis or 30% TD.

M.6.1 Discussion and Results

Figure M.6-1 shows the cross section of the NUHOMS®-32PT DSC. The NUHOMS®-32PT DSC stainless steel basket consists of a welded plate or tube design. The welded plates or tubes form 32 compartments with sufficient space to accommodate aluminum or poison/aluminum inserts and a PWR fuel assembly. The fuel compartment structure is connected to perimeter transition rail assemblies as described shown on the drawings in Section M.1.5. The poison/aluminum plates and aluminum plates are located inside the fuel compartments as shown in Figure M.6-1. Figure M.6-2 through Figure M.6-4 show the fuel compartments that must contain PRAs for loading configurations that require four, eight or sixteen PRAs.

The analysis presented herein is performed for a NUHOMS®-32PT DSC in the NUHOMS® OS197/197H Transfer Casks (TCs) during normal and accident loading conditions. The NUHOMS® OS197/197H TCs consists of an inner stainless steel shell, lead gamma shield, a stainless steel structural shell and a hydrogenous (liquid) neutron shield. This analysis is applicable to any licensed cask of similar construction. The NUHOMS®-32PT DSC/TC configuration is shown to be sub-critical under normal and accident conditions of loading, transfer and storage.

The criticality analysis determines the most reactive configuration for the basket and assembly location. Then criticality calculations evaluate a variety of fuel assembly types, initial enrichments and PRA configurations. Finally, the maximum allowed initial enrichment for each assembly type/PRA configuration is determined. The maximum allowed initial enrichment for each assembly type/PRA configuration is listed in Table M.6-1. The calculations determine k_{eff} with the CSAS25 control module of SCALE-4.4 [6-1] for each assembly type/PRA configuration and initial enrichment, including all uncertainties to assure criticality safety under all credible conditions.

The results of the evaluation demonstrate that the maximum expected k_{eff}, including statistical uncertainty, will be less than the Upper Subcritical Limit (USL) determined from a statistical analysis of benchmark criticality experiments. The statistical analysis procedure includes a confidence band with an administrative safety margin of 0.05.

M.6.2 Package Fuel Loading

The NUHOMS®-32PT DSC is capable of transferring and storing PWR fuel assemblies. Table M.6-2 lists the fuel assemblies considered as authorized contents of the NUHOMS®-32PT DSC.

Table M.6-3 lists the fuel parameters for the PWR fuel assemblies. Reload fuel from other manufacture's with the same parameters are also considered as authorized contents.

For the B&W 15x15 and WE 17x17 class assemblies BPRAs are also included as authorized contents. The only change to the package fuel loading is the addition of BPRAs that are modeled as $^{11}B_4C$. Since BPRAs displace borated moderator in the assembly guide tubes, an evaluation is performed to determine the potential impact of BPRA storage on the system reactivity. No credit is taken for BPRA cladding and absorbers, rather the BPRA is modeled as $^{11}B_4C$ in the entire guide tube of the respective design. Thus, the highly borated moderator between the guide tube and the BPRA rodlet is modeled as $^{11}B_4C$. The inclusion of more Boron-11 and carbon enhances neutron scattering causing the neutron population in the fuel assembly to be slightly increased which increases reactivity. Therefore, these calculations bound any BPRA design that is compatible with B&W 15x15 and WE 17x17 class assemblies. The fuel assembly dimensions reported in Table M.6-3 remain unchanged for the BPRA cases. The models that include BPRAs only differ in that the region inside the guide tubes and instrument tube are modeled as $^{11}B_4C$ instead of moderator or PRAs.

Table M.6-4 lists the minimum B_4C contents for PRAs for the various assembly classes.

M.6.3 Model Specification

The following subsections describe the physical models and materials of the NUHOMS®-32PT DSC as loaded and transferred in the NUHOMS® OS197 or OS197H TC used for input to the CSAS25 module of SCALE-4.4 [6-1] to perform the criticality evaluation. The reactivity of canister under storage conditions is bounded by the TC analysis with zero internal moderator density case. The TC analysis with zero internal moderator density case bounds the storage conditions in the HSM because (1) the canister internals are always dry (purged and backfilled with He) while in the HSM, and (2) the TC contains materials such as steel and lead which provide close reflection of fast neutrons back into the fueled basket while the HSM materials (concrete) are much further from the sides of the DSC and thereby tend to reflect thermalized neutrons back to the canister which are absorbed in the canister materials reducing the system reactivity.

M.6.3.1 Description of Calculational Model

The TC and canister are explicitly modeled using the appropriate geometry options in KENO V.a of the CSAS25 module in SCALE-4.4. Several models are developed to evaluate the fabrication tolerances of the canister, basket, fuel clad outer diameter, fuel assembly locations, fuel assembly type, initial enrichments, PRA locations and storage of BPRAs with the B&W 15x15 and WE 17x17 assembly classes.

The first model is a full active-fuel height and full radial cross section of the canister and TC with reflective boundary conditions on the ends and sides. The model does not explicitly include the water neutron shield. However, the infinite array of TCs without the neutron shield does contain unborated water between the TCs. KENO plots of these models for each assembly class are included in Section M.6.6.2. This model is used to determine the most reactive fuel assembly for a given enrichment and without any PRAs, most reactive assembly-to-assembly pitch, and to determine the most reactive canister configuration accounting for manufacturing tolerances and fuel assembly clad outer diameter tolerances.

The second model is of the most reactive configuration identified above. This model is used to determine the maximum enrichment allowed for each assembly type as a function of the number of PRAs (none, four, eight and sixteen), as appropriate. In addition, the effect of BPRAs for the B&W 15x15 and WE17x17 class assemblies for the various configurations are evaluated.

Figure M.6-5 is a sketch of each KENO V.a unit showing all materials and dimensions for each Unit and an annotated cross section map showing the assembled geometry units in the radial direction of the most reactive configuration identified in this evaluation. The bounding k_{eff} is calculated with a Westinghouse 17x17 LOPAR/Standard assembly with an initial enrichment of 3.4 wt. % U-235, with no PRAs and 32 BPRAs.

M.6.3.2 Package Regional Densities

The Oak Ridge National Laboratory (ORNL) SCALE code package [6-1] contains a standard material data library for common elements, compounds, and mixtures. All the materials used for the TC and canister analysis are available in this data library.

Table M.6-5 provides a complete list of all the relevant materials used for the criticality evaluation. The material density for the B-10 in the poison plates includes a 10% reduction and a 25% reduction for the PRAs.

M.6.4 Criticality Calculations

This section describes the analysis performed for the criticality analysis. The analyses are performed with the CSAS25 module of the SCALE system. A series of calculations are performed to determine the relative reactivity of the various fuel assembly designs evaluated and to determine the most reactive configuration without PRAs and BPRAs. The most reactive fuel for a given enrichment, as demonstrated by the analyses, is the B&W 15x15 Mark B assembly. The most reactive credible configuration is an infinite array of flooded TCs with minimum fuel compartment inner diameter, minimum basket structure thickness and minimum assembly-to-assembly pitch.

As mentioned in Section M.6.1, the NUHOMS®-32PT DSC is evaluated to determine the maximum initial enrichment authorized for each assembly class without PRAs, and with four, eight and 16 PRAs, as applicable.

M.6.4.1 Calculational Method

M.6.4.1.1 Computer Codes.

The CSAS25 control module of SCALE-4.4 [6-1] is used to calculate the effective multiplication factor (k_{eff}) of the fuel in the TC. The CSAS25 control module allows simplified data input to the functional modules BONAMI-S, NITAWL-S, and KENO V.a. These modules process the required cross sections and calculate the k_{eff} of the system. BONAMI-S performs resonance self-shielding calculations for nuclides that have Bondarenko data associated with their cross sections. NITAWL-S applies a Nordheim resonance self-shielding correction to nuclides having resonance parameters. Finally, KENO V.a calculates the k_{eff} of a three-dimensional system. A sufficiently large number of neutron histories are run so that the standard deviation is below 0.0015 for all calculations.

M.6.4.1.2 Physical and Nuclear Data.

The physical and nuclear data required for the criticality analysis include the fuel assembly data and cross-section data as described below.

Table M.6-3 provides the pertinent data for criticality analysis for each fuel assembly evaluated in the NUHOMS®-32PT DSC.

The criticality analysis used the 44-group cross-section library built into the SCALE system. ORNL used ENDF/B-V data to develop this broad-group library specifically for criticality analysis of a wide variety of thermal systems.

M.6.4.1.3 Bases and Assumptions.

The analytical results reported in Section M.3.7 demonstrate that the TC containment boundary and canister basket structure do not experience any significant distortion under hypothetical accident conditions. Therefore, for both normal and hypothetical accident conditions the TC geometry is identical except for the neutron shield and skin. As discussed above, the neutron shield and skin are conservatively removed and the interstitial space modeled as water.

The TC is modeled with KENO V.a using the available geometry input. This option allows a model to be constructed that uses regular geometric shapes to define the material boundaries. The following conservative assumptions are also incorporated into the criticality calculations:

1. No burnable poisons are accounted for in the fuel,

2. Water density is at optimum moderator density,

3. Unirradiated fuel – no credit taken for fissile depletion due to burnup or fission product poisoning,

4. The maximum fuel enrichment is modeled as uniform everywhere throughout the assembly. Natural uranium blankets and axial or radial enrichment zones are modeled as enriched uranium,

5. All fuel rods are filled with 100% moderator in the pellet/cladding gap,

6. Only the active fuel length of each assembly type is explicitly modeled with reflective boundary conditions on the ends; therefore the model is effectively infinitely long,

7. The neutron shield and stainless steel skin of the TC are stripped away and the infinite array of TCs are pushed close together with moderator in the interstitial spaces,

8. The least material condition (LMC) is assumed for the fuel compartment and fuel structure assemblies are pushed together toward the center maximizing reactivity; the reduction in steel thickness also reduces neutron absorption in the steel in the basket,

9. The transition rails between the basket and the canister shell are modeled as 100% aluminum. Steel and open space in the transition rails reduces reactivity because these materials have much higher absorption cross sections as compared to the aluminum,

10. Only 90% credit is taken for the B-10 in the poison plates and 75% credit for the B-10 in PRAs are credited in the KENO models,

11. Temperature is 20°C (293K),

12. Ninety six percent theoretical density for fuel which conservatively increases the total fuel content in the model, and

13. All stainless steel, including XM-19, is modeled as SS304; the small differences in the composition of the various stainless steels have no effect on results of the calculation.

M.6.4.1.4 Determination of k_{eff}.

The Monte Carlo calculations performed with CSAS25 (KENO V.a) use a flat neutron starting distribution. The total number of histories traced for each calculation is approximately 500,000. This number of histories is sufficient to converge the source and produce standard deviations of less than 0.15% in k_{eff}. The maximum k_{eff} for the calculation is determined with the following formula:

$$k_{eff} = k_{KENO} + 2\sigma_{KENO.}$$

M.6.4.2 Fuel Loading Optimization

Determination of the Most Reactive Fuel Type

All fuel lattices listed in Table M.6-3 are evaluated to determine the most reactive fuel assembly type with initial enrichments of 3.3 wt. % U-235. The fuel types are analyzed with water in the fuel pellet cladding annulus and are centered in the fuel compartments. Nominal basket dimensions are used in the KENO models. The effect of moderator density is also evaluated using the most reactive fuel type, B&W 15x15 Mark B.

The canister/TC model for this evaluation differs from the actual design in the following ways:

the boron 10 content in the poison plates is 10% lower than the minimum required,

the neutron shield and the skin of the TC are conservatively replaced with water between the TCs, and

the stainless steel and aluminum transition rails provide support to the fuel compartment grid are modeled as solid aluminum.

In all other respects, the model is the same as that described in Sections M.6.3.1 and M.6.3.2. KENO plots of these models are included in Section M.6.6.2.

A typical input file is included in Section M.6.6.3. The results of these calculations are listed in Table M.6-6. The most reactive fuel type evaluated for the canister design for a given initial enrichment, without PRAs and without BPRAs, is the B&W 15x15 Mark B assembly.

Determination of the Most Reactive Configuration

The fuel-loading configuration of the canister/TC affects the reactivity of the package. Several series of analyses determine the most reactive configuration for the canister/TC.

For this analysis, the most reactive fuel type is used to determine the most reactive configuration. The canister/TC is modeled over the active fuel height of the B&W 15x15 Mark B assembly with reflective boundary conditions on all sides. This represents and infinite array in the x-y direction of canisters/TCs that are conservatively infinite in length. The first model in this series of calculations is identical to the model used above. The canister/TC model for this evaluation differs from the actual design in the following ways:

the boron 10 content in the poison plates is 10% lower than the minimum required,

the stainless steel/aluminum transition rails provide support to the fuel compartment grid are modeled as various solid materials to determine the most reactive condition, and

the neutron shield and the skin of the TC are conservatively replaced with water between the TCs.

Each evaluation is performed at 100% moderator density and again at 60% moderator density which is the most reactive moderator density as demonstrated by the results in Table M.6-6.

The first series of analyses examines the effect of the different materials used in the transition rails between the basket structure and canister shell on reactivity. The transition rails includes stainless steel and aluminum. Two cases with 2500 ppm borated water and pure water in the transition rail region are also included for completeness. The results in Table M.6-7 show a transition rail region filled with aluminum results in the most reactive condition. Therefore, all further analysis assumes solid aluminum in this region.

The second set of analysis evaluates the sensitivity of the system reactivity on fuel cladding OD. The model starts with the worst case above and the assembly cladding O.D. is varied from 0.420 to 0.440 inches. The results of this analysis demonstrate that cladding O.D. or thickness has a statistically insignificant effect on system reactivity. Therefore, the nominal clad thicknesses listed in Table M.6-3 are used for the balance of this evaluation. The results of the fuel clad OD evaluation are listed in Table M.6-8.

The third set of analyses evaluates the effect of neutron poison/aluminum plate thickness on the system reactivity. The model starts with the nominal clad OD model above. The poison plates consist of a poison/aluminum laminate. The minimum B-10 loading is specified. Therefore, if the poison plate thickness is reduced below the nominal, then the B-10 loading must be increased in order to conserve the areal density. For this evaluation only the aluminum laminate thickness is varied. For the solid aluminum plate, the overall plate thickness is varied. Based on the results in Table M.6-9 the effect due to the variation in plate thickness is within the statistical uncertainty of the calculation. The nominal value, however, produced the maximum k_{eff} for both the 100 and 60% moderator density. Therefore, the nominal plate thickness is used for the balance of this evaluation.

The fourth set of analyses evaluates the effect of basket grid structure plate/tube thickness on reactivity. The model starts with the nominal poison/aluminum plate thickness above and the basket structure plate/tube thickness is varied from 0.235 to 0.26 inches. The results in Table M.6-10 show that the effect of basket structure plate/tube thickness has a statistically insignificant effect on reactivity. The most reactive calculated condition occurs with minimum basket structure plate/tube thickness because it allows the fuel assemblies to move slightly closer together. The balance of this evaluation uses the minimum basket structure plate/tube thickness because it represents the most reactive configuration.

The fifth set of analyses evaluates the effect of fuel compartment size on the system reactivity. The model starts with the minimum basket structure plate/tube thickness modeled as above because it represents the most reactive condition. For this evaluation the fuel compartment width is varied from 8.715 to 8.928 inches square. Note that these dimensions are the basket structure plate to plate distance or tube inner diameter. The actual space remaining for the fuel assemblyis obtained by subtracting the poison/aluminum plate thickness. The results of the evaluation are given in Table M.6-11. The results show that the effect is within the statistical uncertainty of calculation. The most

reactive configuration is with the minimum fuel compartment size because the assembly-to-assembly pitch is minimized. The balance of this evaluation use the minimum fuel compartment width because it represents the most reactive configuration.

The final series of sensitivity analyses determined the most reactive fuel assembly-to-assembly pitch. The most reactive configurations occur at the minimum assembly-to-assembly pitch. For assemblies with large cross sections such as the B&W 15x15 Mark B, however, there is little space for the assemblies to move with in the minimum fuel compartment modeled. The results in Table M.6-12 demonstrate that for the B&W 15x15 Mark B assembly the effect is within the statistical uncertainty of the calculation. For smaller assemblies such as the WE 14x14, this effect would be statistically significant because the assemblies have more space in which to move inside the fuel compartment, therefore the minimum assembly-to-assembly pitch is used for the balance of this analysis.

Determination of the Maximum Initial Enrichment for each Fuel Class and PRA Configuration

The most reactive configuration as determined in Section B above is with solid aluminum in the transition rail region, nominal poison/aluminum plate thickness, minimum basket structure plate/tube thickness, minimum fuel compartment width and the minimum assembly-to-assembly pitch. The following analysis uses this configuration to determine the maximum allowed initial enrichment as a function of initial enrichment and PRA configuration for each assembly class. Only the assembly type and PRA configuration is changed for each model. The most reactive assembly type for each assembly class is used for each evaluation. In addition, for each case the internal moderator density is varied to determine the peak reactivity for the specific configuration. The maximum initial enrichment for each assembly class and PRA configuration are provided in Table M.6-1.

The canister/TC model for this evaluation differs from the actual design in the following ways:

the boron 10 content in the poison plates is 10% lower than the minimum required,

the boron 10 content in the PRAs is 25% lower than the minimum required,

the stainless steel/aluminum transition rails that provide support to the fuel compartment grid are modeled as various solid materials to determine the most reactive condition,

BPRAs, when modeled, are modeled as solid $^{11}B_4C$ in the guide tubes and instrument tubes,

the neutron shield and the skin of the TC are conservatively replaced with water between the TCs, and

the worst case material conditions, as determined in Section B above, are modeled.

The input file for the case with the highest calculated reactivity is included in Section M.6.6.4.

WE 17x17 Class Assemblies

The most reactive WE 17x17 class assembly is the WE 17x17 LOPAR/standard assembly as demonstrated in Table M.6-6. The results for the WE 17x17 class assembly calculations are listed in Table M.6-13 and Table M.6-14 for cases without and with BPRAs, respectively.

CE 16x16 Class Assemblies

The most reactive CE 16x16 class assembly is the CE 16x16 system 80 assembly as demonstrated in Table M.6-6. The results for the CE 16x16 class assembly calculations are listed in Table M.6-15 for cases without BPRAs. BPRAs are not authorized to be stored with CE 16x16 class assemblies.

B&W 15x15 Class Assemblies

The most reactive B&W 15x15 class assembly is the B&W 15x15 Mark B assembly as demonstrated in Table M.6-6. The results for the B&W 15x15 class assembly calculations are listed in Table M.6-16 and Table M.6-17 for cases without and with BPRAs, respectively.

CE 15x15 Class Assemblies

The most reactive CE 15x15 class assembly is the CE 15x15 Palisades assembly as demonstrated in Table M.6-6. The results for the CE 15x15 class assembly calculations are listed in Table M.6-18 for cases without BPRAs. BPRAs are not authorized to be stored with CE 15x15 class assemblies.

WE 15x15 Class Assemblies

The most reactive WE 15x15 class assembly is the WE 15x15 Standard assembly as demonstrated in Table M.6-6. The results for the WE 15x15 class assembly calculations are listed in Table M.6-19 for cases without BPRAs. BPRAs are not authorized to be stored with WE 15x15 class assemblies.

CE 14x14 Class Assemblies

The most reactive CE 14x14 class assembly is the CE 14x14 Fort Calhoun assembly as demonstrated in Table M.6-6. The results for the CE 14x14 class assembly calculations are listed in Table M.6-20 for cases without BPRAs. BPRAs are not authorized to be stored with CE 14x14 class assemblies.

WE 14x14 Class Assemblies

The most reactive WE 14x14 class assembly is the WE 14x14 ZCA/ZCB assembly as demonstrated in Table M.6-6. The results for the WE 14x14 class assembly calculations are listed in Table M.6-21 for cases without BPRAs. BPRAs are not authorized to be stored with WE 14x14 class assemblies.

M.6.4.3 Criticality Results

Table M.6-22 lists the bounding results for all conditions of storage. The highest calculated k_{eff}, including 2σ uncertainty, is for the WE 17x17 LOPAR/Standard assembly with an initial U-235 enrichment of 3.4 wt. %, no PRAs, and 32 BPRAs. The maximum allowed initial enrichment for each assembly type/PRA configuration is listed in Table M.6-1.

These criticality calculations were performed with CSAS25 of SCALE-4.4. For each case, the result includes (1) the KENO-calculated k_{KENO}, (2) the one sigma uncertainty σ_{KENO}, and (3) the final k_{eff}, which is equal to $k_{KENO} + 2\sigma_{KENO}$.

The criterion for subcriticality is that

$$k_{KENO} + 2\sigma_{KENO} \bullet \text{USL},$$

where USL is the upper subcritical limit established by an analysis of benchmark criticality experiments. From Section M.6.5, the minimum USL over the parameter range is 0.9411. From Table M.6-22 for the most reactive case,

$$k_{KENO} + 2\sigma_{KENO} = 0.9389 + 2\ (0.0010) = 0.9409 \bullet 0.9411.$$

M.6.5 Critical Benchmark Experiments

The criticality safety analysis of the NUHOMS® OS197/197H TC containing the NUHOMS® -32PT DSC uses the CSAS25 module of the SCALE system of codes. The CSAS25 control module allows simplified data input to the functional modules BONAMI-S, NITAWL-S, and KENO V.a. These modules process the required cross-section data and calculate the k_{eff} of the system. BONAMI-S performs resonance self-shielding calculations for nuclides that have Bondarenko data associated with their cross sections. NITAWL-S applies a Nordheim resonance self-shielding correction to nuclides having resonance parameters. Finally, KENO V.a calculates the effective neutron multiplication (k_{eff}) of a 3-D system.

The analysis presented herein uses the fresh fuel assumption for criticality analysis. The analysis employs the 44-group ENDF/B-V cross-section library because it has a small bias, as determined by 121 benchmark calculations. The Upper Subcritical Limit (USL-1) was determined using the results of these 121 benchmark calculations.

The benchmark problems used to perform this verification are representative of benchmark arrays of commercial light water reactor (LWR) fuels with the following characteristics:

(1) water moderation,

(2) boron neutron absorbers,

(3) unirradiated light water reactor type fuel (no fission products or "burnup credit") near room temperature (vs. reactor operating temperature),

(4) close reflection, and

(5) uranium oxide.

The 121 uranium oxide experiments were chosen to model a wide range of uranium enrichments, fuel pin pitches, assembly separation, concentration of soluble boron and control elements in order to test the codes ability to accurately calculate k_{eff}. These experiments are discussed in detail in Reference [6-2].

M.6.5.1 Benchmark Experiments and Applicability

A summary of all of the pertinent parameters for each experiment is included in Table M.6-23 along with the results of each run. The best correlation is observed for fuel assembly separation distance with a correlation of 0.68. All other parameters show much lower correlation ratios indicating no real correlation. All parameters were evaluated for trends and to determine the most conservative USL.

The USL is calculated in accordance to NUREG/CR-6361 [6-2]. USL Method 1 (USL-1) applies a statistical calculation of the bias and its uncertainty plus an administrative margin (0.05) to the linear fit of results of the experimental benchmark data. The basis for the administrative margin is from Reference [6-3]. Results from the USL evaluation are presented in Table M.6-24.

The criticality evaluation used the same cross section set, fuel materials and similar material/geometry options that were used in the 121 benchmark calculations as shown in Table M.6-23. The modeling techniques and the applicable parameters listed in Table M.6-25 for the actual criticality evaluations fall within or very close the range of those addressed by the benchmarks in Table M.6-23.

M.6.5.2 Results of the Benchmark Calculations

The results from the comparisons of physical parameters of each of the fuel assembly types to the applicable USL value are presented in Table M.6-25. The minimum value of the USL is determined to be 0.9411 based on comparisons to the limiting assembly parameters as shown in Table M.6-25.

M.6.6 Appendix

M.6.6.1 References

6-1 Oak Ridge National Laboratory, RSIC Computer Code Collection, "SCALE: A Modular Code System for Performing Standardized Computer Analysis for Licensing Evaluations for Workstations and Personal Computers," NUREG/CR-0200, Revision 6, ORNL/NUREG/CSD-2/V2/R6.

6-2 U.S. Nuclear Regulatory Commission, "Criticality Benchmark Guide for Light-Water-Reactor fuel in Transportation and Storage Packages," NUREG/CR-6361, Published March 1997, ORNL/TM-13211.

6-3 U.S. Nuclear Regulatory Commission, "Recommendations for Preparing the Criticality Safety Evaluation of Transportation Packages," NUREG/CR-5661, Published April 1997, ORNL/TM-11936.

M.6.6.2 KENO Plots of Various Cases

Table M.6-1
Maximum Initial Enrichment For Each Configuration

Assembly Class	Assembly Type	Maximum Initial Enrichment, wt. % U-235			
		No PRAs	4 PRAs	8 PRAs	16 PRAs
WE 17x17[1]	Westinghouse 17x17 LOPAR/Std	3.40	4.00	4.50	5.00
	Westinghouse 17x17 OFA/Vantage 5,+[2]				
CE 16x16[3]	CE 16x16 System 80	3.80	4.30	4.70	5.00
B&W 15x15[1]	B&W 15x15 Mark B	3.30	3.90	NA	5.00
CE 15x15	CE 15x15 Palasades	3.40	Not Evaluated	Not Evaluated	Not Evaluated
	Exxon/ANF 15x15 CE				
WE 15x15	Westinghouse 15x15 Std/ZC	3.40	4.00	4.60	5.00
	Exxon/ANF 15x15 WE				
CE 14x14	CE 14x14 Std/Generic	3.80	4.60	5.00	Not Evaluated
	CE 14x14 Fort Calhoun				
WE 14x14	Westinghouse 14x14 ZCA/ZCB	4.00	5.00	Not Evaluated	Not Evaluated
	Westinghouse 14x14 OFA				
	Exxon/ANF 14x14 WE				

NOTES:

(1) With or without BPRAs in locations without PRAs

(2) Includes all Vantage versions (5, +, ++, etc.).

(3) The length of CE 16x16 system 80 fuel assemblies is longer than the length currently allowed in the NUHOMS®-32PT system. However, this assembly is included in the criticality analysis to demonstrate that it is an acceptable fuel assembly type with respect to the criticality safety analysis.

Table M.6-2
Authorized Contents for NUHOMS®-32PT System

Assembly Type[1]	Array
Westinghouse 17x17 LOPAR/Standard	17x17
Westinghouse 17x17 OFA/Vantage 5	17x17
CE 16x16 System 80[2]	16x16
B&W 15x15 Mark B	15x15
CE 15x15 Palisades	15x15
Exxon/ANF 15x15 CE	15x15
Exxon/ANF 15x15 WE	15x15
Westinghouse 15x15 Standard/ZC	15x15
CE 14x14 Standard/Generic	14x14
CE 14x14 Fort Calhoun	14x14
Exxon/ANF 14x14 WE	14x14
Westinghouse 14x14 ZCA/ZCB	14x14
Westinghouse 14x14 OFA	14x14

NOTES:

(1) Reload fuel from other manufacturers with these parameters are also acceptable.

(2) The length of CE 16x16 system 80 fuel assemblies is longer than the length currently allowed in the NUHOMS®-32PT system. However, this assembly is included in the criticality analysis to demonstate that it is an acceptable fuel assembly type with respect to the criticality safety analysis

Table M.6-3
Parameters For PWR Assemblies[3]

Manufacturer[1]	Array	Version	Active Fuel Length (in)	Number Fuel Rods per Assembly	Pitch (in)	Fuel Pellet OD (in)
WE	17x17	LOPAR	144	264	0.496	0.3225
WE	17x17	OFA/Van 5	144	264	0.496	0.3088
CE	16x16	System 80	150	236	0.506	0.3255
B&W	15x15	Mark B	141.8	208	0.568	0.3686
CE	15x15	Palisades	132	216	0.550	0.3580
Exxon/ANF	15x15	CE	131.8	216	0.550	0.3565
Exxon/ANF	15x15	WE	144	204	0.563	0.3565
WE	15x15	Std/ZC	144	204	0.563	0.3559
CE	14x14	Std/Gen	137	176	0.580	0.3765
CE	14x14	Ft. Calhoun	128	176	0.580	0.3815
Exxon/ANF	14x14	WE	142	179	0.556	0.3505
WE	14x14	ZCA/ZCB	144	179	0.556	0.3659
WE	14x14	OFA	144	179	0.556	0.3444

Manufacturer [1]	Array	Version	Clad Thickness (in)	Clad OD (in)	Guide Tube OD (in)	Instrument Tube ID (in)
WE	17x17	LOPAR	0.0225	0.374	24@0.474 1@0.480	24@0.422 1@0.450
WE	17x17	OFA/Van 5	0.0225	0.360	24@0.482 1@0.476	24@0.450 1@0.460
CE	16x16	System 80	0.0250	0.382	5@0.768	5@0.687
B&W	15x15	Mark B	0.0265	0.430	16@0.530 1@0.493	16@0.498 1@441
CE	15x15	Palisades	0.0260	0.418	8@0.4135	8@0.3655
Exxon/ANF	15x15	CE	0.0300	0.417	8Guide Bars[2] 1@0.417	1@0.363
Exxon/ANF	15x15	WE	0.0300	0.424	20@0.544 1@0.544	20@0.510 1@0.510
WE	15x15	Std/ZC	0.0242	0.422	20@0.546 1@0.546	20@0.512 1@0.512
CE	14x14	Std/Gen	0.0280	0.440	5@1.115	5@1.035
CE	14x14	Ft. Calhoun	0.0280	0.440	5@1.115	5@1.035
Exxon/ANF	14x14	WE	0.0300	0.424	16@0.541 1@0.480	16@0.507 1@0.448
WE	14x14	ZCA/ZCB	0.0225	0.422	16@0.539 1@0.422	16@0.505 1@0.392
WE	14x14	OFA	0.0243	0.400	16@0.526 1@0.400	16@0.492 1@0.353

NOTES:

(1) Reload fuel from other manufacturers with these parameters are also acceptable.

(2) Guide Bars are solid Zircaloy-4 approximately 0.40 inches x 0.45 inches

(3) All dimensions shown are nominal

Table M.6-4
Poison Rod Assembly (PRA) Description

Assembly Class	Minimum Number of Rods/PRA	Modeled B_4C Content per Rod (g/cm)	Minimum B_4C Content per Rod (g/cm)
WE 17x17	24	0.59	0.79
CE 16x16	5	1.34	1.78
B&W 15x15	16	0.72	0.96
WE 15x15	20	0.72	0.96
CE 14x14	5	3.14	4.19
WE 14x14	16	0.72	0.96

Table M.6-5
Material Property Data

Material	Density g/cm^3	Element	Weight %	Atom Density (atoms/b-cm)
UO_2 (Enrichment - 3.4 wt%)	10.52	U-235	3.00	8.0797E-04
		U-238	85.15	2.2666E-02
		O	11.85	4.6948E-02
UO_2 (Enrichment - 5.0 wt%)	10.52	U-235	4.41	1.1882E-03
		U-238	83.73	2.2290E-02
		O	11.86	4.6956E-02
Zircaloy-4	6.56	Zr	98.23	4.2541E-02
		Sn	1.45	4.8254E-04
		Fe	0.21	1.4856E-04
		Cr	0.10	7.5978E-05
		Hf	0.01	2.2133E-06
Borated Water (2500 ppm Boron)	1.000	H	0.11	6.6769E-02
		O	0.89	3.3385E-02
		B-10	4.602E-04	2.7713E-05
		B-11	2.038E-03	1.1155E-04
Water	0.998	H	11.1	6.6769E-02
		O	88.9	3.3385E-02
Stainless Steel (SS304)	7.94	C	0.080	3.1877E-04
		Si	1.000	1.7025E-03
		P	0.045	6.9468E-05
		Cr	19.000	1.7473E-02
		Mn	2.000	1.7407E-03
		Fe	68.375	5.8545E-02
		Ni	9.500	7.7402E-03
Aluminum	2.70	Al	100.0	6.0307E-02
Lead	11.34	Pb	100.0	3.2969E-02
Aluminum - Boron Poison Plate (0.0063 g/cm^2 B-10)	2.465	B-10	1.34	1.9847E-03
		Al	98.66	5.4276E-02
B_4C in PRA	0.756	B-10	14.42	6.5599E-03
		B-11	63.83	2.6405E-02
		C	21.75	8.2411E-03
$^{11}B_4C$ in BPRA	2.555	B-11	78.56	1.0988E-01
		C	21.44	2.7470E-02

Table M.6-6
Most Reactive Fuel Type

Manufacturer	Array	Version	k_{KENO}	1σ	k_{eff}
Most Reactive Fuel Type at 3.3 wt.% U-235, w/o PRAs, 2500 ppm Boron					
WE	17x17	LOPAR	0.8862	0.0009	0.8880
WE	17x17	OFA/Van 5	0.8579	0.0011	0.8601
CE	16x16	System 80	0.8293	0.0009	0.8311
B&W	15x15	Mark B	0.8932	0.0008	0.8948
CE	15x15	Palisades	0.8766	0.0009	0.8784
Exxon/ANF	15x15	CE	0.8734	0.0009	0.8752
Exxon/ANF	15x15	WE	0.8625	0.0008	0.8641
WE	15x15	Std/ZC	0.8760	0.0009	0.8778
CE	14x14	Std/Gen	0.8196	0.0009	0.8214
CE	14x14	Ft. Calhoun	0.8235	0.0009	0.8253
Exxon/ANF	14x14	WE	0.7821	0.0009	0.7839
WE	14x14	ZCA/ZCB	0.8012	0.0009	0.8030
WE	14x14	OFA	0.7638	0.0008	0.7654
B&W 15x15 Mark B - Internal Moderator Density (IMD) Evaluation					
Assembly Design		IMD Condition	k_{KENO}	1σ	k_{eff}
B&W 15x15 Mark B		100% TD	0.8932	0.0008	0.8948
B&W 15x15 Mark B		90% TD	0.9053	0.0008	0.9069
B&W 15x15 Mark B		80% TD	0.9170	0.0009	0.9188
B&W 15x15 Mark B		70% TD	0.9238	0.0009	0.9256
B&W 15x15 Mark B		60% TD	0.9270	0.0010	0.9290
B&W 15x15 Mark B		50% TD	0.9223	0.0008	0.9239

Table M.6-7
Transition Rail Material Evaluation Results

Model Description	k_{KENO}	1σ	k_{eff}
Transition Rail Material Evaluation - 100% IMD			
Aluminum	0.8932	0.0008	0.8948
2500 ppm Borated Water	0.8873	0.0009	0.8891
Pure Water	0.8893	0.0008	0.8909
Stainless Steel	0.8918	0.0008	0.8934
Transition Rail Material Evaluation - 60% IMD			
Aluminum	0.9270	0.0010	0.9290
2500 ppm Borated Water	0.9188	0.0010	0.9208
Pure Water	0.9189	0.0011	0.9211
Stainless Steel	0.9261	0.0009	0.9279

Table M.6-8
Fuel Clad OD Evaluation Results

Model Description	k_{KENO}	1σ	k_{eff}
Fuel Clad O.D. Evaluation - 100% IMD			
Fuel Clad O.D. = 0.420 inches	0.8889	0.0009	0.8907
Fuel Clad O.D. = 0.422 inches	0.8884	0.0008	0.8900
Fuel Clad O.D. = 0.424 inches	0.8915	0.0010	0.8935
Fuel Clad O.D. = 0.426 inches	0.8904	0.0009	0.8922
Fuel Clad O.D. = 0.428 inches	0.8922	0.0009	0.8940
Fuel Clad O.D. = 0.430 inches	0.8932	0.0008	0.8948
Fuel Clad O.D. = 0.432 inches	0.8933	0.0008	0.8949
Fuel Clad O.D. = 0.434 inches	0.8919	0.0009	0.8937
Fuel Clad O.D. = 0.436 inches	0.8953	0.0009	0.8971
Fuel Clad O.D. = 0.438 inches	0.8948	0.0008	0.8964
Fuel Clad O.D. = 0.440 inches	0.8939	0.0009	0.8957
Fuel Clad O.D. Evaluation - 60% IMD			
Fuel Clad O.D. = 0.420 inches	0.9293	0.0009	0.9311
Fuel Clad O.D. = 0.422 inches	0.9272	0.0010	0.9292
Fuel Clad O.D. = 0.424 inches	0.9273	0.0011	0.9295
Fuel Clad O.D. = 0.426 inches	0.9268	0.0009	0.9286
Fuel Clad O.D. = 0.428 inches	0.9270	0.0008	0.9286
Fuel Clad O.D. = 0.430 inches	0.9270	0.0010	0.9290
Fuel Clad O.D. = 0.432 inches	0.9267	0.0008	0.9283
Fuel Clad O.D. = 0.434 inches	0.9258	0.0009	0.9276
Fuel Clad O.D. = 0.436 inches	0.9259	0.0009	0.9277
Fuel Clad O.D. = 0.438 inches	0.9260	0.0009	0.9278
Fuel Clad O.D. = 0.440 inches	0.9251	0.0010	0.9271

Table M.6-9
Poison/Aluminum and Aluminum Plate Thickness Evaluation Results

Table M.6-10
Basket Grid Structure Plate/Tube Thickness Evaluation Results

Table M.6-11
Fuel Compartment Width Evaluation Results

Table M.6-12
Assembly-to-Assembly Pitch Evaluation

Model Description	k_{KENO}	1σ	k_{eff}
Assembly-to-Assembly Pitch Evaluation - 100% IMD			
Maximum Assembly-to-Assembly Pitch	0.8983	0.0008	0.8999
Assemblies Centered in Sleeves	0.9006	0.0008	0.9022
Minimum Assembly-to-Assembly Pitch	0.9030	0.0009	0.9048
Assembly-to-Assembly Pitch Evaluation - 60% IMD			
Maximum Assembly-to-Assembly Pitch	0.9330	0.0009	0.9348
Assemblies Centered in Sleeves	0.9320	0.0009	0.9338
Minimum Assembly-to-Assembly Pitch	0.9317	0.0009	0.9335

Table M.6-13
WE 17x17 Class Assembly without BPRAs Results

Model Description	k_{KENO}	1σ	k_{eff}
Initial Enrichment 3.4 wt% U-235 - No PRAs, w/o BPRAs			
Internal Moderator at 100%TD	0.9099	0.0008	0.9115
Internal Moderator at 90%TD	0.9216	0.0009	0.9234
Internal Moderator at 80%TD	0.9313	0.0009	0.9331
Internal Moderator at 70%TD	0.9355	0.0010	0.9375
Internal Moderator at 60%TD	0.9369	0.0009	0.9387
Internal Moderator at 50%TD	0.9282	0.0008	0.9298
Internal Moderator at 40%TD	0.9115	0.0008	0.9131
Initial Enrichment 4.0 wt% U-235 - 4 PRAs, w/o BPRAs			
Internal Moderator at 100%TD	0.9201	0.0008	0.9217
Internal Moderator at 90%TD	0.9269	0.0008	0.9285
Internal Moderator at 80%TD	0.9322	0.0009	0.9340
Internal Moderator at 70%TD	0.9333	0.0009	0.9351
Internal Moderator at 60%TD	0.9263	0.0009	0.9281
Internal Moderator at 50%TD	0.9151	0.0009	0.9169
Internal Moderator at 40%TD	0.8913	0.0008	0.8929
Initial Enrichment 4.5 wt% U-235 - 8 PRAs, w/o BPRAs			
Internal Moderator at 100%TD	0.9262	0.0008	0.9278
Internal Moderator at 90%TD	0.9313	0.0009	0.9331
Internal Moderator at 80%TD	0.9386	0.0009	0.9404
Internal Moderator at 70%TD	0.9357	0.0010	0.9377
Internal Moderator at 60%TD	0.9283	0.0010	0.9303
Internal Moderator at 50%TD	0.9110	0.0011	0.9132
Internal Moderator at 40%TD	0.8855	0.0009	0.8873
Initial Enrichment 5.0 wt% U-235 - 16 PRAs, w/o BPRAs			
Internal Moderator at 100%TD	0.8998	0.0011	0.9020
Internal Moderator at 90%TD	0.8943	0.0014	0.8971
Internal Moderator at 80%TD	0.8895	0.0013	0.8921
Internal Moderator at 70%TD	0.8820	0.0011	0.8842
Internal Moderator at 60%TD	0.8649	0.0010	0.8669
Internal Moderator at 50%TD	0.8408	0.0010	0.8428
Internal Moderator at 40%TD	0.8074	0.0010	0.8094

Table M.6-14
WE 17x17 Class Assembly with BPRAs Results

Model Description	k_{KENO}	1σ	k_{eff}
Initial Enrichment 3.4 wt% U-235 - No PRAs, with BPRAs			
Internal Moderator at 100%TD	0.9256	0.0008	0.9272
Internal Moderator at 90%TD	0.9342	0.0009	0.9360
Internal Moderator at 80%TD	0.9385	0.0009	0.9403
Internal Moderator at 70%TD	0.9389	0.0010	0.9409
Internal Moderator at 60%TD	0.9357	0.0008	0.9373
Internal Moderator at 50%TD	0.9236	0.0011	0.9258
Internal Moderator at 40%TD	0.9017	0.0009	0.9035
Internal Moderator at 0%TD	0.5821	0.0005	0.5831
Initial Enrichment 4.0 wt% U-235 - 4 PRAs, with BPRAs			
Internal Moderator at 100%TD	0.9317	0.0009	0.9335
Internal Moderator at 90%TD	0.9347	0.0010	0.9367
Internal Moderator at 80%TD	0.9357	0.0009	0.9375
Internal Moderator at 70%TD	0.9314	0.0008	0.9330
Internal Moderator at 60%TD	0.9240	0.0009	0.9258
Internal Moderator at 50%TD	0.9075	0.0009	0.9093
Internal Moderator at 40%TD	0.8830	0.0009	0.8848
Initial Enrichment 4.5 wt% U-235 - 8 PRAs, with BPRAs			
Internal Moderator at 100%TD	0.9339	0.0009	0.9357
Internal Moderator at 90%TD	0.9368	0.0011	0.9390
Internal Moderator at 80%TD	0.9338	0.0009	0.9356
Internal Moderator at 70%TD	0.9257	0.0009	0.9275
Internal Moderator at 60%TD	0.9123	0.0010	0.9143
Internal Moderator at 50%TD	0.8932	0.0011	0.8954
Internal Moderator at 40%TD	0.8656	0.0010	0.8676
Initial Enrichment 5.0 wt% U-235 - 16 PRAs, with BPRAs			
Internal Moderator at 100%TD	0.9008	0.0013	0.9034
Internal Moderator at 90%TD	0.8949	0.0015	0.8979
Internal Moderator at 80%TD	0.8879	0.0015	0.8909
Internal Moderator at 70%TD	0.8742	0.0013	0.8768
Internal Moderator at 60%TD	0.8550	0.0010	0.8570
Internal Moderator at 50%TD	0.8311	0.0009	0.8329
Internal Moderator at 40%TD	0.7964	0.0010	0.7984

Table M.6-15
CE 16x16 Class Assembly without BPRAs Results

Model Description	k_{KENO}	1σ	k_{eff}
Initial Enrichment 3.8 wt% U-235 - No PRAs, w/o BPRAs			
Internal Moderator at 100%TD	0.9000	0.0011	0.9022
Internal Moderator at 90%TD	0.9140	0.0009	0.9158
Internal Moderator at 80%TD	0.9262	0.0009	0.9280
Internal Moderator at 70%TD	0.9357	0.0010	0.9377
Internal Moderator at 60%TD	0.9374	0.0010	0.9394
Internal Moderator at 50%TD	0.9330	0.0008	0.9346
Internal Moderator at 40%TD	0.9206	0.0010	0.9226
Initial Enrichment 4.3 wt% U-235 - 4 PRAs, w/o BPRAs			
Internal Moderator at 100%TD	0.9082	0.0009	0.9100
Internal Moderator at 90%TD	0.9188	0.0009	0.9206
Internal Moderator at 80%TD	0.9280	0.0009	0.9298
Internal Moderator at 70%TD	0.9365	0.0009	0.9383
Internal Moderator at 60%TD	0.9351	0.0008	0.9367
Internal Moderator at 50%TD	0.9280	0.0011	0.9302
Internal Moderator at 40%TD	0.9128	0.0010	0.9148
Initial Enrichment 4.7 wt% U-235 - 8 PRAs, w/o BPRAs			
Internal Moderator at 100%TD	0.9193	0.0010	0.9213
Internal Moderator at 90%TD	0.9277	0.0009	0.9295
Internal Moderator at 80%TD	0.9355	0.0009	0.9373
Internal Moderator at 70%TD	0.9371	0.0010	0.9391
Internal Moderator at 60%TD	0.9372	0.0010	0.9392
Internal Moderator at 50%TD	0.9263	0.0009	0.9281
Internal Moderator at 40%TD	0.9090	0.0009	0.9108
Initial Enrichment 5.0 wt% U-235 - 16 PRAs, w/o BPRAs			
Internal Moderator at 100%TD	0.9106	0.0009	0.9124
Internal Moderator at 90%TD	0.9150	0.0010	0.9170
Internal Moderator at 80%TD	0.9192	0.0010	0.9212
Internal Moderator at 70%TD	0.9171	0.0009	0.9189
Internal Moderator at 60%TD	0.9118	0.0010	0.9138
Internal Moderator at 50%TD	0.9004	0.0009	0.9022
Internal Moderator at 40%TD	0.8775	0.0009	0.8793

Table M.6-16
B&W 15x15 Class Assembly without BPRAs Results

Model Description	k_{KENO}	1σ	k_{eff}
Initial Enrichment 3.3 wt% U-235 - No PRAs, w/o BPRAs			
Internal Moderator at 100%TD	0.9030	0.0009	0.9048
Internal Moderator at 90%TD	0.9152	0.0009	0.9170
Internal Moderator at 80%TD	0.9249	0.0008	0.9265
Internal Moderator at 70%TD	0.9331	0.0009	0.9349
Internal Moderator at 60%TD	0.9317	0.0009	0.9335
Internal Moderator at 50%TD	0.9239	0.0009	0.9257
Internal Moderator at 40%TD	0.9078	0.0008	0.9094
Internal Moderator at 30%TD	0.8735	0.0009	0.8753
Internal Moderator at 20%TD	0.8132	0.0009	0.8150
Internal Moderator at10%TD	0.7178	0.0007	0.7192
Internal Moderator at 0%TD	0.5676	0.0006	0.5688
Initial Enrichment 3.9 wt% U-235 - 4 PRAs, w/o BPRAs			
Internal Moderator at 100%TD	0.9200	0.0009	0.9218
Internal Moderator at 90%TD	0.9293	0.0010	0.9313
Internal Moderator at 80%TD	0.9330	0.0010	0.9350
Internal Moderator at 70%TD	0.9351	0.0010	0.9371
Internal Moderator at 60%TD	0.9326	0.0008	0.9342
Internal Moderator at 50%TD	0.9195	0.0009	0.9213
Internal Moderator at 40%TD	0.8985	0.0008	0.9001
Initial Enrichment 5.0 wt% U-235 - 16 PRAs, w/o BPRAs			
Internal Moderator at 100%TD	0.9189	0.0010	0.9209
Internal Moderator at 90%TD	0.9202	0.0010	0.9222
Internal Moderator at 80%TD	0.9176	0.0009	0.9194
Internal Moderator at 70%TD	0.9095	0.0011	0.9117
Internal Moderator at 60%TD	0.8953	0.0009	0.8971
Internal Moderator at 50%TD	0.8769	0.0010	0.8789
Internal Moderator at 40%TD	0.8450	0.0009	0.8468

Table M.6-17
B&W 15x15 Class Assembly with BPRAs Results

Model Description	k_{KENO}	1σ	k_{eff}
Initial Enrichment 3.3 wt% U-235 - No PRAs, with BPRAs			
Internal Moderator at 100%TD	0.9182	0.0009	0.9200
Internal Moderator at 90%TD	0.9272	0.0010	0.9292
Internal Moderator at 80%TD	0.9332	0.0008	0.9348
Internal Moderator at 70%TD	0.9360	0.0009	0.9378
Internal Moderator at 60%TD	0.9341	0.0010	0.9361
Internal Moderator at 50%TD	0.9213	0.0010	0.9233
Internal Moderator at 40%TD	0.9002	0.0008	0.9018
Initial Enrichment 3.9 wt% U-235 - 4 PRAs, with BPRAs			
Internal Moderator at 100%TD	0.9313	0.0008	0.9329
Internal Moderator at 90%TD	0.9382	0.0009	0.9400
Internal Moderator at 80%TD	0.9389	0.0009	0.9407
Internal Moderator at 70%TD	0.9364	0.0008	0.9380
Internal Moderator at 60%TD	0.9294	0.0009	0.9312
Internal Moderator at 50%TD	0.9139	0.0009	0.9157
Internal Moderator at 40%TD	0.8878	0.0008	0.8894
Initial Enrichment 5.0 wt% U-235 - 16 PRAs, with BPRAs			
Internal Moderator at 100%TD	0.9243	0.0010	0.9263
Internal Moderator at 90%TD	0.9228	0.0010	0.9248
Internal Moderator at 80%TD	0.9160	0.0014	0.9188
Internal Moderator at 70%TD	0.9050	0.0010	0.9070
Internal Moderator at 60%TD	0.8886	0.0008	0.8902
Internal Moderator at 50%TD	0.8683	0.0008	0.8699
Internal Moderator at 40%TD	0.8358	0.0009	0.8376

Table M.6-18
CE 15x15 Class Assembly without BPRAs Results

Model Description	k_{KENO}	1σ	k_{eff}
Initial Enrichment 3.4 wt% U-235 - No PRAs, w/o BPRAs			
Internal Moderator at 100%TD	0.9100	0.0009	0.9118
Internal Moderator at 90%TD	0.9188	0.0009	0.9206
Internal Moderator at 80%TD	0.9257	0.0009	0.9275
Internal Moderator at 70%TD	0.9316	0.0011	0.9338
Internal Moderator at 60%TD	0.9267	0.0009	0.9285
Internal Moderator at 50%TD	0.9177	0.0010	0.9197
Internal Moderator at 40%TD	0.8981	0.0009	0.8999

Table M.6-19
WE 15x15 Class Assembly without BPRAs Results

Model Description	k_{KENO}	1σ	k_{eff}
Initial Enrichment 3.4 wt% U-235 - No PRAs, w/o BPRAs			
Internal Moderator at 100%TD	0.9016	0.0009	0.9034
Internal Moderator at 90%TD	0.9149	0.0009	0.9167
Internal Moderator at 80%TD	0.9255	0.0008	0.9271
Internal Moderator at 70%TD	0.9328	0.0009	0.9346
Internal Moderator at 60%TD	0.9364	0.0009	0.9382
Internal Moderator at 50%TD	0.9308	0.0010	0.9328
Internal Moderator at 40%TD	0.9133	0.0008	0.9149
Initial Enrichment 4.0 wt% U-235 - 4 PRAs, w/o BPRAs			
Internal Moderator at 100%TD	0.9107	0.0009	0.9125
Internal Moderator at 90%TD	0.9229	0.0010	0.9249
Internal Moderator at 80%TD	0.9292	0.0010	0.9312
Internal Moderator at 70%TD	0.9307	0.0009	0.9325
Internal Moderator at 60%TD	0.9278	0.0009	0.9296
Internal Moderator at 50%TD	0.9183	0.0009	0.9201
Internal Moderator at 40%TD	0.8959	0.0008	0.8975
Initial Enrichment 4.6 wt% U-235 - 8 PRAs, w/o BPRAs			
Internal Moderator at 100%TD	0.9276	0.0009	0.9294
Internal Moderator at 90%TD	0.9325	0.0009	0.9343
Internal Moderator at 80%TD	0.9363	0.0010	0.9383
Internal Moderator at 70%TD	0.9349	0.0008	0.9365
Internal Moderator at 60%TD	0.9251	0.0009	0.9269
Internal Moderator at 50%TD	0.9130	0.0009	0.9148
Internal Moderator at 40%TD	0.8863	0.0010	0.8883
Initial Enrichment 5.0 wt% U-235 - 16 PRAs, w/o BPRAs			
Internal Moderator at 100%TD	0.8969	0.0012	0.8993
Internal Moderator at 90%TD	0.8985	0.0011	0.9007
Internal Moderator at 80%TD	0.8967	0.0010	0.8987
Internal Moderator at 70%TD	0.8894	0.0009	0.8912
Internal Moderator at 60%TD	0.8780	0.0009	0.8798
Internal Moderator at 50%TD	0.8567	0.0010	0.8587
Internal Moderator at 40%TD	0.8259	0.0009	0.8277

Table M.6-20
CE 14x14 Class Assembly without BPRAs Results

Model Description	k_{KENO}	1σ	k_{eff}
Initial Enrichment 3.8 wt% U-235 - No PRAs, w/o BPRAs			
Internal Moderator at 100%TD	0.8905	0.0011	0.8927
Internal Moderator at 90%TD	0.9078	0.0012	0.9102
Internal Moderator at 80%TD	0.9196	0.0009	0.9214
Internal Moderator at 70%TD	0.9292	0.0009	0.9310
Internal Moderator at 60%TD	0.9347	0.0010	0.9367
Internal Moderator at 50%TD	0.9309	0.0010	0.9329
Internal Moderator at 40%TD	0.9165	0.0010	0.9185
Initial Enrichment 4.6 wt% U-235 - 4 PRAs, w/o BPRAs			
Internal Moderator at 100%TD	0.9103	0.0009	0.9121
Internal Moderator at 90%TD	0.9223	0.0009	0.9241
Internal Moderator at 80%TD	0.9300	0.0010	0.9320
Internal Moderator at 70%TD	0.9371	0.0008	0.9387
Internal Moderator at 60%TD	0.9376	0.0008	0.9392
Internal Moderator at 50%TD	0.9308	0.0009	0.9326
Internal Moderator at 40%TD	0.9155	0.0010	0.9175
Initial Enrichment 5.0 wt% U-235 - 8 PRAs, w/o BPRAs			
Internal Moderator at 100%TD	0.9133	0.0009	0.9151
Internal Moderator at 90%TD	0.9199	0.0010	0.9219
Internal Moderator at 80%TD	0.9271	0.0011	0.9293
Internal Moderator at 70%TD	0.9294	0.0009	0.9312
Internal Moderator at 60%TD	0.9271	0.0008	0.9287
Internal Moderator at 50%TD	0.9181	0.0010	0.9201
Internal Moderator at 40%TD	0.8976	0.0009	0.8994

Table M.6-21
WE 14x14 Class Assembly without BPRAs Results

Model Description	k_{KENO}	1σ	k_{eff}
Initial Enrichment 4.0 wt% U-235 - No PRAs, w/o BPRAs			
Internal Moderator at 100%TD	0.9030	0.0011	0.9052
Internal Moderator at 90%TD	0.9148	0.0009	0.9166
Internal Moderator at 80%TD	0.9257	0.0010	0.9277
Internal Moderator at 70%TD	0.9335	0.0011	0.9357
Internal Moderator at 60%TD	0.9374	0.0010	0.9394
Internal Moderator at 50%TD	0.9343	0.0009	0.9361
Internal Moderator at 40%TD	0.9225	0.0010	0.9245
Initial Enrichment 5.0 wt% U-235 - 4 PRAs, w/o BPRAs			
Internal Moderator at 100%TD	0.9098	0.0009	0.9116
Internal Moderator at 90%TD	0.9189	0.0008	0.9205
Internal Moderator at 80%TD	0.9285	0.0009	0.9303
Internal Moderator at 70%TD	0.9348	0.0009	0.9366
Internal Moderator at 60%TD	0.9364	0.0010	0.9384
Internal Moderator at 50%TD	0.9325	0.0010	0.9345
Internal Moderator at 40%TD	0.9185	0.0010	0.9205

Table M.6-22
Criticality Results

STORAGE

Model Description	k_{KENO}	1σ	k_{eff}
Regulatory Requirements			
Dry Storage (Bounded by infinite array of dry casks)	0.5821	0.0005	0.5831
Normal Conditions (Wet Loading)	0.9256	0.0008	0.9272
Accident Conditions (damaged TC while fuel still wet)	0.9389	0.0010	0.9409

Table M.6-23
Benchmarking Results

Run ID	U Enrich. Wt%	Pitch (cm)	H_2O/fuel volume	Separation of assemblies (cm)	AEG	k_{eff}	1σ
B1645SO1	2.46	1.41	1.015	1.78	32.8194	0.9967	0.0009
B1645SO2	2.46	1.41	1.015	1.78	32.7584	1.0002	0.0011
BW1231B1	4.02	1.511	1.139		31.1427	0.9966	0.0012
BW1231B2	4.02	1.511	1.139		29.8854	0.9972	0.0009
BW1273M	2.46	1.511	1.376		32.2106	0.9965	0.0009
BW1484A1	2.46	1.636	1.841	1.64	34.5304	0.9962	0.0010
BW1484A2	2.46	1.636	1.841	4.92	35.1629	0.9931	0.0010
BW1484B1	2.46	1.636	1.841		33.9421	0.9979	0.0010
BW1484B2	2.46	1.636	1.841	1.64	34.5820	0.9955	0.0012
BW1484B3	2.46	1.636	1.841	4.92	35.2609	0.9969	0.0011
BW1484C1	2.46	1.636	1.841	1.64	34.6463	0.9931	0.0011
BW1484C2	2.46	1.636	1.841	1.64	35.2422	0.9939	0.0012
BW1484S1	2.46	1.636	1.841	1.64	34.5105	1.0001	0.0010
BW1484S2	2.46	1.636	1.841	1.64	34.5569	0.9992	0.0010
BW1484SL	2.46	1.636	1.841	6.54	35.4151	0.9935	0.0011
BW1645S1	2.46	1.209	0.383	1.78	30.1040	0.9990	0.0010
BW1645S2	2.46	1.209	0.383	1.78	29.9961	1.0037	0.0011
BW1810A	2.46	1.636	1.841		33.9465	0.9984	0.0008
BW1810B	2.46	1.636	1.841		33.9631	0.9984	0.0009
BW1810C	2.46	1.636	1.841		33.1569	0.9992	0.0010
BW1810D	2.46	1.636	1.841		33.0821	0.9985	0.0013
BW1810E	2.46	1.636	1.841		33.1600	0.9988	0.0009
BW1810F	2.46	1.636	1.841		33.9556	1.0031	0.0011
BW1810G	2.46	1.636	1.841		32.9409	0.9973	0.0011
BW1810H	2.46	1.636	1.841		32.9420	0.9972	0.0011
BW1810I	2.46	1.636	1.841		33.9655	1.0037	0.0009
BW1810J	2.46	1.636	1.841		33.1403	0.9983	0.0011
EPRU65	2.35	1.562	1.196		33.9106	0.9960	0.0011
EPRU65B	2.35	1.562	1.196		33.4013	0.9993	0.0012
EPRU75	2.35	1.905	2.408		35.8671	0.9958	0.0010
EPRU75B	2.35	1.905	2.408		35.3043	0.9996	0.0010
EPRU87	2.35	2.21	3.687		36.6129	1.0007	0.0011
EPRU87B	2.35	2.21	3.687		36.3499	1.0007	0.0011
NSE71SQ	4.74	1.26	1.823		33.7610	0.9979	0.0012
NSE71W1	4.74	1.26	1.823		34.0129	0.9988	0.0013
NSE71W2	4.74	1.26	1.823		36.3037	0.9957	0.0010
P2438BA	2.35	2.032	2.918	5.05	36.2277	0.9979	0.0013

Table M.6-23
Benchmarking Results

(Continued)

Run ID	U Enrich. Wt%	Pitch (cm)	H_2O/fuel volume	Separation of assemblies (cm)	AEG	k_{eff}	1σ
P2438SLG	2.35	2.032	2.918	8.39	36.2889	0.9986	0.0012
P2438SS	2.35	2.032	2.918	6.88	36.2705	0.9974	0.0011
P2438ZR	2.35	2.032	2.918	8.79	36.2840	0.9987	0.0010
P2615BA	4.31	2.54	3.883	6.72	35.7286	1.0019	0.0014
P2615SS	4.31	2.54	3.883	8.58	35.7495	0.9952	0.0015
P2615ZR	4.31	2.54	3.883	10.92	35.7700	0.9977	0.0014
P2827L1	2.35	2.032	2.918	13.72	36.2526	1.0057	0.0011
P2827L2	2.35	2.032	2.918	11.25	36.2908	0.9999	0.0012
P2827L3	4.31	2.54	3.883	20.78	35.6766	1.0092	0.0012
P2827L4	4.31	2.54	3.883	19.04	35.7131	1.0073	0.0012
P2827SLG	2.35	2.032	2.918	8.31	36.3037	0.9957	0.0010
P3314BA	4.31	1.892	1.6	2.83	33.1881	0.9988	0.0012
P3314BC	4.31	1.892	1.6	2.83	33.2284	0.9992	0.0012
P3314BF1	4.31	1.892	1.6	2.83	33.2505	1.0037	0.0013
P3314BF2	4.31	1.892	1.6	2.83	33.2184	1.0009	0.0013
P3314BS1	2.35	1.684	1.6	3.86	34.8594	0.9956	0.0013
P3314BS2	2.35	1.684	1.6	3.46	34.8356	0.9949	0.0010
P3314BS3	4.31	1.892	1.6	7.23	33.4247	0.9970	0.0013
P3314BS4	4.31	1.892	1.6	6.63	33.4162	0.9998	0.0012
P3314SLG	4.31	1.892	1.6	2.83	34.0198	0.9974	0.0012
P3314SS1	4.31	1.892	1.6	2.83	33.9601	0.9999	0.0012
P3314SS2	4.31	1.892	1.6	2.83	33.7755	1.0022	0.0012
P3314SS3	4.31	1.892	1.6	2.83	33.8904	0.9992	0.0013
P3314SS4	4.31	1.892	1.6	2.83	33.7625	0.9958	0.0011
P3314SS5	2.35	1.684	1.6	7.8	34.9531	0.9949	0.0013
P3314SS6	4.31	1.892	1.6	10.52	33.5333	1.0020	0.0011
P3314W1	4.31	1.892	1.6		34.3994	1.0024	0.0013
P3314W2	2.35	1.684	1.6		35.2167	0.9969	0.0011
P3314ZR	4.31	1.892	1.6	2.83	33.9954	0.9971	0.0013
P3602BB	4.31	1.892	1.6	8.3	33.3221	1.0029	0.0013
P3602BS1	2.35	1.684	1.6	4.8	34.7750	1.0027	0.0012
P3602BS2	4.31	1.892	1.6	9.83	33.3679	1.0039	0.0012
P3602N11	2.35	1.684	1.6	8.98	34.7438	1.0023	0.0012
P3602N12	2.35	1.684	1.6	9.58	34.8391	1.0030	0.0012
P3602N13	2.35	1.684	1.6	9.66	34.9337	1.0013	0.0012
P3602N14	2.35	1.684	1.6	8.54	35.0282	0.9974	0.0013

Table M.6-23
Benchmarking Results

(Continued)

Run ID	U Enrich. Wt%	Pitch (cm)	H_2O/fuel volume	Separation of assemblies (cm)	AEG	k_{eff}	1σ
P3602N21	2.35	2.032	2.918	10.36	36.2821	0.9987	0.0011
P3602N22	2.35	2.032	2.918	11.2	36.1896	1.0025	0.0011
P3602N31	4.31	1.892	1.6	14.87	33.2094	1.0057	0.0013
P3602N32	4.31	1.892	1.6	15.74	33.3067	1.0093	0.0012
P3602N33	4.31	1.892	1.6	15.87	33.4174	1.0107	0.0012
P3602N34	4.31	1.892	1.6	15.84	33.4683	1.0045	0.0013
P3602N35	4.31	1.892	1.6	15.45	33.5185	1.0013	0.0012
P3602N36	4.31	1.892	1.6	13.82	33.5855	1.0004	0.0014
P3602N41	4.31	2.54	3.883	12.89	35.5276	1.0109	0.0013
P3602N42	4.31	2.54	3.883	14.12	35.6695	1.0071	0.0014
P3602N43	4.31	2.54	3.883	12.44	35.7542	1.0053	0.0015
P3602SS1	2.35	1.684	1.6	8.28	34.8701	1.0025	0.0013
P3602SS2	4.31	1.892	1.6	13.75	33.4202	1.0035	0.0012
P3926L1	2.35	1.684	1.6	10.06	34.8519	1.0000	0.0011
P3926L2	2.35	1.684	1.6	10.11	34.9324	1.0017	0.0011
P3926L3	2.35	1.684	1.6	8.5	35.0641	0.9949	0.0012
P3926L4	4.31	1.892	1.6	17.74	33.3243	1.0074	0.0014
P3926L5	4.31	1.892	1.6	18.18	33.4074	1.0057	0.0013
P3926L6	4.31	1.892	1.6	17.43	33.5246	1.0046	0.0013
P3926SL1	2.35	1.684	1.6	6.59	33.4737	0.9995	0.0012
P3926SL2	4.31	1.892	1.6	12.79	33.5776	1.0007	0.0012
P4267B1	4.31	1.8901	1.59		31.8075	0.9990	0.0010
P4267B2	4.31	0.89	1.59		31.5323	1.0033	0.0010
P4267B3	4.31	1.715	1.09		30.9905	1.0050	0.0011
P4267B4	4.31	1.715	1.09		30.5061	0.9996	0.0011
P4267B5	4.31	1.715	1.09		30.1011	1.0004	0.0011
P4267SL1	4.31	1.89	1.59		33.4737	0.9995	0.0012
P4267SL2	4.31	1.715	1.09		31.9460	0.9988	0.0016
P62FT231	4.31	1.891	1.6	5.67	32.9196	1.0012	0.0013
P71F14F3	4.31	1.891	1.6	5.19	32.8237	1.0009	0.0014
P71F14V3	4.31	1.891	1.6	5.19	32.8597	0.9972	0.0014
P71F14V5	4.31	1.891	1.6	5.19	32.8609	0.9993	0.0013
P71F214R	4.31	1.891	1.6	5.19	32.8778	0.9969	0.0012
PAT80L1	4.74	1.6	3.807	2	35.0253	1.0012	0.0012
PAT80L2	4.74	1.6	3.807	2	35.1136	0.9993	0.0015
PAT80SS1	4.74	1.6	3.807	2	35.0045	0.9988	0.0013
PAT80SS2	4.74	1.6	3.807	2	35.1072	0.9960	0.0013

Table M.6-23
Benchmarking Results

(Continued)

Run ID	U Enrich. Wt%	Pitch (cm)	H_2O/fuel volume	Separation of assemblies (cm)	AEG	k_{eff}	1σ
W3269A	5.7	1.422	1.93		33.1480	0.9988	0.0012
W3269B1	3.7	1.105	1.432		32.4055	0.9961	0.0011
W3269B2	3.7	1.105	1.432		32.3921	0.9963	0.0011
W3269B3	3.7	1.105	1.432		32.2363	0.9944	0.0011
W3269C	2.72	1.524	1.494		33.7727	0.9989	0.0012
W3269SL1	2.72	1.524	1.494		33.3850	0.9981	0.0014
W3269SL2	5.7	1.422	1.93		33.0910	1.0005	0.0013
W3269W1	2.72	1.524	1.494		33.5114	0.9966	0.0014
W3269W2	5.7	1.422	1.93		33.1680	1.0014	0.0014
W3385SL1	5.74	1.422	1.932		33.2387	1.0009	0.0012
W3385SL2	5.74	2.012	5.067		35.8818	0.9997	0.0013
Correlation	**0.31**	**0.39**	**0.16**	**0.68**	**-0.03**	**N/A**	**N/A**

Table M.6-24
USL-1 Results

Parameter	Range of Applicability	USL-1
U Enrichment (wt. % U-235)	2.4	0.9423
	2.8	0.9429
	3.3	0.9434
	3.8 – 5.7	0.9437
Fuel Rod Pitch (cm)	0.89	0.9396
	1.1	0.9407
	1.2	0.9411
	1.4	0.9418
	1.6	0.9429
	1.8 – 2.6	0.9438
Water/Fuel Volume Ratio	0.38	0.9420
	1.1	0.9425
	1.7	0.9429
	2.4 –5.1	0.9433
Assembly Separation (cm)	1.4	0.9412
	1.6	0.9413
	4.4	0.9428
	7.1 – 21	0.9442
Average Energy Group Causing Fission (AEG)	30 – 32	0.9434
	33	0.9433
	34	0.9432
	35	0.9431
	36	0.9430
	37	0.9430

Table M.6-25
USL Determination for Criticality Analysis

Parameter	Value from Limiting Analysis	Bounding USL-1
U Enrichment (wt. % U-235)	3.4	0.9434
Fuel Rod Pitch (cm)	1.25984	**0.9411**
Water/Fuel Ratio	1.66	0.9425
Assembly Separation (cm)	1.4	0.9412
Average Energy Group Causing Fission (AEG)	~32	0.9434

Figure M.6-1
NUHOMS®-32PT DSC Cross Section

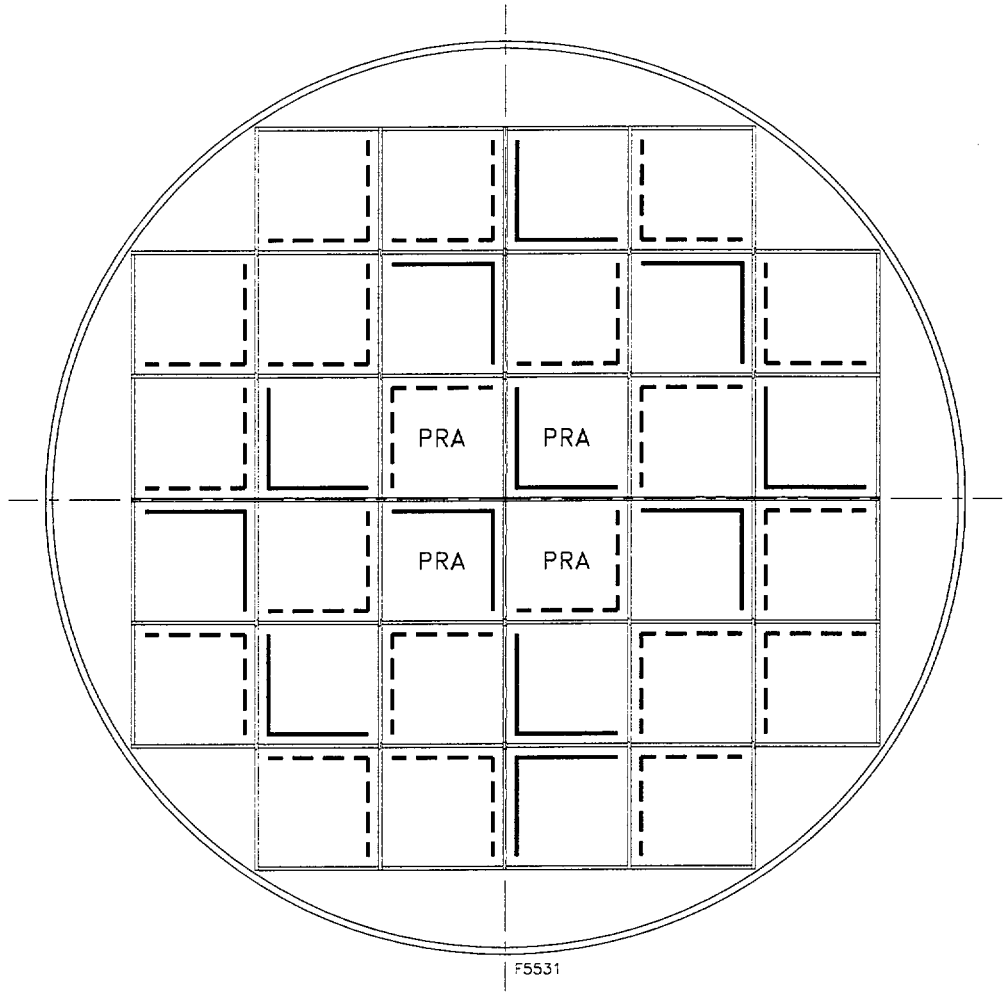

Figure M.6-2
Required PRA Locations for Configurations with Four PRAs

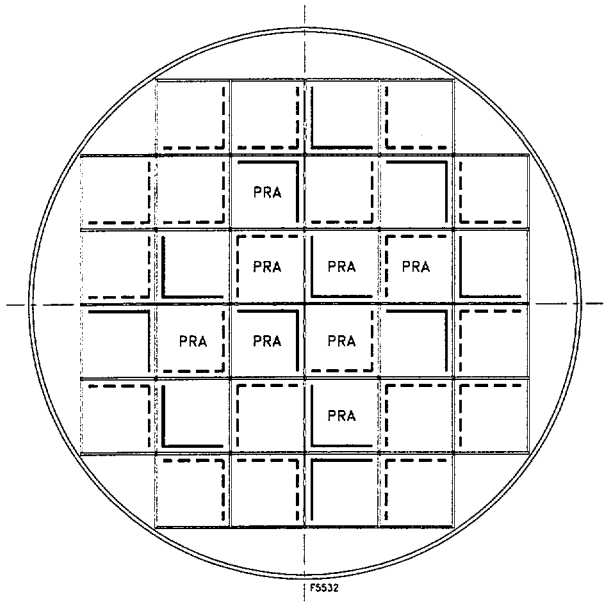

OR

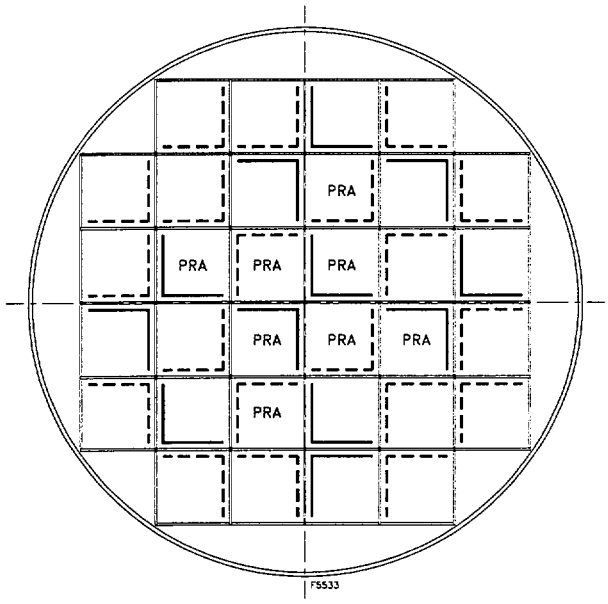

Figure M.6-3
Required PRA Locations for Configurations with Eight PRAs

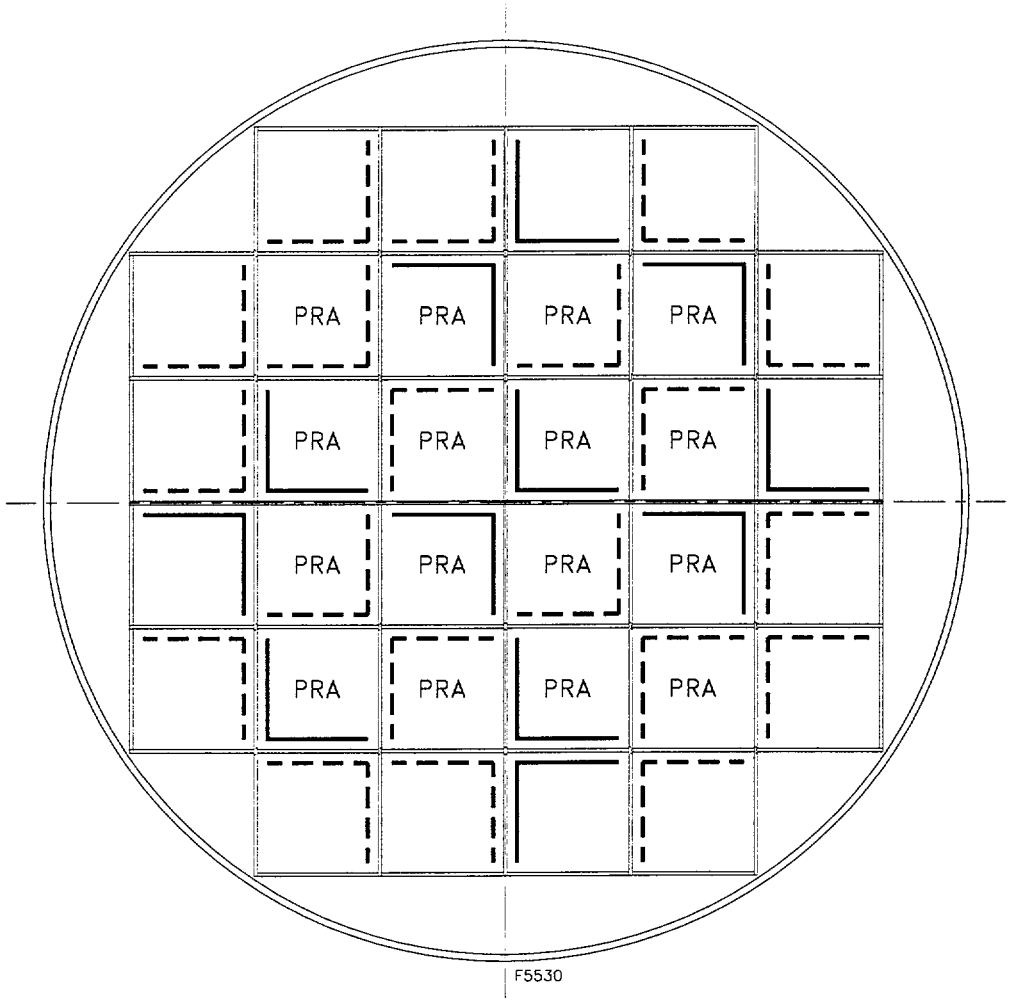

Figure M.6-4
Required PRA Locations for Configurations with Sixteen PRAs

Figure M.6-5
KENO V.a units and Radial Cross Sections of the Model
Part 1 of 18 - (all units 365.76 cm (144 inches) long)

Figure M.6-5
KENO V.a units and Radial Cross Sections of the Model
Part 2 of 18 - (all units 365.76 cm (144 inches) long)

Figure M.6-5
KENO V.a units and Radial Cross Sections of the Model
Part 3 of 18 - (all units 365.76 cm (144 inches) long)

Figure M.6-5
KENO V.a units and Radial Cross Sections of the Model
Part 4 of 18 - (all units 365.76 cm (144 inches) long)

Figure M.6-5
KENO V.a units and Radial Cross Sections of the Model
Part 5 of 18 - (all units 365.76 cm (144 inches) long)

Figure M.6-5
KENO V.a units and Radial Cross Sections of the Model
Part 6 of 18 - (all units 365.76 cm (144 inches) long)

Figure M.6-5
KENO V.a units and Radial Cross Sections of the Model
Part 7 of 18 - (all units 365.76 cm (144 inches) long)

Figure M.6-5
KENO V.a units and Radial Cross Sections of the Model
Part 8 of 18 - (all units 365.76 cm (144 inches) long)

Figure M.6-5
KENO V.a units and Radial Cross Sections of the Model
Part 9 of 18 - (all units 365.76 cm (144 inches) long)

Figure M.6-5
KENO V.a units and Radial Cross Sections of the Model
Part 10 of 18 - (all units 365.76 cm (144 inches) long)

Figure M.6-5
KENO V.a units and Radial Cross Sections of the Model
Part 11 of 18 - (all units 365.76 cm (144 inches) long)

Figure M.6-5
KENO V.a units and Radial Cross Sections of the Model
Part 12 of 18 - (all units 365.76 cm (144 inches) long)

Figure M.6-5
KENO V.a units and Radial Cross Sections of the Model
Part 13 of 18 - (all units 365.76 cm (144 inches) long)

Figure M.6-5
KENO V.a units and Radial Cross Sections of the Model
Part 14 of 18 - (all units 365.76 cm (144 inches) long)

Figure M.6-5
KENO V.a units and Radial Cross Sections of the Model
Part 15 of 18 - (all units 365.76 cm (144 inches) long)

Figure M.6-5
KENO V.a units and Radial Cross Sections of the Model
Part 16 of 18 - (all units 365.76 cm (144 inches) long)

Figure M.6-5
KENO V.a units and Radial Cross Sections of the Model
Part 17 of 18 - (all units 365.76 cm (144 inches) long)

Figure M.6-5
KENO V.a units and Radial Cross Sections of the Model
Part 18 of 18 - (all units 365.76 cm (144 inches) long)

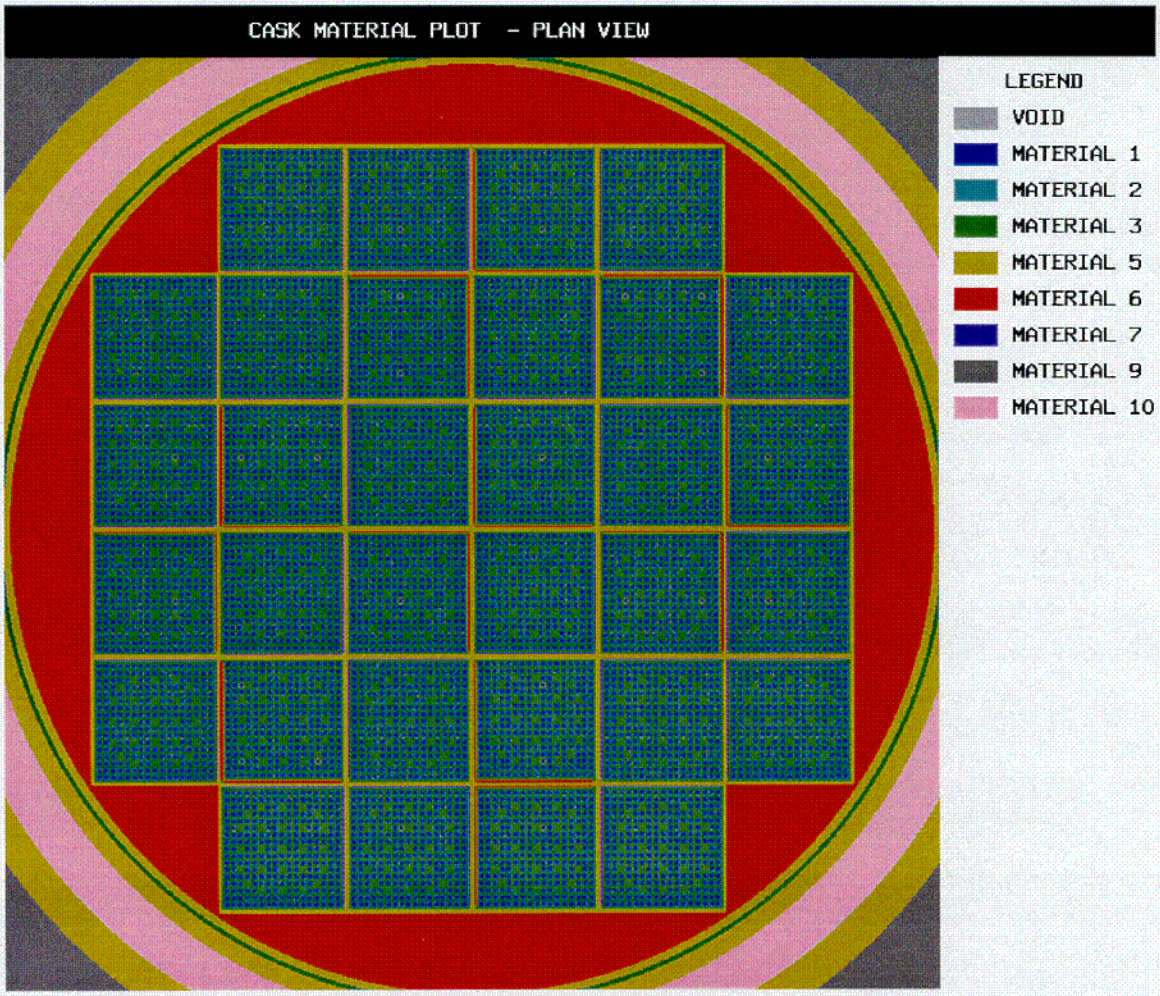

Figure M.6-6
WE 17x17 Class Assembly

C01

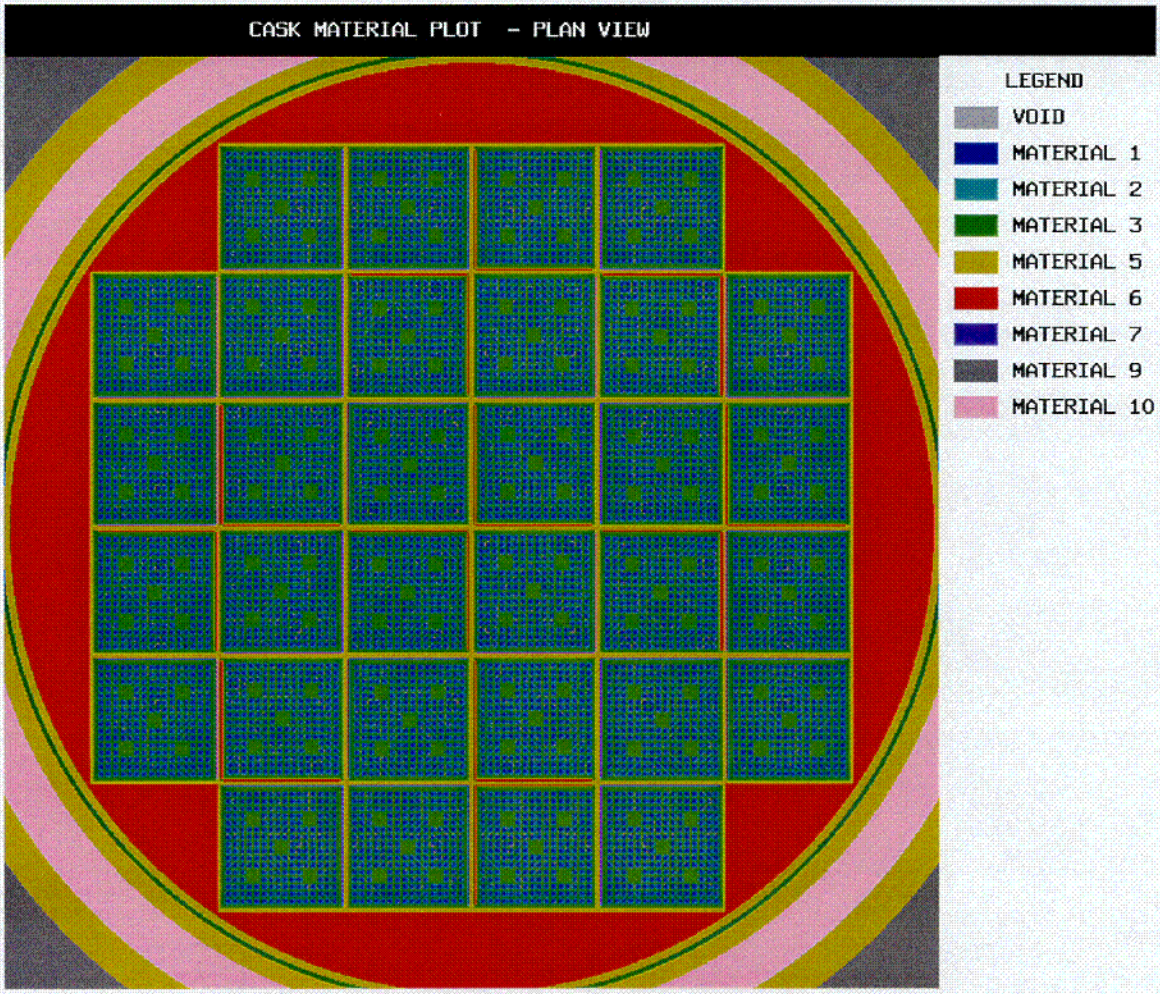

Figure M.6-7
CE 16x16 Class Assembly

C02

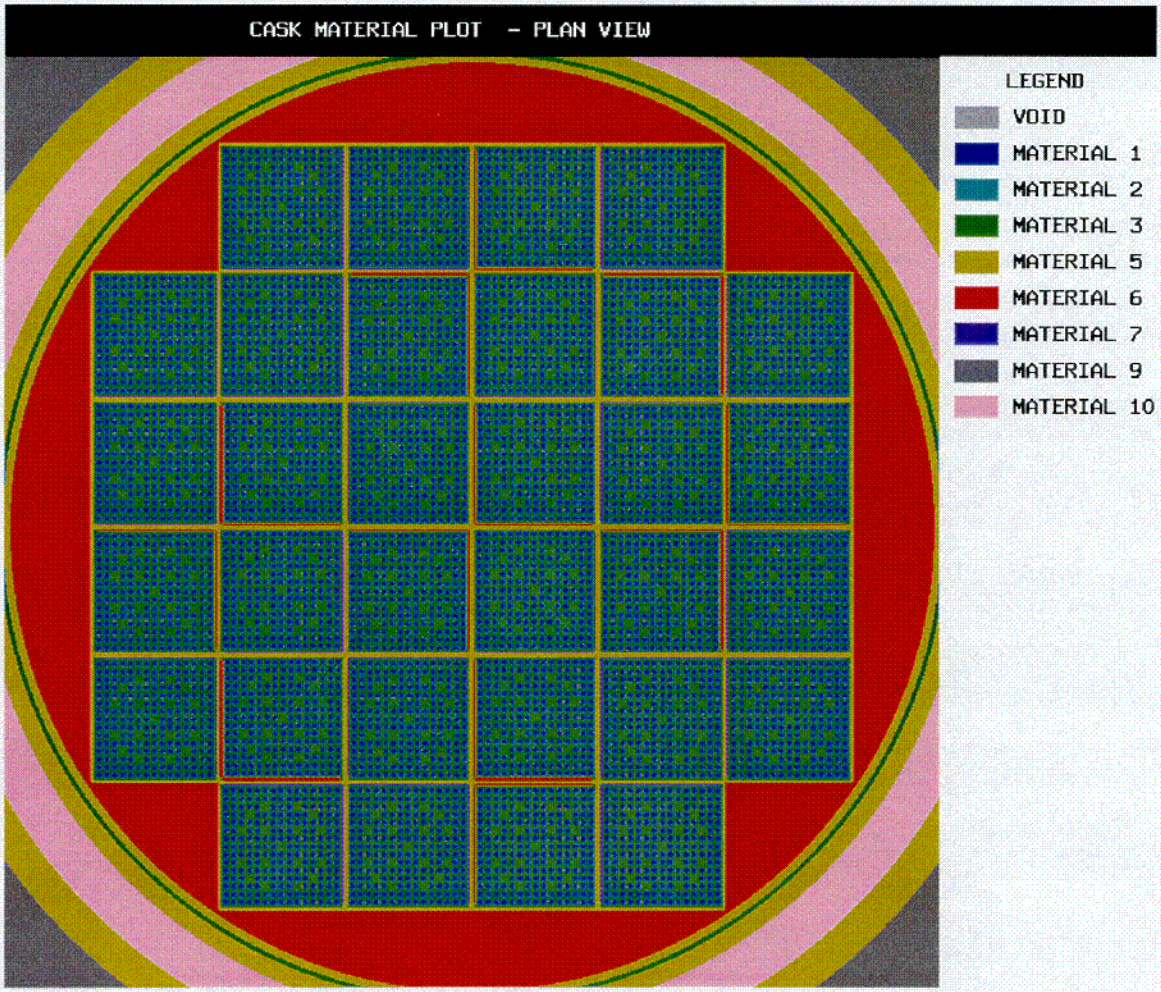

Figure M.6-8
B&W 15x15 Class Assembly

C03

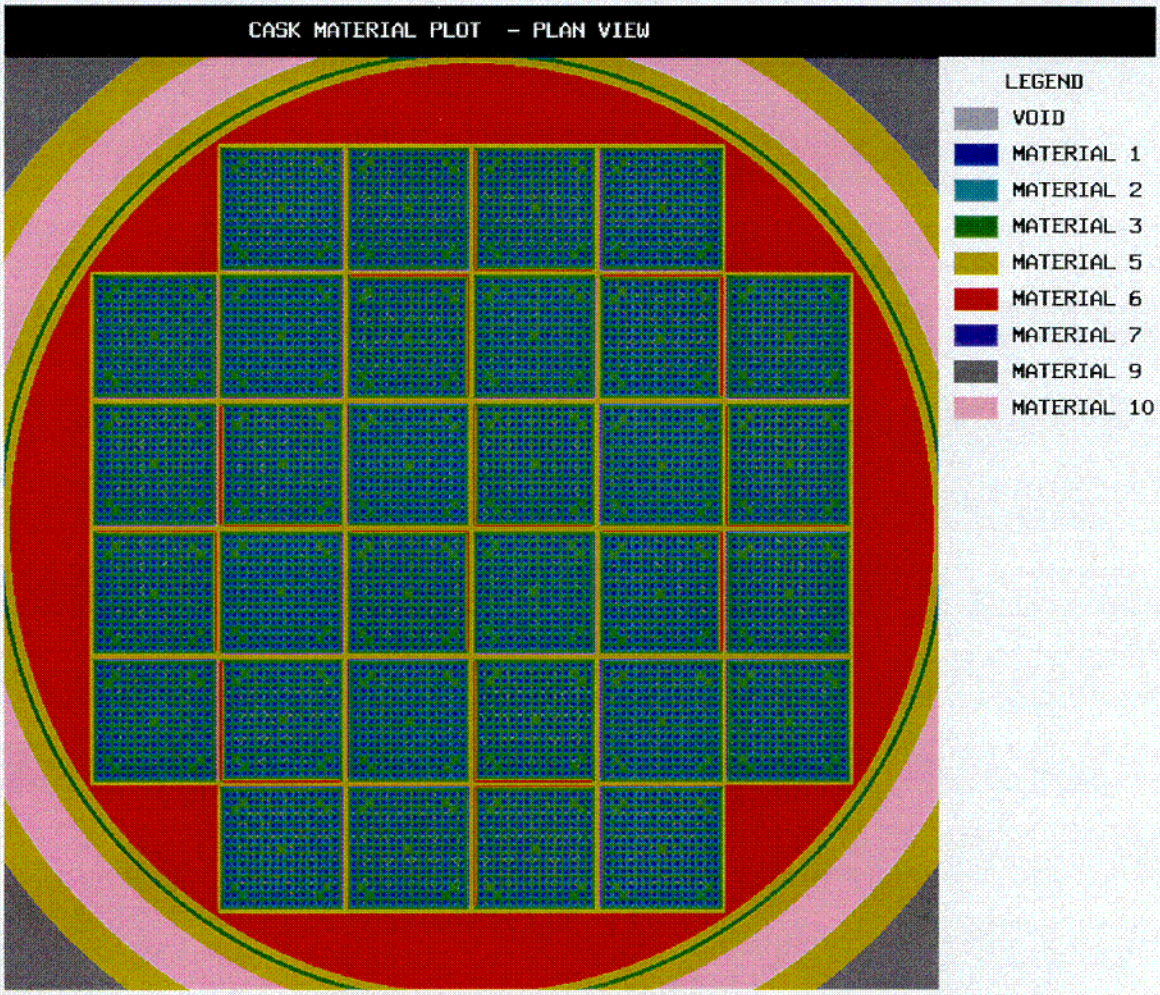

Figure M.6-9
CE 15x15 Class Assembly

C04

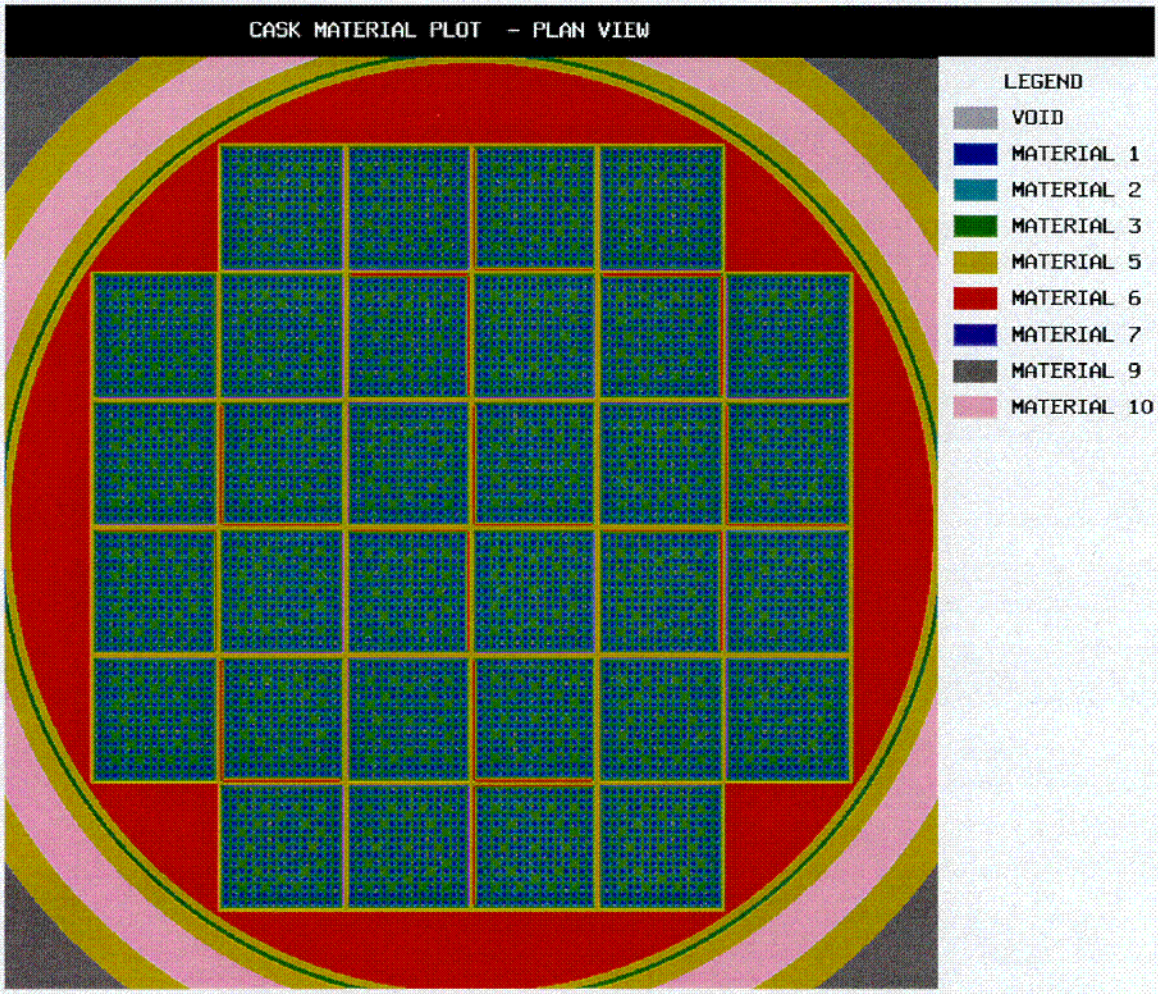

Figure M.6-10
WE 15x15 Class Assembly

C05

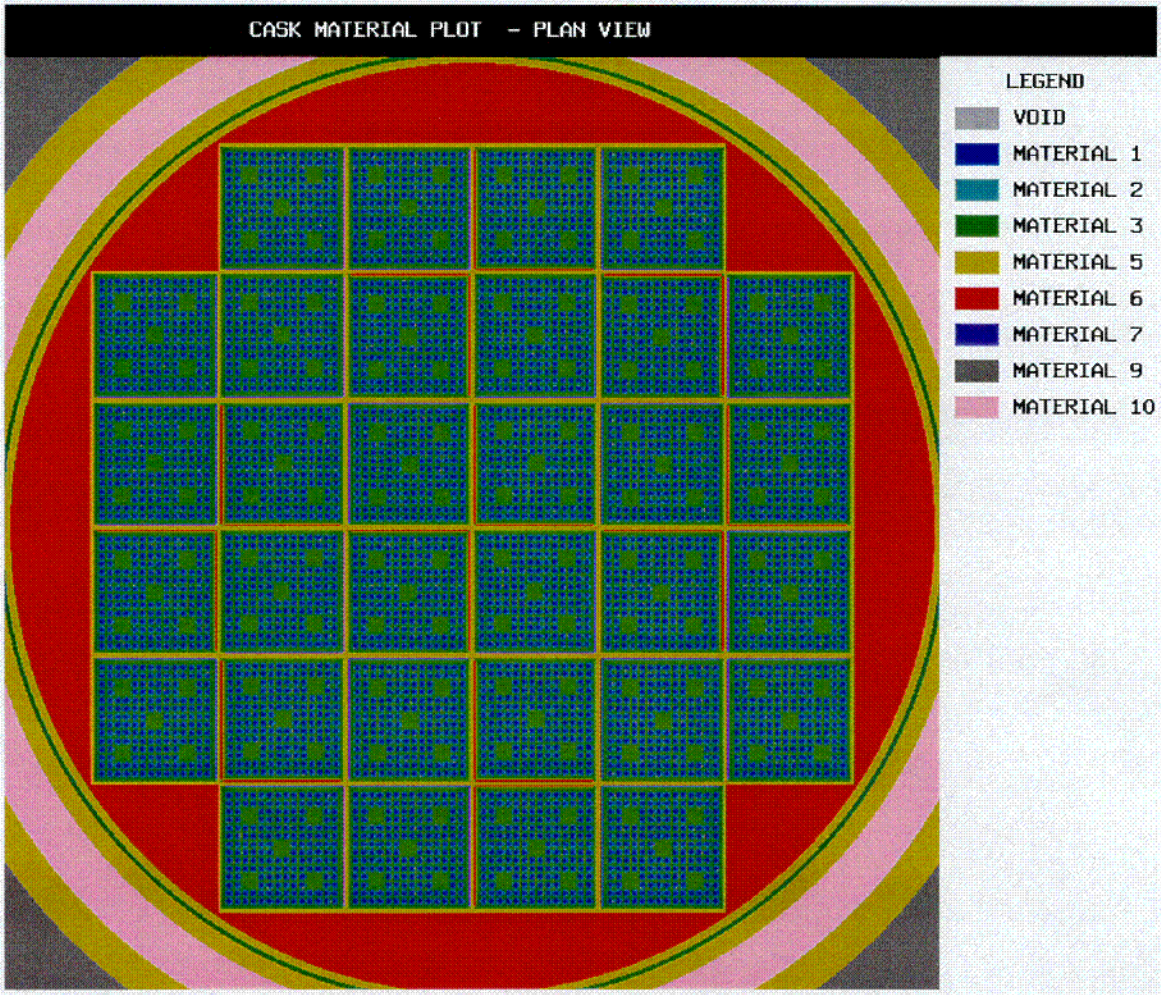

Figure M.6-11
CE 14x14 Class Assembly

C04

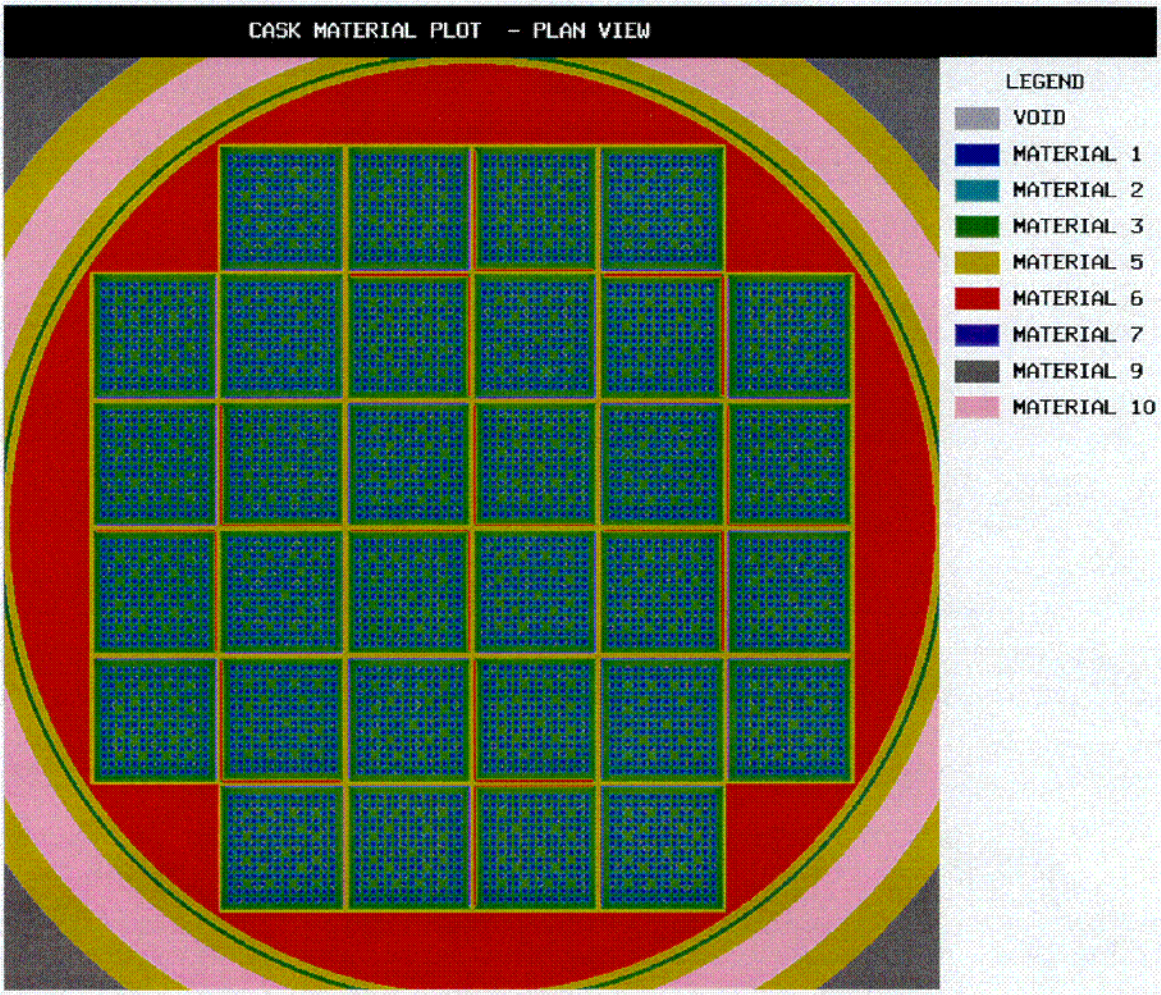

Figure M.6-12
WE 14x14 Class Assembly

C07